U.S. DEPARTMENT OF THE INTERIOR

U.S. GEOLOGICAL SURVEY

Selected geochemical data for the Dillon BLM Resource Area
(including the Virginia City mining district),
Madison and Beaverhead Counties, southwest Montana:
Mineral-resource and mineral-environmental considerations

by J.M. Hammarstrom[1] and B.S. Van Gosen[2]

Open-File Report 98-224-C

1998

[1]Reston, VA
[2]Denver, CO

CONTENTS

Introduction 1
Methods 16
Data 21
Big Muddy mining district 22
Blacktail mining district 25
Cherry Creek mining district 34
Chinatown mining district 39
Horse Prairie mining district 44
Medicine Lodge mining district 49
Monida mining district 52
Pony mining district 55
Red Bluff mining district 59
Revenue mining district 61
Ruby Mountains mining district 63
Sheridan mining district 66
Silver Star mining district 69
Virginia City mining district 72
Mapleton mine 76
Browns Gulch area 76
Alameda-Cornucopia-U.S. Grant mine area 77
Hungry Hollow Gulch 78
Alder Gulch 78
Butcher Gulch 79
Discussion 92
Iron formation 92
Ultramafic rocks 94
Gold vein systems 95
Environmental considerations 97
Summary and conclusions 99
Acknowledgments 100
References cited 101

Figures

Figure 1. Location map for the Dillon BLM Resource Area. 3
Figure 2. Mineral localities in Madison and Beaverhead Counties plotted by mining district. Data are from the MAS/MILS database (Kaas, 1996). Numbers of sites that account for 75 percent of the occurrences and the principal commodities reported for those sites are shown in the inset table. Coordinates shown mark the boundaries of the four 1:250,000-scale quadrangles that cover the Dillon Resource Area. 4
Figure 3. Sample locations plotted by mining district and by sample type. Faint grid outlines 7.5' topographic quadrangle maps. Sample number key in boldface. Mining district key in parentheses. 5
Figure 4. Map of the Chinatown district showing historic mines and prospects and sites sampled for this study. Samples include "cannonballs" (29,30), gossan from the H&S mine dump (31), and a stream sediment sample collected just upstream of the Lucky Strike workings (32). Base topography from the Leadore 1:100,000-scale topographic quadrangle map. 41

Figure 5. Sample sites in the Virginia City mining district. See tables 1 and 16 for map key. Localities for gold mines and prospects and gold placers are plotted from the MAS/MILS database (Kaas, 1996). Boundaries and names of 7.5' quadrangles are shown for reference. Base topography from parts of the Ennis and Dillon 1:100,000-scale topographic quadrangle maps. 75
Figure 6. Chondrite-normalized rare-earth element pattems for iron formation. Element concentrations are normalized to C1 chondrite (Sun and McDonough, 1989). 93
A. Copper Mountain and Carter Creek deposits.
B. Ruby (Johnny Gulch Iron) and Black Butte deposits.
C. Magnetite "cannonballs" from Chinatown placer gold tailings.
Figure 7. Minor element signature of quartz veins plotted by mining district. Open circles, Virginia City; filled circles, Cherry Creek; diamonds, Revenue; square, Horse Prairie; filled triangle, Blacktail; open triangle, Red Bluff. 96
A. Log plot of gold versus zinc.
B. Temary plot of antimony (Sb), tellurium (Te), and selenium (Se).
C. Ternary plot of antimony (Sb), tellurium (Te), and arsenic (As).

Tables

Table 1. Sample locations and descriptions. 6
Table 2. Summary of analytical techniques and detection limits. 17
A. Analytical techniques for each batch of samples. 17
B. Detection limits for each analytical method. 18
Table 3. Analytical data for stream sediment and rock samples from the Big Muddy mining district. 23
Table 4. Analytical data for rock and stream sediment samples from the Blacktail mining district. 27
A. Partial multielement data for a variety of rock types. 27
B. Complete chemical analyses for mafic and ultramafic rocks. 31
Table 5. Analytical data for rock and stream sediment samples from the Cherry Creek mining district. 35
Table 6. Analytical data for rock and stream sediment samples from the Chinatown mining district. 42
Table 7. Analytical data for rock samples from the Horse Prairie mining district. 45
Table 8. Analytical data for rock samples from the Medicine Lodge mining district. 50
Table 9. Analytical data for a soil sample from the Monida mining district. 53
Table 10. Analytical data for rock samples from the Pony mining district. 56
Table 11. Analytical data for rock samples from the Red Bluff mining district. 60
Table 12. Analytical data for rock samples from the Revenue mining district. 62
Table 13. Analytical data for rock samples from the Ruby Mountains mining district. 64
Table 14. Analytical data for rock samples from the Sheridan mining district. 67
Table 15. Analytical data for rock samples from the Silver Star mining district. 70
Table 16. Analytical data for rock and stream sediment samples from the Virginia City mining district. 80
A. Partial multielement data for a variety of rock types. 80
B. Complete chemical analyses for an ultramafic rock sample. 90
Table 17. Summary of selected element concentrations in ultramafic rocks. 94
Table 18. Stream sediment data for selected elements by mining district. 98

INTRODUCTION

Geochemical data on rocks associated with mineral occurrences provide signatures that aid in recognition of the types of mineral deposits that may be present in an area. They also indicate metals, minor elements, or trace elements that may be mobilized from rocks to soils or to waters as rocks are exposed to natural (weathering, landslides) or human-induced (surface disturbance such as road construction or mining) processes. As part of an ongoing study to provide federal land managers with a perspective on the nature of mineral resources in the Dillon BLM Resource Area and intervening areas of the Beaverhead National Forest in Madison and Beaverhead Counties, southwest Montana (fig. 1), 100 samples of rocks and stream sediments were collected during site visits to selected active and abandoned mines, prospects, mineral occurrences, and areas of suspected hydrothermal alteration during the summers of 1994-1996. This report presents geochemical data and sample descriptions for these samples.

The Dillon Resource Area covers parts of the Dillon, Bozeman, Ashton, and Dubois 1° by 2° (1:250,000-scale) quadrangles and includes 52 mining districts (fig. 2). Mining district names and boundaries are based on a recent map of mining districts of Montana (Chavez, 1994), which is available in digital form from the Montana State Library's web site (http://nris.mt.gov/nsdi/nris/ab45.eoo.zip). The area of Beaverhead and Madison Counties includes active mines that produce talc, chlorite, placer garnet, and placer gold, as well as exploration projects for gold, talc, and zeolites (McCulloch, 1994). Based on a search of the U.S. Bureau of Mines MAS/MILS database (Kaas, 1996), the area contains over 1,500 historic mines, prospects, and mineral localities (fig. 2). Gold is the principal commodity reported at over one-third of these localities. Precious and base metals, iron, and phosphate account for 75 percent of the occurrences (see inset table on fig. 2). Other commodities reported in the study area include talc, tungsten, manganese, thorium, pumice, sand and gravel, stone, aluminum minerals, silica, garnet, and clays. We focussed our sampling on mining districts where additional geochemical data would help determine the nature of the occurrences and on the districts most likely to experience minerals activity on federal lands in the reasonably foreseeable future. The districts sampled for this report are shown in color on figures 2 and 3. Parts of the Dillon Resource Area that lie within the Dillon 1° by 2° quadrangle (north of 45° 00' N, west of 112° 00' W) were not extensively sampled for this study; the Dillon quadrangle was thoroughly evaluated in previous studies (Pearson and others, 1992; Berger and others, 1983). A few samples were collected from districts in the Dillon quadrangle that have been the focus of very recent exploration.

Sites in the Dillon Resource Area were chosen to: (1) elucidate the nature and types of mineral deposits that could be present in the study area; (2) obtain more complete, and modern geochemical data for sites that had been mined or studied in the past; (3) develop a geochemical database for rocks to aid interpretation of stream sediment or other geochemical data; and (4) provide independent, objective, baseline geochemical data for areas that are most likely to be explored or developed in the reasonably foreseeable future.

Samples are grouped by mining district (table 1, fig. 3), and field sample numbers are assigned sequential map key numbers for plotting. These map key numbers are used for reference throughout this report. Table 1 includes sample locations (7.5-minute quadrangle name, latitude, longitude, descriptive information), sample descriptions, and analytical job number. Sample numbers followed by an asterisk represent replicates submitted for quality control. Different symbols are used for different samples types in figure 3. Sample types are grouped into the following general categories: Archean gneiss, iron formation, quartz vein, skarn, stream sediment, ultramafic rocks, and other altered rocks. See table 1 for a detailed explanation of sample type and for detailed locations of closely-spaced samples. 7.5 minute quadrangles are shown as a faint grid on figure 3. Samples from the Chinatown (fig. 4) and Virginia City (fig. 5) districts are plotted on more detailed maps, along with locations of gold

placers and lode gold mines, prospects, and occurrences from the U.S. Bureau of Mines MAS/MILS database (Kaas, 1996). Both of these districts have active mining claims and current exploration for gold.

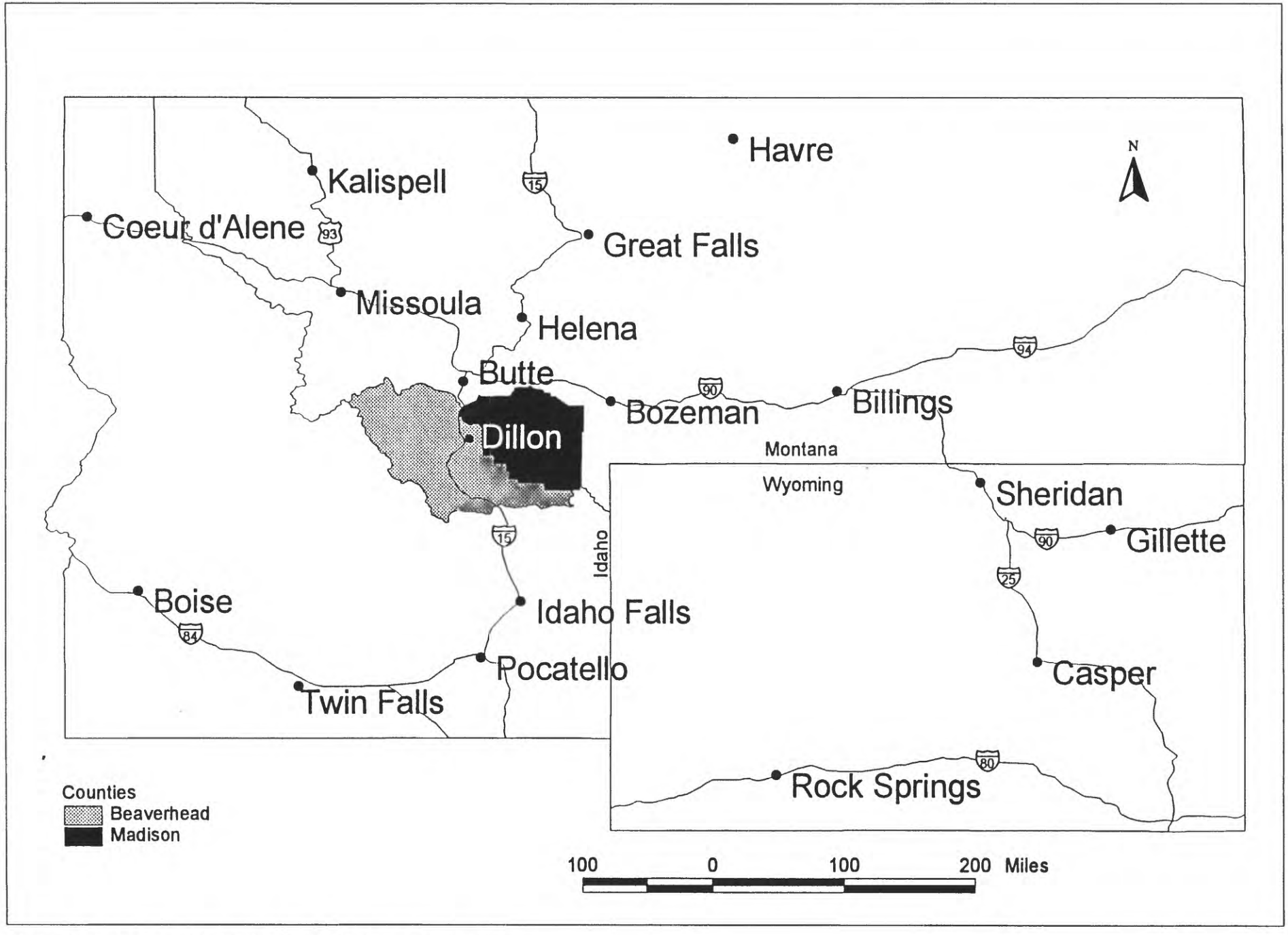

Figure 1. Location map for the Dillon BLM Resource Area.

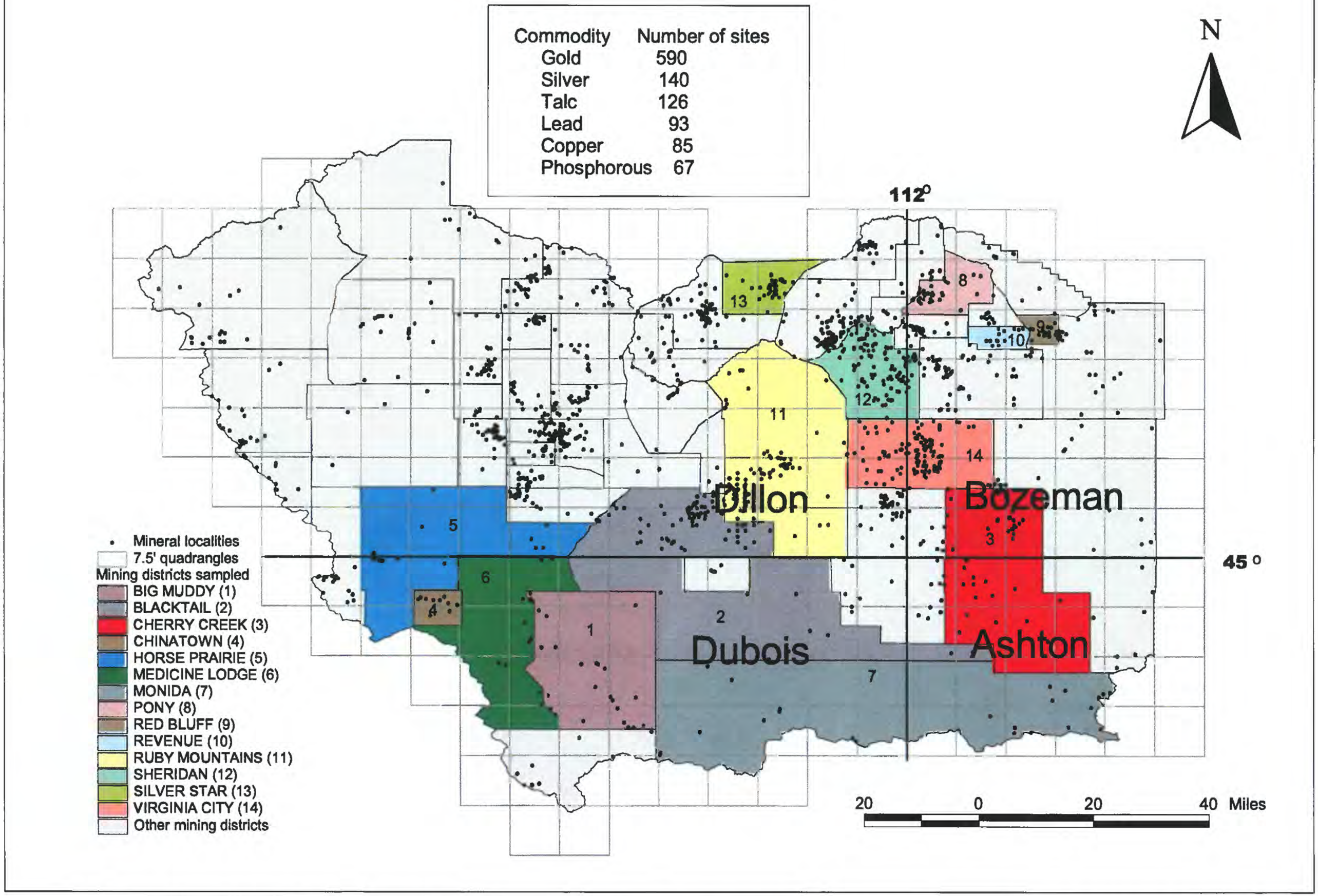

Figure 2. Mineral localities in Madison and Beaverhead Counties plotted by mining district. Data are from the MAS/MILS database (Kaas, 1996). Numbers of sites that account for 75 percent of the occurrences and the principal commodites reported for those sites are shown in the inset table. Coordinates shown mark the boundaries of the four 1:250,000-scale quadrangles that cover the Dillon Resource Area.

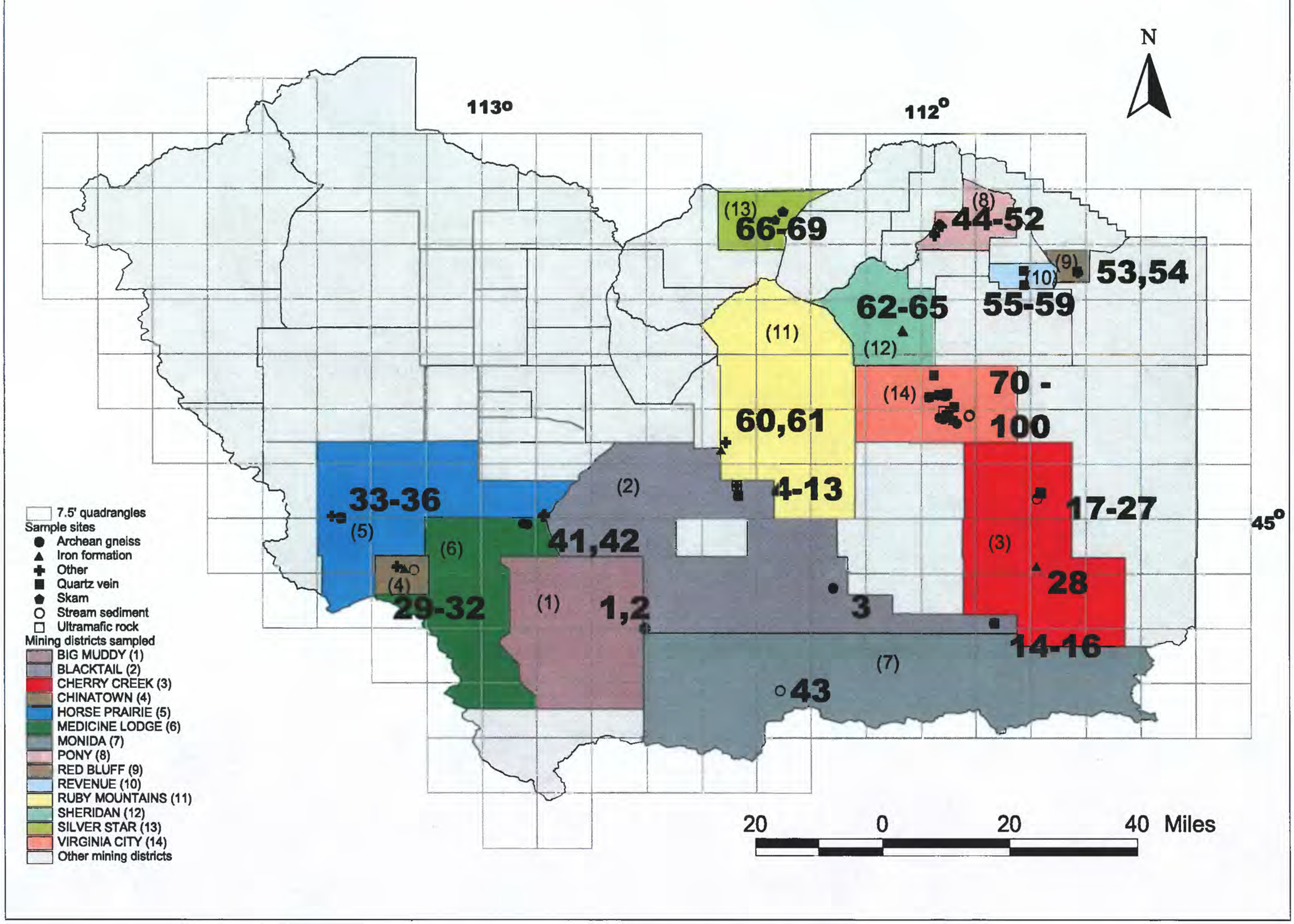

Figure 3. Sample locations plotted by mining district and by sample type. Faint grid outlines 7.5' topographic quadrangle maps. Sample number key in boldface. Mining district key in parentheses.

Table 1. Sample locations and descriptions. Sample numbers followed by an asterisk represent replicates submitted for quality control.

Map key	Mining district	Sample number	Quadrangle (1:24,000 scale)	Location	Description	Latitude North	Longitude West	Analytical Job
1	Big Muddy	96JH34	Dell	Spring Gulch stream bed; SW¼ of NW¼ of sec. 31, T.12S., R.8W.	Dry stream sediment from ephemeral stream bed, below hillside of Red Butte conglomerate (see Haley and Perry, 1991)	44° 44' 56"	112° 37' 53"	AHK1787
2	Big Muddy	96JH35	Dell	Hillside above Spring Gulch; SW¼ of NW¼ of sec. 31, T.12S., R.8W.	Composite sample of outcrop of Red Butte conglomerate (see Haley and Perry, 1991)	44° 44' 58"	112° 37' 49"	AHK1787
3	Blacktail	96JH77	Antone Peak	Snowcrest Range Campground; NE¼ of NW¼ of sec. 34, T.11S., R.5W.	Banded Archean gneiss associated with green quartzite in outcrop along East Fork Blacktail Deer Creek	44° 50' 27"	112° 12' 01"	AHK1787
4	Blacktail	95JH101	Elk Gulch	Elk Creek vermiculite deposit; SE¼ of SE¼ of sec. 2, T.9S., R.7W.	Ultramafic knob just south of, and above, the main prospect trench. Area mapped by Berg (1995) and described by Desmarais (1978, 1981).	45° 04' 31"	112° 25' 14"	AHK1255
5	Blacktail	95JH102	Elk Gulch	Elk Creek vermiculite deposit; SE¼ of SE¼ of sec. 2, T.9S., R.7W.	Ultramafic rock a short several hundred feet away from the vermiculite prospect. Area mapped by Berg (1995) and described by Desmarais (1978, 1981).	45° 04' 31"	112° 25' 14"	AHK1255
6	Blacktail	95JH202*	Elk Gulch	Elk Creek vermiculite deposit; SE¼ of SE¼ of sec. 2, T.9S., R.7W.	Replicate sample for 95JH102	45° 04' 31"	112° 25' 14"	AHK1241
7	Blacktail	E9512	Elk Gulch	southern Ruby Range copper prospect; NE¼ of SE¼ of sec. 14, T.9S., R.7W.	Quartz vein with chalcopyrite in Archean gneiss	45° 03' 02"	112° 25' 05"	AHK1256
8	Blacktail	005AV94	Elk Gulch	southern Ruby Range copper prospect; NE¼ of SE¼ of sec. 14, T.9S., R.7W.	Brecciated Archean gneiss with malachite and iron oxide minerals	45° 03' 02"	112° 25' 05"	AHK0045

Table 1.--Continued

Map key	Mining district	Sample number	Quadrangle (1:24,000 scale)	Location	Description	Latitude North	Longitude West	Analytical Job
9	Blacktail	005BV94*	Elk Gulch	southern Ruby Range copper prospect; NE¼ of SE¼ of sec. 14, T.9S., R.7W.	Replicate sample for 005AV94	45° 03' 02"	112° 25' 05"	AHK0045
10	Blacktail	006AV94	Elk Gulch	Elk Creek vermiculite deposit; SE¼ of SE¼ of sec. 2, T.9S., R.7W.	Altered, intensely folded biotite	45° 04' 31"	112° 25' 14"	AHK0047
11	Blacktail	006BV94	Elk Gulch	Elk Creek vermiculite deposit; SE¼ of SE¼ of sec. 2, T.9S., R.7W.	Altered, biotite-rich layer, perhaps containing vermiculite	45° 04' 31"	112° 25' 14"	AHK0047
12	Blacktail	006CV94	Elk Gulch	Elk Creek vermiculite deposit; SE¼ of SE¼ of sec. 2, T.9S., R.7W.	An ampibolite composed of coarse-grained hornblende.	45° 04' 31"	112° 25' 14"	AHK0047
13	Blacktail	006DV94	Elk Gulch	Elk Creek vermiculite deposit; SE¼ of SE¼ of sec. 2, T.9S., R.7W.	Light green amphibolite, consisting of mostly actinolite.	45° 04' 31"	112° 25' 14"	AHK0047
14	Blacktail	96BV01	Windy Hill	Reported placer site on West Fork Madison River; N½ of sec. 27, T.12S., R.2W.	White bull quartz boulder in dry, but seasonally active stream bed	44° 45' 37"	111° 50' 00"	AHK0045
15	Blacktail	96BV02	Windy Hill	Reported placer site on West Fork Madison River;N½ of sec. 27, T.12S., R.2W.	Olivine basalt boulder (Oligocene basalt of Landon Ridge described by Sonderegger and others, 1982)	44° 45' 37"	111° 50' 00"	AHK0045
16	Blacktail	96BV03	Windy Hill	Reported placer site on West Fork Madison River;N½ of sec. 27, T.12S., R.2W.	Stream sediment from dry, but seasonally active channel.	44° 45' 37"	111° 50' 00"	AHK0046
17	Cherry Creek	96BV10	Bucks Nest	Near Ruby (Johnny Gulch iron) mine; NW¼ and NE¼ of sec. 16, T.9S., R.1W.	Bull quartz lens from schistose banded iron formation. Lenses of bull quartz pinch and swell in thickness, but can be up 2 ft thick. Quartz lenses are concordant with the foliation in the schist.	45° 03' 24"	111° 43' 40"	AHK0045

Table 1.--Continued

Map key	Mining district	Sample number	Quadrangle (1:24,000 scale)	Location	Description	Latitude North	Longitude West	Analytical Job
18	Cherry Creek	96BV11	Bucks Nest	Ruby Creek upstream from reported Ruby Creek placer site; SW¼ of sec. 16, T.9S., R.1W.	Stream sediment from the active channel of Ruby Creek. Collected in a mid-stream bar behind a boulder.	45° 02' 43"	111° 44' 14"	AHK0046
19	Cherry Creek	96BV04	Bucks Nest	Ruby (Johnny Gulch iron) mine; SE¼ of SW¼ of sec. 9, T.9S., R.1W.	Magnetite-rich layers in schist	45° 03' 31"	111° 43' 50"	AHK0045
20	Cherry Creek	96BV05A	Bucks Nest	Ruby (Johnny Gulch iron) mine; SE¼ of SW¼ of sec. 9, T.9S., R.1W.	Magnetite layer of magnetite-quartzite banded iron formation	45° 03' 31"	111° 43' 50"	AHK0045
21	Cherry Creek	96BV05B	Bucks Nest	Ruby (Johnny Gulch iron) mine; SE¼ of SW¼ of sec. 9, T.9S., R.1W.	Bulk sample of magnetite-quartzite layering	45° 03' 31"	111° 43' 50"	AHK0045
22	Cherry Creek	96BV06A	Bucks Nest	Ruby (Johnny Gulch iron) mine; SE¼ of SW¼ of sec. 9, T.9S., R.1W.	Magnetite-free quartz vein discordant to micaceous schist	45° 03' 31"	111° 43' 50"	AHK0045
23	Cherry Creek	96BV06B*	Bucks Nest	Ruby (Johnny Gulch iron) mine; SE¼ of SW¼ of sec. 9, T.9S., R.1W.	Replicate of 96BV06A	45° 03' 31"	111° 43' 50"	AHK0045
24	Cherry Creek	96BV07	Bucks Nest	Ruby (Johnny Gulch iron) mine; SE¼ of SW¼ of sec. 9, T.9S., R.1W.	Sheared, hematitic quartzite	45° 03' 31"	111° 43' 50"	AHK0045
25	Cherry Creek	96BV08	Bucks Nest	Ruby (Johnny Gulch iron) mine; SE¼ of SW¼ of sec. 9, T.9S., R.1W.	Milky white bull quartz from mine dump	45° 03' 31"	111° 43' 50"	AHK0045
26	Cherry Creek	96BV09A	Bucks Nest	Trench 0.3 mi SW of Ruby mine; NW¼ of sec. 16, T.9S., R.1W.	Bulk sample of banded iron formation composed of thin bedded magnetite and quartzite	45° 03' 25"	111° 44' 05"	AHK0045
27	Cherry Creek	96BV09B*	Bucks Nest	Trench 0.3 mi SW of Ruby mine; NW¼ of sec. 16, T.9S., R.1W.	Replicate of 96BV09A	45° 03' 25"	111° 44' 05"	AHK0045

Table 1.--Continued

Map key	Mining district	Sample number	Quadrangle (1:24,000 scale)	Location	Description	Latitude North	Longitude West	Analytical Job
28	Cherry Creek	96BV12	Granite Mountain	Black Butte iron deposit (Granite Mountain area); NW¼ of sec. 9, T.11S., R.1W.	Magnetite-rich banded iron formation in float. This area was mapped by Wier (1965).	44° 53' 25"	111° 44' 19"	AHK0045
29	Chinatown	E9501	Jeff Davis Peak	Chinatown placer in Jeff Davis Creek; NW¼ of sec. 15, T.11S., R.13W.	"Cannonball" with magnetite crystals	44° 52' 59"	113° 10' 38"	AHK1241
30	Chinatown	E9502	Jeff Davis Peak	Chinatown placer in Jeff Davis Creek; NW¼ of sec. 15, T.11S., R.13W.	"Cannonball" with magnetite crystals	44° 52' 59"	113° 10' 38"	AHK1241
31	Chinatown	96JH51	Jeff Davis Peak	H & S Hand mine; NE¼ of SW¼ of sec. 9, T.11S., R.13W.	Gossan from the mine dump	44° 53' 22"	113° 11' 36"	AHK1787
32	Chinatown	96JH50	Jeff Davis Peak	Jeff Davis Creek upstream from Lucky Strike claim; NE¼ of SW¼ of sec. 9, T.11S., R.13W.	Stream sediment	44° 52' 57"	113° 09' 20"	AHK1787
33	Horse Prairie	95JH006	Coyote Creek	Jung Frau mine; SW¼ of SE¼ of sec. 32, T.9S.,R.14W.	Barite vein with tetrahedrite	45° 00' 14"	113° 20' 33"	AHK1256
34	Horse Prairie	95JH003	Coyote Creek	Monument mine; NW¼ of NE¼ of sec. 4, T.10S., R.14W.	Red gossan	45° 00' 01"	113° 19' 18"	AHK1256
35	Horse Prairie	95JH203*	Coyote Creek	Monument mine; NW¼ of NE¼ of sec. 4, T.10S., R.14W.	Replicate sample for 95JH003	45° 00' 01"	113° 19' 18"	AHK1256
36	Horse Prairie	95JH004	Coyote Creek	Monument mine; NW¼ of NE¼ of sec. 4, T.10S., R.14W.	White quartz with copper staining	45° 00' 01"	113° 19' 18"	AHK1256
37	Horse Prairie	96JH39	Dalys	Clark Canyon Reservior area; W½ of sec. 32, T.9S., R.10W.	Chert-rich silicified fault breccia associated with the Armstead thrust fault	45° 00' 30"	112° 51' 29"	AHK1787
38	Horse Prairie	96JH40	Dalys	Clark Canyon Reservior area; W½ of sec. 32, T.9S., R.10W.	Limonitic Beaverhead Conglomerate along small-scale joints near Armstead thrust fault.	45° 00' 28"	112° 51' 26"	AHK1787
39	Horse Prairie	96JH41	Dalys	Clark Canyon Reservior area; W½ of sec. 32, T.9S., R.10W.	Silica-rich fault breccia float - possible jasperoid	45° 00' 23"	112° 51' 31"	AHK1787

Table 1.--Continued

Map key	Mining district	Sample number	Quadrangle (1:24,000 scale)	Location	Description	Latitude North	Longitude West	Analytical Job
40	Horse Prairie	96JH43	Dalys	Clark Canyon Reservior area; W½ of sec. 32, T.9S., R.10W.	Jasperoid(?) - Silicified fault breccia associated with the Armstead thrust fault	45° 00' 14"	112° 51' 39"	AHK1787
41	Medicine Lodge	96JH44A	Garfield Canyon	Clark Canyon Reservior area; SE¼ of SE¼ of sec. 2, T.10S., R.11W.	Altered Archean gneiss below Flathead Sandstone. Gneiss in outcrop in roadcut is highly fractured and altered (chlorite and limonite staining).	44° 59' 16"	112° 54' 24"	AHK1787
42	Medicine Lodge	96JH45	Garfield Canyon	Clark Canyon Reservior area; along north bank of reservoir. NE¼ of NW¼ of sec. 12, T.10S., R.11W.	Highly fractured and limonite-stained leucocratic gneiss. The gneiss contains pods and interbeds of amphibolite.	44° 59' 11"	112° 53' 48"	AHK1787
43	Monida	96JH36	Monida	Centennial Valley - near south bank of Lima Reservior; NE¼ of NW¼ of sec. 22, T.14S., R.6W.	Soil sample from bank of small stream flowing from a spring	44° 36' 25"	112° 19' 20"	AHK1787
44	Pony	95JH021	Pony	Ben Harrison Fraction mine; SE¼ of NE¼ of sec. 21, T.2S., R.3W.	Freshest porphyry from dump nearest road	45° 38' 58"	111° 58' 13"	AHK1256
45	Pony	95JH022	Pony	Ben Harrison Fraction mine; SE¼ of NE¼ of sec. 21, T.2S., R.3W.	Partly altered porphyry at caved adit	45° 38' 58"	111° 58' 13"	AHK1256
46	Pony	95JH023	Pony	Ben Harrison Fraction mine; SE¼ of NE¼ of sec. 21, T.2S., R.3W.	Strongly altered green quartz-eye porphyry	45° 38' 58"	111° 58' 13"	AHK1256
47	Pony	95JH027	Pony	old adit near the Boss Tweed mine; SW¼ of NE¼ of sec.15, T.2S., R.3W.	Gossan - red and yellow varieties	46° 39' 55"	111° 57' 12"	AHK1256
48	Pony	95JH028	Pony	old adit near the Boss Tweed mine; SW¼ of NE¼ of sec.15, T.2S., R.3W.	Gneiss typical of the area	46° 39' 55"	111° 57' 12"	AHK1256

Table 1.--Continued

Map key	Mining district	Sample number	Quadrangle (1:24,000 scale)	Location	Description	Latitude North	Longitude West	Analytical Job
49	Pony	95JH019	Pony	Mountain Meadow claim; SE¼ of SE¼ of sec. 21, T.2S., R.3W.	Chlorite-sericite alteration of granodiorite	45° 38' 39"	111° 58' 10"	AHK1256
50	Pony	95JH020	Pony	Mountain Meadow claim; SE¼ of SE¼ of sec. 21, T.2S., R.3W.	Silicified granodiorite with pyrite, galena, and clay from mine dump	45° 38' 39"	111° 58' 10"	AHK1256
51	Pony	95JH025	Pony	Prospects in NE¼ of NW¼ of sec. 15, T.2S., R.3W.	Gossan	45° 40' 07"	111° 57' 28"	AHK1256
52	Pony	95JH026A	Pony	Prospects in NE¼ of NW¼ of sec. 15, T.2S., R.3W.	Banded gneiss with potassium-feldspar boudin	45° 40' 07"	111° 57' 28"	AHK1241
53	Red Bluff	95JH094	Norris	Adit 0.3 mi NW of Grubstake mine; NE¼ of SE¼ of sec. 19, T.3S., R.1 E.	Fault gouge	45° 33' 36"	111° 38' 39"	AHK1256
54	Red Bluff	95JH096	Norris	Golconda mine; SW¼ of NE¼ of sec. 19, T.3S., R.1E.	Brecciated quartz vein	45° 33' 43"	111° 38' 47"	AHK1256
55	Revenue	95JH083	Maltbys Mound	East Revenue mine - Majesty Mining Company operation; NE¼ of SE¼ of sec. 31, T.3S., R.1W.	High grade ore from pit wall	45° 31' 54"	111° 45' 59"	AHK1256
56	Revenue	95JH283*	Maltbys Mound	East Revenue mine - Majesty Mining Company operation; NE¼ of SE¼ of sec. 31, T.3S., R.1W.	Replicate sample for 95JH083	45° 31' 54"	111° 45' 59"	AHK1256
57	Revenue	95JH084	Maltbys Mound	East Revenue mine - Majesty Mining Company operation; NE¼ of SE¼ of sec. 31, T.3S., R.1W.	Quartz vein with open-space crystal growth	45° 31' 54"	111° 45' 59"	AHK1256
58	Revenue	E9509	Maltbys Mound	East Revenue mine - Majesty Mining Company operation; NE¼ of SE¼ of sec. 31, T.3S., R.1W.	Altered monzogranite with quartz veins	45° 31' 54"	111° 45' 59"	AHK1256
59	Revenue	E9508	Maltbys Mound	Galena mine; NE¼ of sec. 19, T.3S., R.1W.	Sulfide mineral-bearing quartz veins (limonite-stained)	45° 33' 49"	111° 46' 04"	AHK1256

Table 1.--Continued

Map key	Mining district	Sample number	Quadrangle (1:24,000 scale)	Location	Description	Latitude North	Longitude West	Analytical Job
60	Ruby Mountains	96JH30	Christensen Ranch	Carter Creek iron deposit; SW¼ of NW¼ of sec. 10, T.8S., R.7W.	Banded iron formation (see James and Wier, 1972; James, 1990)	45° 09' 18"	112° 27' 23"	AHK1787
61	Ruby Mountains	96JH26	Christensen Ranch	Outcrop on road to Carter Creek iron deposit at 6,070 ft; NW¼ of NE¼ of section 3, T.8S., R.7W.	Silicified, limonitic dolomite - "jasperoid"(?) (see James and Wier, 1972; James, 1990)	45° 10' 24"	112° 26' 45"	AHK1787
62	Sheridan	E9514	Copper Mountain	Banded iron formation on Copper Mountain (see James, 1981; James and Wier, 1962); NE¼ of SW¼ of sec. 1, T.5S., R.4W.	Bulk sample of banded iron formation	45° 25' 46"	112° 02' 35"	AHK1241
63	Sheridan	E9513	Copper Mountain	Copper mine at crest of Copper Mountain (trench); south-center of sec. 1, T.5S., R.4W.	Stained (copper- and iron-) quartzite	45° 25' 30"	112° 02' 20"	AHK1256
64	Sheridan	95JH110	Copper Mountain	Banded iron formation on Copper Mountain (see James, 1981; James and Wier, 1962); NE¼ of SW¼ of sec. 1, T.5S., R.4W.	Banded iron formation - massive magnetite	45° 25' 46"	112° 02' 35"	AHK1241
65	Sheridan	95JH113	Copper Mountain	Banded iron formation on Copper Mountain (see James, 1981; James and Wier, 1962); NE¼ of SW¼ of sec. 1, T.5S., R.4W.	Amphibole-rich iron ore	45° 25' 46"	112° 02' 35"	AHK1241
66	Silver Star	E9505	Silver Star	American pit; NW¼ of NW¼ of sec. 2, T.2S., R.6W.	Fine-grained garnet skarn with disseminated sulfide minerals	45° 41' 52"	112° 18' 48"	AHK1256
67	Silver Star	E9506	Silver Star	American pit; NW¼ of NW¼ of sec. 2, T.2S., R.6W.	Green, fine-grained epidote skarn	45° 41' 52"	112° 18' 48"	AHK1256
68	Silver Star	E9504	Silver Star	Keystone "Black pit"; NW¼ of NW¼ of sec. 2, T.2S., R.6W.	Massive hedenbergite	45° 41' 51"	112° 18' 57"	AHK1256

Table 1.--Continued

Map key	Mining district	Sample number	Quadrangle (1:24,000 scale)	Location	Description	Latitude North	Longitude West	Analytical Job
69	Silver Star	E9507	Silver Star	Mohawk mine (chromite); SE¼ of NW¼ of sec. 10, T.2S., R.6W.	Fine-grained chromite ore	45° 40' 45"	112° 19' 55"	AHK1241
70	Virginia City	E9520	Virginia City	Mapleton mine; NW¼ of SE¼ of sec. 9, T.6S., R.3W.	Limonitic quartz vein from ore bin (may contain tetrahedrite)	45° 19' 33"	111° 58' 21"	AHK1256
71	Virginia City	007AV94	Virginia City	Old adit in Browns Gulch; SW¼ of SW¼ of sec. 28, T.6S., R.3W.	Brecciated gneiss at vein deposit with quartz veins and iron oxide minerals	45° 16' 34"	111° 58' 59"	AHK0045
72	Virginia City	007BV94*	Virginia City	Old adit in Browns Gulch; SW¼ of SW¼ of sec. 28, T.6S., R.3W.	Replicate of sample 007AV94	45° 16' 34"	111° 58' 59"	AHK0045
73	Virginia City	95JH035	Virginia City	Old adit in Browns Gulch; SW¼ of SW¼ of sec. 28, T.6S., R.3W.	Quartz vein with sulfide minerals	45° 16' 34"	111° 58' 59"	AHK1256
74	Virginia City	95JH038	Virginia City	Old adit in Browns Gulch; SW¼ of SW¼ of sec. 28, T.6S., R.3W.	Quartz with pyrite, chalcopyrite, and tetrahedrite(?)	45° 16' 34"	111° 58' 59"	AHK1256
75	Virginia City	008AV94	Cirque Lake	Pacific mine; NW¼ of sec. 15, T.7S., R.3W.	Limonitic, sheared gneiss	45° 13' 46"	111° 57' 30"	AHK0045
76	Virginia City	008BV94	Cirque Lake	Pacific mine; NW¼ of sec. 15, T.7S., R.3W.	Limonitic, sheared gneiss	45° 13' 46"	111° 57' 30"	AHK0045
77	Virginia City	96JH67	Cirque Lake	Ultramafic rocks shown on Hadley's (1969) geologic map of the Varney 15' quadrangle; NE¼ of sec.10, T.7S., R.3W.	Ultramafic (olivine basalt?) rock	45° 14' 45"	111° 56' 57"	AHK1787
78	Virginia City	E9516	Virginia City	Bamboo Chief mine ore stockpile at Roy Moen's mill; SW¼ of sec. 27, T.6S., R.3W.	Siliceous gneiss "ore" with abundant iron oxide mineral staining	45° 16' 51"	111° 57' 39"	AHK1256
79	Virginia City	V9521A	Virginia City	Bamboo Chief mine ore stockpile at Roy Moen's mill; SW¼ of sec. 27, T.6S., R.3W.	Copper-stained, limonitic quartz-rich rock	45° 16' 51"	111° 57' 39"	AHK0045

Table 1.--Continued

Map key	Mining district	Sample number	Quadrangle (1:24,000 scale)	Location	Description	Latitude North	Longitude West	Analytical Job
80	Virginia City	V9521B	Virginia City	Bamboo Chief mine ore stockpile at Roy Moen's mill; SW¼ of sec. 27, T.6S., R.3W.	Oxidized ore - quartz vein with abundant iron oxide minerals	45° 16' 51"	111° 57' 39"	AHK0045
81	Virginia City	E9517	Virginia City	U.S. Grant mine ore stockpile from the lower adit; SW¼ of NW¼ of sec. 26, T.6S., R.3W.	Pyrite-rich quartz vein ore	45° 17' 02"	111° 56' 28"	AHK1256
82	Virginia City	V9522	Virginia City	U.S. Grant mine ore stockpile from the lower adit; SW¼ of NW¼ of sec. 26, T.6S., R.3W.	Quartz vein gossan with pyrite clot	45° 17' 02"	111° 56' 28"	AHK0045
83	Virginia City	95JH118A	Virginia City	Cornucopia mine; SE¼ of sec. 27, T.6S., R.3W.	Amphibolite, garnet-rich, iron oxide mineral stained	45° 16' 47"	111° 56' 44"	AHK1241
84	Virginia City	95JH119	Virginia City	Cornucopia mine; SE¼ of sec. 27, T.6S., R.3W.	Ore - quartz vein with pyrite	45° 16' 47"	111° 56' 44"	AHK1241
85	Virginia City	95JH120	Virginia City	Cornucopia mine; SE¼ of sec. 27, T.6S., R.3W.	Red gossan	45° 16' 47"	111° 56' 44"	AHK1241
86	Virginia City	E9518	Virginia City	Cornucopia mine; SE¼ of sec. 27, T.6S., R.3W.	Iron oxide mineral-stained quartz vein with clots of pyrite	45° 16' 47"	111° 56' 44"	AHK1256
87	Virginia City	009V94	Virginia City	Cornucopia mine; SE¼ of sec. 27, T.6S., R.3W.	Iron oxide mineral-stained quartz vein with clots of pyrite	45° 16' 47"	111° 56' 44"	AHK0045
88	Virginia City	96JH57	Virginia City	Adit in Hungry Hollow Gulch; NE¼ of SE¼ of sec. 2, T.7S., R.3W.	Quartz vein ore (brecciated, vuggy, iron oxide mineral-stained) at adit driven in Archean gneiss	45° 15' 14"	111° 55' 33"	AHK1787
89	Virginia City	96JH58	Virginia City	Adit in Hungry Hollow Gulch; NE¼ of SE¼ of sec. 2, T.7S., R.3W.	Archean gneiss country rock with brown carbonate veinlets. Gneiss is interlayered with amphibolite in the outcrop.	45° 15' 14"	111° 55' 33"	AHK1787
90	Virginia City	96JH60	Cirque Lake	Black Hawk mine; NW¼ of sec. 11, T.7S., R.3W.	Chloritized basalt(?) dike	45° 14' 36"	111° 56' 29"	AHK1787
91	Virginia City	96JH62	Cirque Lake	Mined area in High Up - Irene vein system; NE¼ of sec. 15, T.7S., R.3W.	Gneiss with sulfide mineral-bearing quartz veins	45° 13' 38"	111° 56' 58"	AHK1787

Table 1.--Continued.

Map key	Mining district	Sample number	Quadrangle (1:24,000 scale)	Location	Description	Latitude North	Longitude West	Analytical Job
92	Virginia City	96JH63	Cirque Lake	Mined area in High Up - Irene vein system; NE¼ of sec. 15, T.7S., R.3W.	Stream sediment sample	45° 13' 38"	111° 56' 58"	AHK1787
93	Virginia City	96JH21	Cirque Lake	Bartlett mine - upper adit; NW¼ of NE¼ of sec. 14, T.7S., R.3W.	Massive dolomite	45° 13' 46"	111° 55' 51"	AHK1787
94	Virginia City	96JH23	Cirque Lake	Bartlett mine - upper adit; NW¼ of NE¼ of sec. 14, T.7S., R.3W.	Magnetite-bearing quartz-carbonate rock	45° 13' 46"	111° 55' 51"	AHK1787
95	Virginia City	96JH24	Cirque Lake	Bartlett mine - upper adit; NW¼ of NE¼ of sec. 14, T.7S., R.3W.	Gossan float from dump at main adit	45° 13' 46"	111° 55' 51"	AHK1787
96	Virginia City	95JH055A	Cirque Lake	Millard tunnel - 0.8 mi N-NE of Kearsarge mine; NW¼ of SE¼ of sec. 14, T.7S., R.3W.	Quartz-sulfide "ore"	45° 13' 25"	111° 55' 43"	AHK1241
97	Virginia City	012V94	Cirque Lake	Shaft & prospects east of Kearsarge mine; NW¼ of NW¼ of sec. 24, T.7S., R.3W.	Highly fractured, limonitic potassium feldspar-rich gneiss from dump pile	45° 13' 00"	111° 55' 07"	AHK0045
98	Virginia City	96JH05	Cirque Lake	From bank of Butcher Gulch at 7,460 ft elevation; SE¼ of sec. 7, T.7S., R.2W.	Stream sediment from bank about 20 ft above the flowing stream	45° 14' 08"	111° 53' 22"	AHK1787
99	Virginia City	96JH03	Cirque Lake	In Butcher Gulch at 7,420 ft elevation; SW¼ of SE¼ of sec. 7, T.7S., R.2W.	Stream sediment from active stream bed	45° 14' 00"	111° 53' 31"	AHK1787
100	Virginia City	96JH04	Cirque Lake	In Butcher Gulch at 7,440 ft elevation; SE¼ of sec. 7, T.7S., R.2W.	Stream sedment from active stream bed (upstream from 96JH03)	45° 14' 08"	111° 53' 24"	AHK1787

METHODS

All samples were submitted to ACTLABS, Inc. of Wheat Ridge, CO for sample preparation and analysis. Samples weighing approximately 1 kilogram were crushed with mild steel to avoid contamination with chromium, mechanically split, and pulverized to pass a 150 mesh screen. Analytical techniques utilized for each job are summarized in table 2, along with detection limits for each element. Techniques included multielement instrumental neutron activation (INAA), acid digestion followed by inductively coupled plasma emission spectrometry (ICP), hydride ICP analysis for selected elements (Bi, Ge, Se, Te), x-ray fluorescence (XRF), and lead fire assay inductively coupled plasma - mass spectrometry (ICP/MS) for platinum-group element determination. For most samples, multielement analytical packages were selected that are suitable for gold and base metal exploration, supplemented with special analytical techniques for elements of particular interest, such as tellurium. In addition to the multielement data, complete rock analyses, including major element oxides, were obtained to characterize several samples of mafic and ultramafic rocks.

Table 2. Summary of analytical techniques and detection limits.

A. Analytical techniques for each batch of samples.

Job number	Analytical techniques (Methods refer to ACTLABS, Inc. Protocols)
AHK0045	Method 1H: 48-element combination technique using INAA and 4-acid total digest ICP (See table 2B for elements included and detection limits) Method 1I: Hydride ICP for Bi, Ge, Se, and Te
AHK0046	Method 1H: 48-element combination technique using INAA and 4-acid total digest ICP (See table 2B for elements included and detection limits) Method 1I: Hydride ICP for Bi, Ge, Se, and Te
AHK0047	Method 4E: 49 element total identification package uses ICP, ICP/MS, INAA, and XRF for major element oxides, minor and trace elements including rare earth and actinide elements (See table 2B for elements included and detection limits) Method 1C (PGM option): lead fire assay ICP-ICP/MS analysis for Au, Pt, Pd, Rh, and Ir
AHK1241	Method 1D: 35-element INAA package (See table 2B for elements included and detection limits) Method 1C (PGM option): lead fire assay ICP-ICP/MS analysis for Au, Pt, Pd, Rh, and Ir
AHK1255	Method 4E: 49 element total identification package uses ICP, ICP/MS, INAA, and XRF for major element oxides, minor and trace elements including rare earth and actinide elements (See table 2B for elements included and detection limits) Method 1C (PGM option): lead fire assay ICP-ICP/MS analysis for Au, Pt, Pd, Rh, and Ir Method 1I: Hydride ICP for Bi, Ge, Se, and Te
AHK1256	Method 1D: 35-element INAA package (See table 2B for elements included and detection limits) Method 1I: Hydride ICP for Bi, Ge, Se, and Te
AHK1787	Method 1H: 48-element combination technique using INAA and 4-acid total digest ICP (See table 2B for elements included and detection limits) Method 1I: Hydride ICP for Bi, Ge, Se, and Te For sample 96JH67 only: Method 4E: 49 element total identification package uses ICP, ICP/MS, INAA, and XRF for major element oxides, minor and trace elements including rare earth and actinide elements (See table 2B for elements included and detection limits) Method 1C (PGM option): lead fire assay ICP-ICP/MS analysis for Au, Pt, Pd, Rh, and Ir

Table 2.--Continued.

B. Detection limits for each analytical method [ppb = parts per billion; ppm = parts per million].

Method 1D—35-element INAA package

Au	5 ppb	Hf	1 ppm	Se	5 ppm
Ag	5 ppm	Hg	1 ppm	Sr	0.05%
As	2 ppm	Ir	5 ppb	Sm	0.1 ppm
Ba	100 ppm	La	1 ppm	Sn	0.01%
Br	1 ppm	Lu	0.05 ppm	Ta	1 ppm
Ca	1%	Mo	5 ppm	Th	0.5 ppm
Ce	3 ppm	Na	0.05%	Tb	0.5 ppm
Co	5 ppm	Nd	5 ppm	U	0.5 ppm
Cr	10 ppm	Ni	50 ppm	W	4 ppm
Cs	2 ppm	Rb	30 ppm	Yb	0.2 ppm
Eu	0.2 ppm	Sb	0.2 ppm	Zn	50 ppm
Fe	0.02%	Sc	0.1 ppm		

Method 1C—Lead Fire Assay - ICP - ICP/MS

Au	1 ppb
Pt	0.1 ppb
Pd	0.1 ppb
Rh	0.1 ppb
Ir	0.1 ppb

Method 1H—4 acid total digestion ICP technique

Ag	0.5 ppm	K	0.01%	Pb	5 ppm
Al	0.01%	Mg	0.01%	Sr	1 ppm
Be	2 ppm	Mn	1 ppm	Ti	0.01%
Bi	5 ppm	Mo	2 ppm	V	2 ppm
Ca	0.01%	Ni	1 ppm	Y	2 ppm
Cd	0.5 ppm	P	0.001%	Zn	1 ppm
Cu	1 ppm				

Table 2.--Continued.

B. Detection limits for each analytical method, continued [ppb = parts per billion; ppm = parts per million].

Method 1H—INAA technique

Au	2 ppb	Hf	1 ppm	Se	3 ppm
As	0.5 ppm	Hg	1 ppm	Sm	0.1 ppm
Ba	50 ppm	Ir	5 ppb	Sn	0.01%
Br	0.5 ppm	La	0.5 ppm	Ta	0.5 ppm
Ce	3 ppm	Lu	0.05 ppm	Th	0.2 ppm
Co	1 ppm	Na	0.01%	Tb	0.5 ppm
Cr	5 ppm	Nd	5 ppm	U	0.5 ppm
Cs	1 ppm	Rb	5 ppm	W	1 ppm
Eu	0.2 ppm	Sb	0.1 ppm	Yb	0.2 ppm
Fe	0.01%	Sc	0.1 ppm		

Method 1I—Hydride ICP technique

Bi	0.2 ppm
Ge	0.2 ppm
Se	0.2 ppm
Te	0.2 ppm

Method 4F—Other whole rock analyses (completed on samples 95JH101 and 95JH102 in analytical job AHK1255).

Element-oxide	Detection Limit	Analytical technique
FeO	0.1%	Titration
S	0.01%	Leco
SO_4	0.01%	Leco
Cl	0.01%	INAA
CO_2	0.01%	Leco
H_2O+, H_2O-	0.1%	Gravimetric

Table 2.–Continued.

B. Detection limits for each analytical method, continued [ppb = parts per billion; ppm = parts per million].

Method 4E—49-element total identification package using ICP, INAA, ICP/MS, and XRF

Ag	0.5 ppm	MgO	0.01%
Al_2O_3	0.01%	MnO	0.01%
As	1 ppm	Mo	2 ppm
Au	1 ppb	Na_2O	0.01%
B	0.5 ppm	Ni	1 ppm
Ba	1 ppm	P_2O_5	0.01%
Be	2 ppm	Pb	5 ppm
Bi	5 ppm	Rb	10 ppm
Br	0.5 ppm	Sb	0.1 ppm
CaO	0.01%	Se	0.5 ppm
Cd	0.5 ppm	SiO_2	0.01%
Co	0.1 ppm	Sr	1 ppm
Cr	0.5 ppm	Ta	0.3 ppm
Cs	0.2 ppm	TiO_2	0.01%
Cu	1 ppm	V	1 ppm
Fe_2O_3	0.01%	W	1 ppm
Hf	0.2 ppm	Y	1 ppm
Ir	1 ppb	Zn	1 ppm
K_2O	0.01%	Zr	1 ppm

RARE EARTH AND ACTINIDE ELEMENTS

Sc	0.01 ppm	Tb	0.1 ppm
La	0.1 ppm	Yb	0.05 ppm
Ce	1 ppm	Lu	0.01 ppm
Nd	1 ppm	U	0.1 ppm
Sm	0.01 ppm	Th	0.1 ppm
Eu	0.05 ppm		

DATA

Results are tabulated by mining districts in tables 3 - 16, and a brief discussion of samples and results by district accompanies the tables. The regional metallogenic, petrogenetic, and(or) environmental significance of these data is discussed in a summary section following the discussion of mining districts.

Elements are listed in alphabetical order in the data tables. Some elements appear more than once in the listing because they were analyzed by different techniques. For example, some analytical jobs included silver (Ag) by ICP, whereas other jobs included silver by INAA; these data are reported separately because different techniques have different detection limits (see table 2, part b). Data for precious and base metals are highlighted to make the tables easier to read.

Stream sediment data included in this report were collected to fill in some areas that were not covered in the systematic stream sediment surveys conducted for the National Uranium Resource Evaluation (NURE) studies of the 1980's (Bolivar, 1980; Shannon, 1980). All of these data are being evaluated as part of the ongoing assessment of the Dillon Resource Area. The thresholds (highest background concentrations) for the Dillon area are not yet available; however, a threshold gold concentration of 50 ppb (parts per billion) was used to determine anomalous gold concentrations in stream sediments of the Gallatin National Forest (Carlson and Lee, in prep.) and this may be a reasonable threshold value to consider for the stream sediment data in this report.

We have included all of the data as reported from the laboratory. However, we offer the users of these data a caveat about the tungsten data. Tungsten was acquired by INAA in all cases. Jobs AHK0045 and AHK1787 used the laboratory method 1H, which has a detection level of 1 ppm (parts per million) for tungsten, and jobs AHK1241 and AHK1256 used method 1D, which has a detection level of 4 ppm. Plots of data for tantalum versus tungsten and for cobalt versus tungsten were examined to test for contamination from tungsten carbide materials that might have been used inadvertently in sample preparation for some jobs. These plots are inconclusive, but do show that most samples analyzed by method 1D have higher reported tungsten concentrations than those analyzed by method 1H. Although there could be real variation present in the samples in this study, discrepancies in samples from the same site lead us to suspect that there may be a problem with the data for this element. For example, in table 16A, samples 84-87 are all from a dump from the same orebody. The analyses for samples 84 and 86 (analyzed by method 1D) reported 550 and 880 ppm tungsten whereas similar sample 87 (analyzed by method 1H) had <1 ppm tungsten.

Big Muddy mining district (Table 3)

Two samples near Dell, along the eastern edge of the Big Muddy mining district were analyzed to determine precious metal values for background information from samples of Red Butte conglomerate (Haley and Perry, 1991). Both samples (table 3, map key 1 and 2) are below detection limits for gold and silver.

Table 3. Analytical data for stream sediment and rock samples from the Big Muddy mining district.
[See text for explanation of methods]

Map key			1	2
Sample number			96JH34	96JH35
Job number			AHK1787	AHK1787
Element	Units	Method		
Ag	ppm	ICP	<0.4	<0.4
Ag	ppm	INAA	<5	<5
Al	%	ICP	1.03	0.88
As	ppm	INAA	6.3	7.7
Au	ppb	INAA	<2	<2
Ba	ppm	INAA	210	150
Be	ppm	ICP	<2	<2
Bi	ppm	ICP-HY	<1	<1
Bi	ppm	ICP	<5	<5
Br	ppm	INAA	1.6	1
Ca	%	ICP	17.12	22.52
Ca	%	INAA	19	23
Cd	ppm	ICP	<0.5	<0.5
Ce	ppm	INAA	20	15
Co	ppm	INAA	2	1
Cr	ppm	INAA	16	15
Cs	ppm	INAA	<1	<1
Cu	ppm	ICP	2	2
Eu	ppm	INAA	0.4	0.3
Fe	%	INAA	0.58	0.51
Ge	ppm	ICP-HY	<0.2	<0.2
Hf	ppm	INAA	3	2
Hg	ppm	INAA	<1	<1
Ir	ppb	INAA	<5	<5
K	%	ICP	0.55	0.46
La	ppm	INAA	10	8.4
Lu	ppm	INAA	0.16	<0.05
Mg	%	ICP	1.07	1.33
Mn	ppm	ICP	303	211
Mo	ppm	ICP	<2	<2
Mo	ppm	INAA	2	3
Na	%	INAA	0.07	0.03
Nd	ppm	INAA	8	9
Ni	ppm	ICP	5	3
Ni	ppm	INAA	<20	<20

Table 3.--Continued.

Map key			1	2
P	%	ICP	0.023	0.023
Pb	ppm	ICP	27	<5
Rb	ppm	INAA	16	<15
Sb	ppm	INAA	0.4	0.3
Sc	ppm	INAA	1.5	1.3
Se	ppm	ICP-HY	<0.2	0.3
Se	ppm	INAA	<3	<3
Sm	ppm	INAA	1.5	1.2
Sn	%	INAA	<0.01	<0.01
Sr	ppm	ICP	169	162
Sr	%	INAA	<0.05	<0.05
Ta	ppm	INAA	<0.5	<0.5
Tb	ppm	INAA	<0.5	<0.5
Te	ppm	ICP-HY	<0.2	<0.2
Th	ppm	INAA	2.5	2
Ti	%	ICP	0.05	0.04
U	ppm	INAA	1.3	1.5
V	ppm	ICP	14	15
W	ppm	INAA	<1	<1
Y	ppm	ICP	12	12
Yb	ppm	INAA	1.1	0.9
Zn	ppm	ICP	14	18
Zn	ppm	INAA	<50	<50

Blacktail mining district (Table 4)

Samples from the Blacktail mining district (fig. 3, table 1, table 4, map key 3 to 16) include unmineralized Archean gneiss associated with green quartzite in the Snowcrest Range, rocks associated with the Elk Creek vermiculite deposit and copper prospects in the Ruby Range, and sediments from reported placer sites for which no production data are available.

There are a number of small, mafic to ultramafic bodies of apparent Archean age that intrude Archean rocks of the Ruby Range metamorphic complex (Desmarais, 1978, 1981) in the Dillon Resource Area. The nature of these bodies is uncertain because of their complex metamorphic history. They may have been emplaced as igneous intrusions, or they may have been emplaced as cold ultramafic bodies during tectonism (Desmarais, 1981). Compositionally, the bodies include locally serpentinized metaperidotite (harzburgite) and metapyroxenite; the bodies tend to be aligned parallel to the regional metamorphic foliation (Garihan, 1979). Multiple phases of ultramafic rocks have been described for the Ruby Range bodies, and primary cumulate textures may have been obscured by metamorphism; however, they do not appear to represent dismembered stratiform ultramafic complexes and are probably more akin to gabbroic bodies, which can contain economic concentrations of nickel, copper, cobalt and(or) precious metals including PGE (platinum group elements) (Page, 1986). The Ruby Range bodies have been prospected for nickel and copper (Sinkler, 1942; Geach, 1972) and the contact zones have been explored for vermiculite (Berg, 1995).

Fourteen samples (includes two replicates) from the Blacktail mining district were analyzed. Gold is detected in all samples of Archean gneiss associated with reported copper prospects (fig. 3, table 4, map key 3, 7, and 8) in concentrations ranging from 8 to 262 ppb. Silver values for these same samples range from below detection limits to 20 ppm. Analysis of map key 9 is a replicate of analysis 8. Agreement between the two analyses is excellent for some elements; however, concentrations of metals of economic interest, such as gold and silver, are variable and may reflect sample heterogeneity.

Ultramafic rocks, amphibolite, and biotite gneiss from the area of the Elk Creek vermiculite deposit were sampled to acquire complete major element chemical analysis, as well as metals and platinum-group elements (fig. 3, tables 1 and 4B, map key 4-6, 10-13). The area of the vermiculite deposits was mapped and sampled by Berg (1995) and studied by Desmarais (1978, 1981). Locally, some of the rocks contain annabergite, a hydrated nickel arsenate mineral. This is the nickel mineral that constitutes the "ore" at the Dillon nickel prospect (Sinkler, 1942). Berg (1995) reported gold, platinum, and palladium values for four samples of ultramafic rocks from the area of the Elk Creek vermiculite deposit. Our samples 95JH101 and 95JH102 (fig. 3, tables 1 and 4B, map key 4 and 5) are from the same general area as Berg's chip sample of outcrop on the west side of the mill (Berg sample EC-466). Sample 95JH202 (tables 1 and 4A, map key 6) is a replicate sample for 95JH102 (for trace elements only). These rocks are part of the fault-bounded Wolf Creek pluton, a N55E-trending weathered peridotite body, described by Sinkler (1942) and Heinrich (1949, 1960). Heinrich (1960) interpreted the numerous, small ultramafic bodies in the area as one intrusion, cut by faults. Both Berg (1995) and Desmarais (1978) interpret the bodies as individual bodies that were emplaced before Precambrian folding, although the nature of the emplacement (tectonic emplacement of serpentinite or magmatic intrusion) is uncertain. The vermiculite deposit formed from weathering of biotite in quartzofeldspathic gneiss at the contact of the ultramafic bodies, where a biotite schist (tables 1 and 4B, map key 10 and 11) developed from a metasomatic reaction during regional metamorphism (Desmarais, 1978). Where the ultramafic rock is in contact with amphibolite (tables 1 and 4B, map key 12 and 13), the biotite schist is absent (Berg, 1995; Desmarais, 1978).

Major-element analyses (table 4B) for the two samples from the ultramafic peridotite body total about 100% and are somewhat less magnesian than average peridotite. Samples 95JH101 and 95JH102 are more siliceous, more aluminous, and less magnesian than "average" peridotite (Nockolds, 1954). Chromium concentrations are typical (about 2,000 ppm Cr) for ultramafic rocks, and nickel concentrations are relatively low (<1,000 ppm) for rocks of ultramafic composition (Hawkes and Webb, 1962). Major element totals for biotite schist and amphibolite (table 4B, map key 10-13) are low (74 to 87 weight percent), indicating the hydrous nature of the mineral assemblages. Sample 006BV94 (table 4B, map key 11) approximates an altered biotite in composition with over 5 weight percent K_2O. Similarly, sample 006CV94 (table 4B, map key 12) approximates an amphibole in composition. These analyses reflect the nearly monomineralic nature of the metasomatic zones that developed at the ultramafic contact.

Chromium and nickel are erratically distributed in these zones, but remain elevated (hundreds to thousands of ppm).

Copper, cobalt, and other base metals are negligible. Precious metals are variable: gold is present at the 1 to 108 ppb level in both the ultramafic rocks and the metasomatic zones. Gold concentrations determined by INAA are consistently elevated relative to gold done by ICP/MS. We have no a priori reason to reject the higher values, but users of these data should be aware of these discrepancies, which may reflect systematic lab error, nugget effects, or sample contamination. A replicate sample of 95JH102 (table 4B, map key 5) was analyzed in a separate job (table 4A, map key 6) and the concentrations of gold by INAA (<2 ppb) and gold by ICP/MS are comparable to the values reported for 95JH102 (4 and 1 ppb, respectively). PGE values for the sample and replicate agree very well; individual PGE concentrations are below 14 ppb, and Pt>Pd for all samples.

Table 4. Analytical data for rock and stream sediment samples from the Blacktail mining district.
A. Partial multielement data.
[See text for explanation of methods; n.d., not determined; *, replicate sample]

Map key			3	6	7	8	9	14
Sample number			96JH77	95JH202*	E9512	005AV94	005BV94*	96BV01
Job number			AHK1787	AHK1241	AHK1256	AHK0045	AHK0045	AHK0045
Element	Units	Method						
Ag	ppm	ICP	<0.4	n.d.	n.d.	9.9	19.6	<0.4
Ag	ppm	INAA	<5	<5	9	10	20	<5
Al	%	ICP	7.68	n.d.	n.d.	5.29	4.05	0.02
As	ppm	INAA	<0.5	2.0	7.2	38	78	0.6
Au	ppb	ICP/MS	n.d.	2	n.d.	n.d.	n.d.	n.d.
Au	ppb	INAA	8	<2	54	262	138	4
Ba	ppm	INAA	540	<50	440	230	490	<50
Be	ppm	ICP	<2	n.d.	n.d.	<2	<2	<2
Bi	ppm	ICP-HY	<0.2	n.d.	1.3	1	1	<0.2
Bi	ppm	ICP	<5	n.d.	n.d.	<5	6	<5
Br	ppm	INAA	<0.5	<0.5	17	8	8.4	<0.5
Ca	%	ICP	0.56	n.d.	n.d.	2.3	2.07	0.01
Ca	%	INAA	<1	4	<1	3	2	<1
Cd	ppm	ICP	<0.5	n.d.	n.d.	<0.5	0.8	<0.5
Ce	ppm	INAA	48	11	4	25	24	<3
Co	ppm	INAA	5	96	240	150	160	<1
Cr	ppm	INAA	11	4000	<5	15	28	20
Cs	ppm	INAA	<1	<1	<1	<1	<1	<1
Cu	ppm	ICP	89	n.d.	n.d.	95,343	99,999	9
Eu	ppm	INAA	0.6	<0.2	<0.2	1.3	1.5	<0.2
Fe	%	INAA	1.56	7.6	3.34	6.39	9.02	0.34
Ge	ppm	ICP-HY	<0.2	n.d.	<0.2	<0.2	<0.2	<0.2
Hf	ppm	INAA	4	1	<1	2	2	<1
Hg	ppm	INAA	<1	<1	<1	<1	<1	<1
Ir	ppb	ICP/MS	n.d.	9.1	n.d.	n.d.	n.d.	n.d.
Ir	ppb	INAA	<5	<5	<5	<5	<5	<5
K	%	ICP	1.26	n.d.	n.d.	0.4	0.29	0.01
La	ppm	INAA	27	5.5	1.9	28	32	<0.5
Lu	ppm	INAA	0.05	0.15	<0.05	0.28	0.31	<0.05
Mg	%	ICP	0.98	n.d.	n.d.	0.72	0.68	0.04
Mn	ppm	ICP	185	n.d.	n.d.	206	197	26
Mo	ppm	ICP	<2	n.d.	n.d.	<2	2	<2
Mo	ppm	INAA	<1	<1	6	<1	<1	<1
Na	%	INAA	4.33	0.15	0.02	2.6	1.45	<0.01
Nd	ppm	INAA	11	<5	<5	16	13	<5
Ni	ppm	ICP	5	n.d.	n.d.	153	170	5
Ni	ppm	INAA	180	1000	92	130	100	<20

Table 4.--Continued

Map key			3	6	7	8	9	14
P	%	ICP	0.037	n.d.	n.d.	0.026	0.026	0.002
Pb	ppm	ICP	8	n.d.	n.d.	6	10	<5
Pd	ppb	ICP/MS	n.d.	2.6	n.d.	n.d.	n.d.	n.d.
Pt	ppb	ICP/MS	n.d.	13.4	n.d.	n.d.	n.d.	n.d.
Rb	ppm	INAA	<15	<15	<15	40	<15	<15
Rh	ppb	ICP/MS	n.d.	2.1	n.d.	n.d.	n.d.	n.d.
Sb	ppm	INAA	<0.1	0.1	0.2	1.3	2.2	0.1
Sc	ppm	INAA	3.7	16.0	0.2	5.4	4.5	0.1
Se	ppm	ICP-HY	<0.2	n.d.	4.8	16.3	31.5	<0.2
Se	ppm	INAA	<3	<3	<3	11	30	<3
Sm	ppm	INAA	1.9	0.9	0.1	2.6	2.6	<0.1
Sn	%	INAA	<0.01	<0.01	<100	<0.02	<0.02	<0.01
Sr	ppm	ICP	189	n.d.	n.d.	356	302	2
Sr	%	INAA	<0.05	<0.05	<0.05	<0.05	<0.05	<0.05
Ta	ppm	INAA	<0.5	<0.5	1.3	<0.5	<0.5	<0.5
Tb	ppm	INAA	0.6	<0.5	<0.5	<0.5	<0.5	<0.5
Te	ppm	ICP-HY	0.2	n.d.	1.6	0.5	0.8	0.2
Th	ppm	INAA	5.3	2.3	<0.5	0.9	1.4	<0.2
Ti	%	ICP	0.14	n.d.	n.d.	0.14	0.11	0.01
U	ppm	INAA	<0.5	<0.5	3	27	53	<0.5
V	ppm	ICP	21	n.d.	n.d.	275	538	2
W	ppm	INAA	<1	36	760	<1	<1	<1
Y	ppm	ICP	5	n.d.	n.d.	18	22	2
Yb	ppm	INAA	<0.2	0.9	<0.2	1.3	1.6	<0.2
Zn	ppm	ICP	23	n.d.	n.d.	94	101	6
Zn	ppm	INAA	94	94	<50	71	108	<50

Table 4.--Continued

Map key			15	16
Sample number			96BV02	96BV03
Job number			AHK0045	AHK0046
Element	Units	Method		
Ag	ppm	ICP	<0.4	<0.4
Ag	ppm	INAA	<5	<5
Al	%	ICP	7.13	3.97
As	ppm	INAA	<0.5	8.9
Au	ppb	INAA	12	<2
Ba	ppm	INAA	1200	1300
Be	ppm	ICP	<2	<2
Bi	ppm	ICP-HY	0.3	<0.2
Bi	ppm	ICP	<5	<5
Br	ppm	INAA	<0.5	1.9
Ca	%	ICP	5.22	4.13
Ca	%	INAA	5	5
Cd	ppm	ICP	<0.5	<0.5
Ce	ppm	INAA	36	59
Co	ppm	INAA	29	7
Cr	ppm	INAA	380	55
Cs	ppm	INAA	1	3
Cu	ppm	ICP	62	15
Eu	ppm	INAA	1.2	1.4
Fe	%	INAA	5.69	2.3
Ge	ppm	ICP-HY	0.2	<0.2
Hf	ppm	INAA	3	12
Hg	ppm	INAA	<1	<1
Ir	ppb	INAA	<5	<5
K	%	ICP	2.07	1.56
La	ppm	INAA	24	28
Lu	ppm	INAA	0.3	0.5
Mg	%	ICP	3.78	1.87
Mn	ppm	ICP	1027	1476
Mo	ppm	ICP	<2	<2
Mo	ppm	INAA	<1	2
Na	%	INAA	2.04	0.36
Nd	ppm	INAA	15	26
Ni	ppm	ICP	82	21
Ni	ppm	INAA	<22	<20
P	%	ICP	0.137	0.163
Pb	ppm	ICP	14	17
Rb	ppm	INAA	93	57
Sb	ppm	INAA	0.2	0.6

Table 4.--Continued

Map key			15	16
Sc	ppm	INAA	20	6.8
Se	ppm	ICP-HY	0.7	0.2
Se	ppm	INAA	<3	<3
Sm	ppm	INAA	3.5	4.8
Sn	%	INAA	<0.02	<0.01
Sr	ppm	ICP	521	113
Sr	%	INAA	<0.05	<0.05
Ta	ppm	INAA	<0.5	<0.5
Tb	ppm	INAA	0.5	0.9
Te	ppm	ICP-HY	0.4	<0.2
Th	ppm	INAA	4	8.9
Ti	%	ICP	0.40	0.21
U	ppm	INAA	1.5	3.2
V	ppm	ICP	159	52
W	ppm	INAA	<1	<1
Y	ppm	ICP	19	22
Yb	ppm	INAA	1.8	3.3
Zn	ppm	ICP	86	59
Zn	ppm	INAA	56	102

Table 4. Analytical data for rock samples from the Blacktail mining district.
B.Complete chemical analyses for mafic and ultramafic rocks.
[n.d., not determined; total iron reported as Fe_2O_3 for entries 10-13]

Major elements, in weight per cent						
Map key	**4**	**5**	**10**	**11**	**12**	**13**
Sample number	**95JH101**	**95JH102**	**006AV94**	**006BV94**	**006CV94**	**006DV94**
Job number	AHK1255	AHK1255	AHK0047	AHK0047	AHK0047	AHK0047
SiO_2	48.07	51.7	50.34	40.25	41.25	56.52
Al_2O_3	10.42	5.05	5.54	11.98	15.43	2.09
Fe_2O_3	10.13	11.32	11.42	12.25	15.8	9.19
FeO	7.1	7.9	n.d.	n.d.	n.d.	n.d.
MnO	0.17	0.16	0.102	0.081	0.221	0.152
MgO	23.02	26.72	3.54	9.12	1.53	8.77
CaO	5.62	3.42	2.84	0.42	10.57	0.8
Na_2O	0.67	0.15	0.12	0.37	1.64	0.1
K_2O	0.14	0.06	0.04	5.55	0.51	<0.01
TiO_2	0.35	0.26	0.11	1.25	1.44	0.03
P_2O_5	0.03	0.05	0.02	0.05	0.11	0.02
LOI	0.84	0.64	n.d.	n.d.	n.d.	n.d.
TOTAL	99.5	99.5	74.1	81.3	87.3	77.7
S	<0.003	<0.003	n.d.	n.d.	n.d.	n.d.
H_2O	0.05	0.37	n.d.	n.d.	n.d.	n.d.
CO_2	<0.003	0.051	n.d.	n.d.	n.d.	n.d.

Table 4.-- Continued

Minor and trace elements								
Map key			4	5	10	11	12	13
Sample number			95JH101	95JH102	006AV94	006BV94	006CV94	006DV94
Element	Units	Method						
Ag	ppm	ICP	<0.5	<0.5	<0.4	<0.4	0.5	<0.4
As	ppm	INAA	2	3	2	2	2	2
Au	ppb	INAA	108	4	2	23	9	4
Au	ppb	ICP/MS	1	1	1	10	3	1
Ba	ppm	INAA	219	15	42	2005	153	6
Be	ppm	ICP	1	<1	<1	<1	3	<1
Bi	ppm	ICP	<5	<5	<5	<5	<5	<5
Bi	ppm	ICP-HY	<0.2	<0.2	n.d.	n.d.	n.d.	n.d.
Br	ppm	INAA	1	<1	<1	<1	<1	<1
Cd	ppm	ICP	1	1	<0.5	<0.5	0.7	<0.5
Ce	ppm	INAA	26	11	6	332	22	4
Co	ppm	INAA	85	93	47	64	66	89
Cr	ppm	INAA	2260	3340	901	1160	331	3660
Cs	ppm	INAA	<0.2	<0.2	0.3	18.4	<0.2	0.4
Cu	ppm	ICP	11	99	2	3	8	2
Eu	ppm	INAA	0.6	0.1	0.3	1.5	1.4	0.1
Ga	ppm	XRF	5	13	n.d.	n.d.	n.d.	n.d.
Ge	ppm	ICP-HY	<0.2	<0.2	n.d.	n.d.	n.d.	n.d.
Hf	ppm	INAA	2.2	0.9	0.7	50.4	1.9	0.3
Hg	ppm	INAA	<1	<1	<1	<1	<1	<1
Ir	ppb	INAA	<1	<1	<1	18	<1	34
Ir	ppb	ICP/MS	2.8	3.2	<0.1	3.9	0.7	3.2
La	ppm	INAA	13.7	4.3	1	179	9.2	0.9
Lu	ppm	INAA	<0.01	<0.01	<0.01	<0.01	1	<0.01
Mo	ppm	ICP	<2	<2	<2	4	<2	<2
Nb	ppm	XRF	2	2	n.d.	n.d.	n.d.	n.d.
Nd	ppm	INAA	9	3	4	136	12	2
Ni	ppm	ICP	815	926	1385	709	160	2028
Pb	ppm	ICP	8	8	<5	<5	<5	<5
Pb	ppm	XRF	6	9	n.d.	n.d.	n.d.	n.d.
Pd	ppb	ICP/MS	1.9	2.8	0.8	2.0	2.6	0.8
Pt	ppb	ICP/MS	7.6	12.2	2.3	5.9	3.2	5.0
Rb	ppm	INAA	<10	<10	<10	202	<10	<10
Rb	ppm	XRF	<2	<2	n.d.	n.d.	n.d.	n.d.
Rh	ppb	ICP/MS	1.1	1.7	<0.1	0.9	0.6	1.2
S	ppm	XRF	<50	<50	n.d.	n.d.	n.d.	n.d.
Sb	ppm	INAA	<0.1	<0.1	<0.1	<0.1	<0.1	<0.1
Sc	ppm	INAA	16	13	8	11	53	5

Table 4.--Continued.

Minor and trace elements								
Map key			4	5	10	11	12	13
Se	ppm	ICP-HY	0.3	0.2	n.d.	n.d.	n.d.	n.d.
Se	ppm	INAA	<1	<1	<1	5	<1	<1
Sm	ppm	INAA	1.9	0.8	1.4	16.7	3.1	0.1
Sn	ppm	XRF	<5	10	n.d.	n.d.	n.d.	n.d.
Sr	ppm	ICP	16	2	6	12	90	2
Ta	ppm	INAA	<0.3	<0.3	<0.3	2	1	<0.3
Tb	ppm	INAA	0.4	0.2	0.4	1.5	0.9	<0.1
Te	ppm	ICP-HY	0.2	0.2	n.d.	n.d.	n.d.	n.d.
Th	ppm	INAA	4	1	<0.1	63	1	1
U	ppm	INAA	1	<0.1	<0.1	5	1	<0.1
V	ppm	ICP	90	69	37	92	376	<5
W	ppm	INAA	37	<1	<1	<1	<1	<1
Y	ppm	ICP	14	6	21	23	34	5
Yb	ppm	INAA	1	1	3	3	4	1
Zn	ppm	ICP	46	24	48	115	109	87
Zr	ppm	ICP	83	40	23	1961	68	11

Cherry Creek mining district (Table 5)

The Cherry Creek mining district borders the eastern flanks of the Gravelly Range in Madison County. Samples include banded iron formation and related rocks from the Ruby (Johnny Gulch) mine in the northern part of the district near the Yellowstone talc mine, a stream sediment from a reported placer site along Ruby Creek (for which no production data are available), and a sample of banded iron formation from the Black Butte deposit near Granite Mountain (Wier, 1965) in the southern part of the district. Additional samples were collected in this study to provide additional data and corroboration of anomalous gold values reported by Stanley (1988).

In the 1930's, gold was reportedly produced from a quartz vein cutting iron formation at the Ruby Mine (Hogberg, 1960). Stanley (1988) reported gold concentrations of 1 to over 4,500 ppb for 23 samples from the mine area; the two high concentration samples are grab samples of finely banded iron formation from a dump (4,688 ppb gold) and a channel sample of fault gouge (2,038 ppb gold). All other samples contained 155 ppb gold or less, and most were in the range of 1 to 10 ppb gold. Our samples (table 5, map key 17, 19 to 27) all contain 35 ppb gold or less and negligible concentrations of silver (<5 ppm) and arsenic (10 ppm or less). No gold (<2 ppb) was detected in a stream sediment sample (table 5, map key 18) collected just upstream of the reported placer site in Ruby Creek.

Table 5. Analytical data for rock and stream sediment samples from the Cherry Creek mining district. [See text for explanation of methods;*, replicate samples]

Map key			17	18	19	20	21	22
Sample number			96BV10	96BV11	96BV04	96BV05A	96BV05B	96BV06A
Job number			AHK0045	AHK0046	AHK0045	AHK0045	AHK0045	AHK0045
Element	Units	Method						
Ag	ppm	ICP	<0.4	<0.4	<0.4	<0.4	<0.4	<0.4
Ag	ppm	INAA	<5	<5	<5	<5	<5	<5
Al	%	ICP	0.03	2.65	0.07	0.05	0.03	0.38
As	ppm	INAA	1.3	10	10	2.8	1.4	8.2
Au	ppb	INAA	27	<2	15	<2	<2	4
Ba	ppm	INAA	<50	780	<50	<50	<50	76
Be	ppm	ICP	<2	<2	<2	<2	<2	<2
Bi	ppm	ICP-HY	<0.2	<0.2	1.5	1.1	0.8	<0.2
Bi	ppm	ICP	<5	<5	<5	<5	<5	<5
Br	ppm	INAA	0.7	3.2	<0.5	<0.5	<0.5	1.1
Ca	%	ICP	2.03	7.9	0.19	0.12	0.19	0.02
Ca	%	INAA	<1	9	<1	<1	<1	<1
Cd	ppm	ICP	<0.5	0.8	1.3	<0.5	1	<0.5
Ce	ppm	INAA	<3	66	<3	<3	<3	4
Co	ppm	INAA	<1	6	1	<1	<1	3
Cr	ppm	INAA	11	93	15	13	10	58
Cs	ppm	INAA	<1	3	<1	<1	<1	<1
Cu	ppm	ICP	3	11	13	13	10	7
Eu	ppm	INAA	<0.2	1.2	0.2	<0.2	<0.2	<0.2
Fe	%	INAA	0.32	2.32	31.5	46.7	33.8	0.99
Ge	ppm	ICP-HY	<0.2	<0.2	2.4	4.8	3.4	0.2
Hf	ppm	INAA	<1	21	<1	<1	<1	<1
Hg	ppm	INAA	<1	<1	<1	<1	<1	<1
Ir	ppb	INAA	<5	<5	<5	<5	<5	<5
K	%	ICP	0.02	1.27	0.02	0.01	0.01	0.20
La	ppm	INAA	<0.5	37	2.1	1.2	1.6	2.7
Lu	ppm	INAA	<0.05	0.79	0.05	<0.05	<0.05	<0.05
Mg	%	ICP	0.01	1.56	0.15	0.06	0.08	0.06
Mn	ppm	ICP	39	881	2453	319	165	258
Mo	ppm	ICP	<2	<2	<2	<2	<2	<2
Mo	ppm	INAA	<1	<1	4	<1	<1	<1
Na	%	INAA	0.01	0.27	0.01	<0.01	<0.01	0.01
Nd	ppm	INAA	<5	32	<5	<5	<5	<5
Ni	ppm	ICP	2	15	8	5	3	13
Ni	ppm	INAA	<20	<20	<20	<22	<20	<20
P	%	ICP	0.005	0.179	0.035	0.033	0.033	0.004
Pb	ppm	ICP	<5	15	<5	<5	7	<5
Rb	ppm	INAA	<15	49	<15	<15	<15	<15

Table 5.--Continued

Map key			17	18	19	20	21	22
Sb	ppm	INAA	0.2	0.6	0.3	0.6	0.4	0.2
Sc	ppm	INAA	0.1	7.2	0.2	0.2	0.1	0.8
Se	ppm	ICP-HY	0.2	0.6	0.5	0.4	0.6	0.4
Se	ppm	INAA	<3	<3	<3	<3	<3	<3
Sm	ppm	INAA	<0.1	5.1	0.1	0.1	0.1	0.3
Sn	%	INAA	<0.01	<0.01	<0.01	<0.01	<0.01	<0.01
Sr	ppm	ICP	53	86	17	5	4	4
Sr	%	INAA	<0.05	<0.05	<0.05	<0.05	<0.05	<0.05
Ta	ppm	INAA	<0.5	0.7	<0.5	<0.5	<0.5	<0.5
Tb	ppm	INAA	<0.5	1.1	<0.5	<0.5	<0.5	<0.5
Te	ppm	ICP-HY	0.2	<0.2	0.5	0.5	0.4	0.3
Th	ppm	INAA	<0.2	14	<0.2	<0.2	<0.2	1.1
Ti	%	ICP	0.01	0.22	0.01	0.01	0.01	0.02
U	ppm	INAA	<0.5	4.4	2.8	<0.5	<0.5	<0.5
V	ppm	ICP	2	41	50	4	2	11
W	ppm	INAA	<1	<1	<1	<1	<1	<1
Y	ppm	ICP	2	25	6	5	4	2
Yb	ppm	INAA	<0.2	4.6	0.3	<0.2	<0.2	0.3
Zn	ppm	ICP	41	71	2	2	2	8
Zn	ppm	INAA	<50	109	<50	<50	<50	<50

Table 5.–Continued

Map key			23	24	25	26	27	28
Sample number			96BV06B*	96BV07	96BV08	96BV09A	96BV09B*	96BV12
Job number			AHK0045	AHK0045	AHK0045	AHK0045	AHK0045	AHK0045
Element	Units	Method						
Ag	ppm	ICP	<0.4	<0.4	<0.4	<0.4	<0.4	<0.4
Ag	ppm	INAA	<5	<5	<5	<5	<5	<5
Al	%	ICP	0.31	0.15	0.03	0.03	0.03	0.17
As	ppm	INAA	5.9	10	1.2	<0.5	1.7	2.7
Au	ppb	INAA	4	4	3	6	35	18
Ba	ppm	INAA	50	150	<50	<50	<50	<50
Be	ppm	ICP	<2	<2	<2	<2	<2	<2
Bi	ppm	ICP-HY	<0.2	0.2	<0.2	0.4	0.6	0.4
Bi	ppm	ICP	<5	<5	<5	6	7	<5
Br	ppm	INAA	1.5	5	<0.5	<0.5	<0.5	<0.5
Ca	%	ICP	0.01	0.05	0.01	0.03	0.03	0.56
Ca	%	INAA	<1	<1	<1	<1	<1	<1
Cd	ppm	ICP	<0.5	<0.5	<0.5	<0.5	<0.5	<0.5
Ce	ppm	INAA	4	5	<3	<3	<3	3
Co	ppm	INAA	3	5	<1	<1	<1	5
Cr	ppm	INAA	43	13	10	11	10	18
Cs	ppm	INAA	<1	<1	<1	<1	<1	1
Cu	ppm	ICP	7	26	2	6	5	4
Eu	ppm	INAA	<0.2	<0.2	<0.2	<0.2	<0.2	<0.2
Fe	%	INAA	0.72	8.33	0.32	23	26.6	30.4
Ge	ppm	ICP-HY	<0.2	<0.2	<0.2	1.4	1.3	0.4
Hf	ppm	INAA	<1	<1	<1	<1	<1	<1
Hg	ppm	INAA	<1	<1	<1	<1	<1	<1
Ir	ppb	INAA	<5	<5	<5	<5	<5	<5
K	%	ICP	0.17	0.04	0.01	0.01	0.01	0.03
La	ppm	INAA	2.2	2.4	<0.5	0.6	0.9	1.3
Lu	ppm	INAA	<0.05	<0.05	<0.05	<0.05	<0.05	0.1
Mg	%	ICP	0.04	0.07	0.01	0.02	0.02	1.3
Mn	ppm	ICP	292	4850	36	271	303	257
Mo	ppm	ICP	<2	2	<2	<2	<2	<2
Mo	ppm	INAA	<1	3	<1	<1	<1	<1
Na	%	INAA	0.02	0.02	0.01	<0.01	<0.01	0.03
Nd	ppm	INAA	<5	<5	<5	<5	<5	<5
Ni	ppm	ICP	10	11	2	2	3	7
Ni	ppm	INAA	<20	<20	<20	<20	<20	<20
P	%	ICP	0.002	0.011	0.002	0.012	0.012	0.034
Pb	ppm	ICP	6	12	<5	<5	<5	<5
Rb	ppm	INAA	<15	<15	<15	<15	<15	28
Sb	ppm	INAA	0.2	0.2	0.2	<0.1	<0.1	0.2

Table 5.--Continued

Map key			23	24	25	26	27	28
Sc	ppm	INAA	0.6	0.9	0.1	0.1	0.2	1
Se	ppm	ICP-HY	0.3	<0.2	0.3	<0.2	<0.2	<0.2
Se	ppm	INAA	<3	<3	<3	<3	<3	<3
Sm	ppm	INAA	0.3	0.3	<0.1	<0.1	<0.1	0.2
Sn	%	INAA	<0.01	<0.01	<0.01	<0.01	<0.01	<0.01
Sr	ppm	ICP	4	19	2	3	3	8
Sr	%	INAA	<0.05	<0.05	<0.05	<0.05	<0.05	<0.05
Ta	ppm	INAA	<0.5	<0.5	<0.5	<0.5	<0.5	<0.5
Tb	ppm	INAA	<0.5	<0.5	<0.5	<0.5	<0.5	<0.5
Te	ppm	ICP-HY	0.2	0.2	0.2	0.4	0.3	0.2
Th	ppm	INAA	0.7	0.4	<0.2	<0.2	<0.2	0.4
Ti	%	ICP	0.02	0.01	0.01	0.01	0.01	0.02
U	ppm	INAA	<0.5	2.2	<0.5	<0.5	<0.5	<0.5
V	ppm	ICP	10	43	2	2	2	8
W	ppm	INAA	<1	<1	<1	<1	<1	<1
Y	ppm	ICP	2	4	2	2	2	7
Yb	ppm	INAA	<0.2	0.2	<0.2	<0.2	0.2	0.5
Zn	ppm	ICP	6	21	5	2	2	21
Zn	ppm	INAA	<50	<50	<50	<50	<50	<50

Chinatown mining district (Table 6)

Chinatown is an historic placer gold district that was worked in the 1800's, and then intermittently in the 20th century with reported production of 3,500 ounces of gold from 1902 to 1965 (Geach, 1972, p. 168). The lode source of the gold has never been identified, and the area continues to be explored. In 1995, there were 28 active lode and placer mining claims recorded with the Bureau of Land Management in sections 10, 11, and 15 of T.11S., R.13 W. (MCRS, 1996). These are in the area of the Lucky Strike Mine and the historic Raven No. 28 prospect (fig. 4). The historic placer workings were concentrated along Jeff Davis Creek, an east-west gulch (fig. 4) that drains Archean granitic gneiss and Tertiary sedimentary and volcanic rocks (probably equivalents of the Eocene Challis Volcanic Group) (M'Gonigle and Hait, 1997).

The source of the placer gold in this district is one of the geologic puzzles of southwest Montana. Numerous theories have been postulated, but none to date have adequately accounted for the localization of gold in Jeff Davis Gulch. The following description of the area is based on information provided by Elizabeth Brenner Younggren (written communication, 1995), Geach (1972), and site visits by the authors. Minor placer gold was recovered from the next drainage to the south, Maiden Creek; however, no placer gold has been recovered from the drainage to the north, Shenon Creek. Placer workings in Jeff Davis Gulch appear to exploit terrace gravels that contain rounded boulders of a variety of rock types. Among these rock types are unusual boulders of magnetite, informally referred to as "cannonballs". Because gold is associated with iron formation at some localities in the Archean terrane of southwestern Montana (for example, at the Mineral Hill Mine near Jardine), we analyzed two of these "cannonballs" (table 6, map key 29 and 30) for gold and trace elements. These data allow us to compare the chemistry of the "cannonballs" with banded iron formation that occurs in Archean-age Cherry Creek Group metasupracrustal rocks well to the east of the Chinatown district (see discussion of "Iron formation").

A glacial origin for the deposits seems unlikely, given the lack of evidence for glaciation in the area (Brenner Younggren, 1995). Sources to the west, postulated on the basis of Lyden's (1948) observation that gold grain size fines towards the mountain front, require a reversal in modern drainage patterns. Stream reversals are documented in other parts of southwest Montana, where the modern drainage system developed as recently (in geologic time) as the last 2 to 3 million years (Loen, 1995). Lode sources for productive gold placer deposits in southwestern Montana are not always apparent. For example, placer gold deposits in the Bannack area to the north appear to be "displaced" relative to their likely lode source, and a lode source for the voluminous Virginia City placer deposits has not been unequivocally established (Loen, 1995). Bannack has been suggested as a possible source area for the Chinatown gold, but it would be difficult to explain the distant transport of large boulders and the localization of the gold in Jeff Davis Gulch relative to surrounding areas.

Neither of the two known lode deposits along Jeff Davis Gulch, the H&S lead-zinc mine and the Lucky Strike claim (no recorded production), appear to represent a lode source for the placer, although many workers have suggested that the gold is related to Tertiary igneous rocks that are known to be associated with these two mineralized areas. M'Gonigle and Dalrymple (1996) showed that the volcanic rocks (rhyolitic tuffs and ash flow tuffs) exposed in the Horse Prairie (Chinatown) area and Medicine Lodge basin are correlative with the Eocene Challis Volcanic Group of central Idaho and were emplaced between 48.8 and 45.0 Ma.

The H&S mine sits above the gulch and is downstream from many of the placer workings. The H&S mine explores a brecciated contact between Archean gneiss, schist, and marble and a shallow, Tertiary intrusion described by Geach (1972) as a felsite. According to Geach (1972), who provided a plan map of the underground workings, the mine produced a small amount (40 ounces) of gold; primary production was for lead (about 700,000 pounds), zinc (15,000 pounds), copper (700 pounds) and silver (11,000 ounces). The ore at the H & S mine is mainly galena and the oxidized lead carbonate mineral, cerussite.

The Lucky Strike workings (exploration adits and prospects pits) were developed along the contact of a Tertiary(?) porphyritic latite that intrudes brecciated Archean gneiss along the southern margin of a diorite body of unknown age (M'Gonigle and Hait, 1997). Most of the active claims explore the western contact of this diorite body, adjacent Tertiary(?) intrusive felsic rocks, and the area of the range front fault. The latite crops out as an intrusive body in the gulch and as small dikes along the margin of the diorite, and locally contains pyrite and chalcopyrite (M'Gonigle and Hait, 1997).

Winters and others (1994) reported geochemical data for several samples from this area. For six samples at the H&S mine, they detected gold in only one sample, a chip sample across a breccia zone at the upper adit that assayed 0.034 grams/metric ton (0.001 ounces/short ton) gold. Our gossan sample (table 6, map key 31) from the H&S contains significantly less gold than the chip sample, 4 ppb gold (0.004 grams/metric ton). No significant metal values were obtained by Winters and others (1994) for sulfide-bearing rhyolite and altered quartz monzonite (probably the diorite body of M'Gonigle and Hait, 1997) at the Raven No. 28 (fig. 4) claims. Their analyses for the Lucky Strike claim include a select sample from the adit dump that assayed 0.021 grams/metric ton (0.0006 ounces/short ton) gold and a chip sample across a shear zone that assayed 0.12 grams/metric ton (0.004 ounces/short ton) gold. We detected 9 ppb gold (0.009 grams/metric ton) in a stream sediment (table 6, map key 32) from Jeff Davis Creek, just upstream of the Lucky Strike workings. Given the historic placer activity in the creek, one might not expect to see anomalous gold concentrations remaining, so the relatively low content is not particularly significant in evaluating the lode source area. What is significant is that the only location where base metals and silver are present with any gold is at the H&S mine; the lack of these metals with the gold at the Lucky Strike, the Raven (also known as Oxide) claims, and in the stream sediments indicate that the geochemical signature of altered rocks associated with the Tertiary(?) intrusions is distinct. Brenner Younggren (1995) reported a maximum gold concentration of 168 ppb in a drill core at the contact between Tertiary(?) volcanic rocks and Archean gneiss; she also noted localized high-grade samples (>10 ppm gold) in prospect pits along range front faults.

In summary, gold is present in the district but a gold-rich mineral deposit has not been delineated to date. There are a number of small-scale base metal occurrences associated with major thrust faults in southwest Montana; none of these have been significant past producers. Although the eastern and northern contacts of the diorite body have not been thoroughly explored, the concentration of historic workings along the western margin suggest that this is the most prospective area for further exploration. Perhaps this area is at the intersection of an east-west structure that defines the gulch and a north-south structure along the western margin of the diorite ("MP fault" on M'Gonigle and Hait, 1997), where metal-bearing fluids may have been channeled. The gold may be associated with the Tertiary intrusive event, or may represent Archean gold that was remobilized during Late Cretaceous Laramide-style deformation, subsequent Sevier-style (thin skin) thrusting, or still younger Tertiary Basin and Range-style block faulting (Perry and others, 1988).

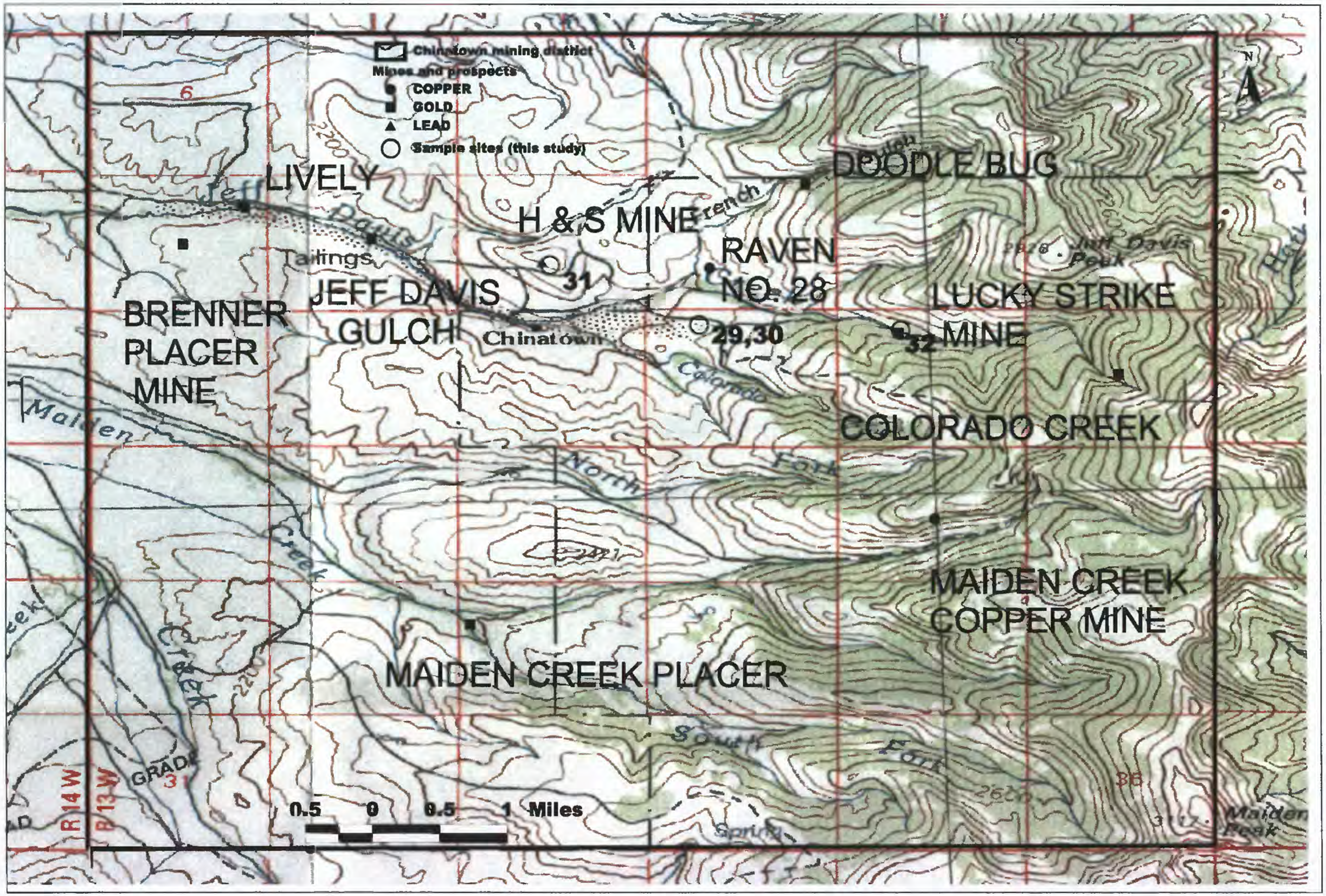

Figure 4. Map of the Chinatown district showing historic mines and prospects and sites sampled for this study. Samples include "cannonballs" (29,30), gossan from the H&S mine dump (31), and a stream sediment sample collected just upstream of the Lucky Strike workings (32). Base topography from the Leadore 1:100,000-scale topographic quadrangle map.

Table 6. Analytical data for rock and stream sediment samples from the Chinatown mining district. [See text for explanation of methods; n.d., not determined]

Map key			29	30	31	32
Sample number			E9501	E9502	96JH51	96JH50
Job number			AHK1241	AHK1241	AHK1787	AHK1787
Element	Units	Method				
Ag	ppm	ICP	n.d.	n.d.	2.3	<0.4
Ag	ppm	INAA	<5	<5	<5	<5
Al	%	ICP	n.d.	n.d.	2.97	6.53
As	ppm	INAA	5.2	4.7	9.4	5.9
Au	ppb	ICP/MS	6	19	n.d.	n.d.
Au	ppb	INAA	4	17	4	9
Ba	ppm	INAA	<50	<50	30000	1600
Be	ppm	ICP	n.d.	n.d.	4	2
Bi	ppm	ICP-HY	n.d.	n.d.	1.0	<1
Bi	ppm	ICP	n.d.	n.d.	<5	<5
Br	ppm	INAA	2.4	2.1	<0.5	4.1
Ca	%	ICP	n.d.	n.d.	0.23	0.31
Ca	%	INAA	<1	<1	<1	<1
Cd	ppm	ICP	n.d.	n.d.	6.8	<0.5
Ce	ppm	INAA	37	14	66	100
Co	ppm	INAA	26	20	7	3
Cr	ppm	INAA	160	150	47	16
Cs	ppm	INAA	<1	<1	1	3
Cu	ppm	ICP	n.d.	n.d.	25	11
Eu	ppm	INAA	0.6	0.2	3.3	1.9
Fe	%	INAA	30.6	31.7	16.1	2.05
Ge	ppm	ICP-HY	n.d.	n.d.	<0.2	<0.2
Hf	ppm	INAA	7	7	5	13
Hg	ppm	INAA	5	<1	<1	<1
Ir	ppb	INAA	<5	<5	<5	<5
Ir	ppb	ICP/MS	1.1	0.9	n.d.	n.d.
K	%	ICP	n.d.	n.d.	1.8	4.19
La	ppm	INAA	17.0	3.1	36	50
Lu	ppm	INAA	2.45	1.28	0.35	0.83
Mg	%	ICP	n.d.	n.d.	0.17	0.44
Mn	ppm	ICP	n.d.	n.d.	46476	303
Mo	ppm	ICP	n.d.	n.d.	4	2
Mo	ppm	INAA	41	34	33	6
Na	%	INAA	0.01	<0.01	0.06	1.43
Nd	ppm	INAA	15	<5	20	36
Ni	ppm	ICP	n.d.	n.d.	28	6
Ni	ppm	INAA	<27	<29	96	<20
P	%	ICP	n.d.	n.d.	0.019	0.038

Table 6.--Continued.

Map key			29	30	31	32
Pb	ppm	ICP	n.d.	n.d.	1841	27
Pd	ppb	ICP/MS	0.2	0.2	n.d.	n.d.
Pt	ppb	ICP/MS	<0.1	<0.1	n.d.	n.d.
Rb	ppm	INAA	<15	38	90	130
Rh	ppb	ICP/MS	0.2	<0.1	n.d.	n.d.
Sb	ppm	INAA	0.4	0.4	7.2	0.8
Sc	ppm	INAA	15.0	18.0	5.8	3.5
Se	ppm	ICP-HY	n.d.	n.d.	0.6	<0.2
Se	ppm	INAA	<3	<3	<3	<3
Sm	ppm	INAA	4.9	1.4	5.1	6.8
Sn	%	INAA	<0.01	<0.01	<0.01	<0.01
Sr	ppm	ICP	n.d.	n.d.	399	117
Sr	%	INAA	<0.05	<0.05	0.06	<0.05
Ta	ppm	INAA	120	140	0.7	1.6
Tb	ppm	INAA	1.7	0.5	0.9	1.3
Te	ppm	ICP-HY	n.d.	n.d.	0.5	0.2
Th	ppm	INAA	0.4	0.9	4.7	16
Ti	%	ICP	n.d.	n.d.	0.1	0.19
U	ppm	INAA	2.1	3.0	12	4.6
V	ppm	ICP	n.d.	n.d.	24	20
W	ppm	INAA	89	63	<1	<1
Y	ppm	ICP	n.d.	n.d.	26	31
Yb	ppm	INAA	14.0	7.3	2.2	5.3
Zn	ppm	ICP	n.d.	n.d.	1997	71
Zn	ppm	INAA	129	127	1920	57

Horse Prairie mining district (Table 7)

There are a number of northwest-trending quartz veins within Early Proterozoic gneiss and schist (Ruppel and others, 1993) in the western part of the Horse Prairie district that were discovered in the 1880's and mined intermittently from 1902 until 1928 (Geach, 1972, p. 31). All of the mines and prospects appear to line up along a northwest trend (near latitude 45° N on fig. 3). Although the principal commodity reported varies among the sites (copper, lead), all of these occurrences appear to represent a family of related, probably coeval veins that follow northwest-trending contacts or structures. Most of the veins are described as quartz veins with iron and manganese oxides, galena, the oxidized lead carbonate mineral cerrusite, chalcopyrite, and in some cases tetrahedrite is reported. This area was described as the Monument (or Beaverhead) mining district by Geach (1972, p. 31) who reported total production of gold (114 ounces), silver (10,181 ounces), copper (98,982 pounds), and lead (49,862 pounds). This area is on BLM lands.

Samples from the Jung Frau (fig. 3, tables 1 and 7, map key 33) and Monument (fig. 3, tables 1 and 7, map key 34-36) mines in the western part of the Horse Prairie district were sampled to characterize the minor element signature of these vein deposits. A few lode claims are maintained in the vicinity of the Jung Frau mine, but no claim activity is recorded in the Monument area (MCRS, 1996). The Jung Frau patented claim explores a tetrahedrite-bearing barite vein along a shear zone in Archean gneiss; no production is recorded. The elevated concentrations of silver (76 ppm) and antimony (210 ppm) in our sample of the barite vein reflect the presence of tetrahedite; gold was below detection levels (<2 ppb). This is the only reported occurrence of barite in the Horse Prairie area. Our data confirm the presence of barite (400,000 ppm Ba in the sample and confirmation by x-ray diffraction) at this locality, which was previously reported as an unverified barite occurrence by Berg (1988).

The Monument mine produced a small amount of copper and silver from workings along the contact of an iron-and copper-stained quartzite with biotite schist (Geach, 1972, p. 31); no gold was reported. Our samples of gossan and copper-stained quartz from the surface workings at the Monument mine have an unusual geochemical signature. All three samples contained gold (244 to 419 ppb), arsenic (640 to 1,700 ppm), bismuth (26 to 57 ppm), cobalt (210 to 1,000 ppm), antimony (5 to 16 ppm), and tellurium (0.3 to 1.1 ppm). These types of vein deposits may account for the presence of small amounts of gold (a few flakes per pan) reported for placer attempts in Horse Prairie Valley (Brenner Younggren, oral communication, 1996). We did not analyze these samples for copper or lead; zinc concentrations ranged from 110 ppm (quartz vein) to 430 ppm (gossan). Geach (1972) noted that the workings explored narrow quartz veins in gneiss and schist; to the northwest, the gneiss is in contact with white, micaceous quartz sandstone and to the southeast, the gneiss is covered by Tertiary volcanic rocks. We interpret these veins as polymetallic veins; they may have formed along northwest structures that developed during Late Cretaceous Laramide-style deformation or subsequent Sevier-style deformation (Perry and others, 1988), or they may represent fluids associated with the Eocene Challis volcanic event that concentrated along such structures. Although the data set is limited, these veins appear to have a distinctive geochemical signature compared to Chinatown. No historic placers or recent placer claims are associated with the veins in the Monument mine area.

In the southeastern corner of the Horse Prairie district near Clark Canyon Reservoir (fig. 3, map key 37-40), the Beaverhead Conglomerate is highly fractured and silicified along the Armstead thrust fault. Silicified breccia and jasperoid (table 7, map key 37-40) were sampled to look for mineralization associated with fault movement along the Armstead thrust. None of these samples contain any significant metal values.

Table 7. Analytical data for rock samples from the Horse Prairie mining district.
[See text for explanation of methods; n.d., not determined; *, replicate samples]

Map key			33	34	35	36	37	38
Sample number			95JH006	95JH003	95JH203 *	95JH004	96JH39	96JH40
Job number			AHK1256	AHK1256	AHK1256	AHK1256	AHK1787	AHK1787
Element	Units	Method						
Ag	ppm	ICP	n.d.	n.d.	n.d.	n.d.	0.6	0.7
Ag	ppm	INAA	76	26	19	<5	<5	<5
Al	%	ICP	n.d.	n.d.	n.d.	n.d.	0.47	0.48
As	ppm	INAA	73	890	1700	640	180	590
Au	ppb	INAA	<2	244	276	419	4	<2
Ba	ppm	INAA	400,000	790	760	900	560	510
Be	ppm	ICP	n.d.	n.d.	n.d.	n.d.	<2	2
Bi	ppm	ICP-HY	<0.2	26.6	39.6	56.8	<1	<1
Bi	ppm	ICP	n.d.	n.d.	n.d.	n.d.	<5	<5
Br	ppm	INAA	6.2	3.6	<0.5	2.5	<0.5	3.3
Ca	%	ICP	n.d.	n.d.	n.d.	n.d.	0.72	0.92
Ca	%	INAA	<1	<1	<1	<1	<1	<1
Cd	ppm	ICP	n.d.	n.d.	n.d.	n.d.	<0.5	<0.5
Ce	ppm	INAA	<3	27	30	42	18	14
Co	ppm	INAA	5	380	1,000	210	<1	4
Cr	ppm	INAA	<5	53	78	14	25	27
Cs	ppm	INAA	<1	<1	<1	<1	1	<1
Cu	ppm	ICP	n.d.	n.d.	n.d.	n.d.	2	6
Eu	ppm	INAA	<0.2	0.6	<0.2	0.7	1	0.9
Fe	%	INAA	0.41	4.79	5.77	0.92	0.83	2.14
Ge	ppm	ICP-HY	<0.2	<0.2	<0.2	<0.2	<0.2	<0.2
Hf	ppm	INAA	<1	2	<1	4	<1	<1
Hg	ppm	INAA	<1	<1	<1	<1	<1	<1
Ir	ppb	INAA	<5	<5	<5	<5	<5	<5
K	%	ICP	n.d.	n.d.	n.d.	n.d.	0.07	0.08
La	ppm	INAA	4.2	18	17	27	31	38
Lu	ppm	INAA	<0.05	<0.05	0.1	0.2	0.3	0.47
Mg	%	ICP	n.d.	n.d.	n.d.	n.d.	0.02	0.08
Mn	ppm	ICP	n.d.	n.d.	n.d.	n.d.	57	58
Mo	ppm	ICP	n.d.	n.d.	n.d.	n.d.	2	2
Mo	ppm	INAA	<1	22	22	<1	4	4
Na	%	INAA	<0.01	0.04	0.07	0.05	0.02	0.03
Nd	ppm	INAA	<5	6	14	15	21	22
Ni	ppm	ICP	n.d.	n.d.	n.d.	n.d.	2	11
Ni	ppm	INAA	<23	210	360	150	<20	48
P	%	ICP	n.d.	n.d.	n.d.	n.d.	0.086	0.352
Pb	ppm	ICP	n.d.	n.d.	n.d.	n.d.	<5	9
Rb	ppm	INAA	<15	53	120	88	<15	<15

Table 7.--Continued

Map key			33	34	35	36	37	38
Sb	ppm	INAA	210	12	16	5.1	1.7	8.8
Sc	ppm	INAA	0.8	6.8	8.6	7.5	0.8	1.6
Se	ppm	ICP-HY	0.2	1.1	1.8	0.6	0.6	<0.2
Se	ppm	INAA	<3	<3	<3	<3	<3	<3
Sm	ppm	INAA	0.1	1.6	1.5	2.4	3	3
Sn	%	INAA	<0.01	<0.01	<0.01	<0.01	<0.01	<0.01
Sr	ppm	ICP	n.d.	n.d.	n.d.	n.d.	719	1,369
Sr	ppm	INAA	6,400	<500	<500	<500	900	1,500
Ta	ppm	INAA	<0.5	<0.5	<0.5	0.8	<0.5	0.6
Tb	ppm	INAA	<0.5	<0.5	<0.5	<0.5	0.6	0.7
Te	ppm	ICP-HY	0.2	0.6	1.1	0.3	<0.2	<0.2
Th	ppm	INAA	<0.5	10	16	6.6	1	0.9
Ti	%	ICP	n.d.	n.d.	n.d.	n.d.	0.03	0.03
U	ppm	INAA	<0.6	24	30	28	2.5	4.1
V	ppm	ICP	n.d.	n.d.	n.d.	n.d.	34	149
W	ppm	INAA	47	93	130	190	5	25
Y	ppm	ICP	n.d.	n.d.	n.d.	n.d.	59	91
Yb	ppm	INAA	<0.2	0.3	0.7	1.4	2	3.2
Zn	ppm	ICP	n.d.	n.d.	n.d.	n.d.	8	110
Zn	ppm	INAA	110	260	430	110	<50	106

Table 7.--Continued

Map key			39	40
Sample number			96JH41	96JH43
Job number			AHK1787	AHK1787
Element	Units	Method		
Ag	ppm	ICP	<0.4	<0.4
Ag	ppm	INAA	<5	<5
Al	%	ICP	0.13	0.25
As	ppm	INAA	190	110
Au	ppb	INAA	<2	<2
Ba	ppm	INAA	200	160
Be	ppm	ICP	<2	<2
Bi	ppm	ICP-HY	<1	<1
Bi	ppm	ICP	<5	<5
Br	ppm	INAA	<0.5	<0.5
Ca	%	ICP	0.12	0.75
Ca	%	INAA	<1	1
Cd	ppm	ICP	<0.5	<0.5
Ce	ppm	INAA	7	11
Co	ppm	INAA	<1	1
Cr	ppm	INAA	16	43
Cs	ppm	INAA	<1	1
Cu	ppm	ICP	2	2
Eu	ppm	INAA	<0.2	0.2
Fe	%	INAA	0.74	1.09
Ge	ppm	ICP-HY	<0.2	<0.2
Hf	ppm	INAA	<1	<1
Hg	ppm	INAA	<1	<1
Ir	ppb	INAA	<5	<5
K	%	ICP	0.04	0.06
La	ppm	INAA	8.5	24
Lu	ppm	INAA	0.09	0.1
Mg	%	ICP	0.01	0.01
Mn	ppm	ICP	50	77
Mo	ppm	ICP	<2	<2
Mo	ppm	INAA	<1	2
Na	%	INAA	0.01	0.03
Nd	ppm	INAA	<5	5
Ni	ppm	ICP	2	3
Ni	ppm	INAA	<20	<20
P	%	ICP	0.021	0.101
Pb	ppm	ICP	6	11
Rb	ppm	INAA	<15	<15
Sb	ppm	INAA	1.8	1.8

Table 7.–Continued

Map key			39	40
Sc	ppm	INAA	0.8	1.4
Se	ppm	ICP-HY	0.9	0.2
Se	ppm	INAA	<3	<3
Sm	ppm	INAA	0.3	0.6
Sn	%	INAA	<0.01	<0.01
Sr	ppm	ICP	54	247
Sr	ppm	INAA	<500	<500
Ta	ppm	INAA	<0.5	<0.5
Tb	ppm	INAA	<0.5	<0.5
Te	ppm	ICP-HY	<0.2	0.3
Th	ppm	INAA	0.9	2.4
Ti	%	ICP	0.04	0.05
U	ppm	INAA	1.3	2.8
V	ppm	ICP	19	27
W	ppm	INAA	8	12
Y	ppm	ICP	7	7
Yb	ppm	INAA	0.6	0.6
Zn	ppm	ICP	9	7
Zn	ppm	INAA	<50	<50

Medicine Lodge mining district (Table 8)

An outcrop along the beach area at the northwest corner of Clark Canyon Reservoir exposes chloritized, iron-stained, altered Archean gneiss overlain by Cambrian Flathead Sandstone. The gneiss contains pods and interbeds of amphibolite, and some leucocratic gneiss layers are garnetiferous. The gneiss is cut by pegmatites that contain coarse-grained biotite. These rocks are in the core of the Armstead anticline. No metallic mineral occurrences are associated with them; the scattered mineral localities in the vicinity (fig. 2) refer to phosphate leases and a reported sillimanite occurrence. The sillimanite of the Armstead area occurs in a package of rocks consisting of marble, gneiss (graphite, biotite, hornblende, and garnetiferous varieties), and schist, which were described by Lowell (1965). Heinrich (1949) described these rocks as similar to those in the Blacktail Mountains and south end of the Ruby Range, and assigned them to the Archean Cherry Creek group. We analyzed two samples (tables 1 and 8, map key 41 and 42) of fractured, altered gneiss to check for any anomalous metal concentrations and to obtain trace element geochemistry that might provide useful in correlating these rocks with Cherry Creek rocks well to the east. All precious and base metal concentrations are at or near detection limits.

Table 8. Analytical data for rock samples from the Medicine Lodge mining district.
[See text for explanation of methods]

Map key			41	42
Sample number			96JH44A	96JH45
Job number			AHK1787	AHK1787
Element	Units	Method		
Ag	ppm	ICP	<0.4	<0.4
Ag	ppm	INAA	<5	<5
Al	%	ICP	6.91	5.78
As	ppm	INAA	1.1	<0.5
Au	ppb	INAA	<2	<2
Ba	ppm	INAA	140	760
Be	ppm	ICP	2	2
Bi	ppm	ICP-HY	<1	<1
Bi	ppm	ICP	<5	<5
Br	ppm	INAA	1.4	<0.5
Ca	%	ICP	0.05	0.79
Ca	%	INAA	<1	<1
Cd	ppm	ICP	<0.5	<0.5
Ce	ppm	INAA	170	21
Co	ppm	INAA	7	<1
Cr	ppm	INAA	<5	<5
Cs	ppm	INAA	2	<1
Cu	ppm	ICP	3	2
Eu	ppm	INAA	1.7	1.6
Fe	%	INAA	1.83	0.44
Ge	ppm	ICP-HY	<0.2	<0.2
Hf	ppm	INAA	8	2
Hg	ppm	INAA	<1	<1
Ir	ppb	INAA	<5	<5
K	%	ICP	2.59	2.8
La	ppm	INAA	89	13
Lu	ppm	INAA	0.22	0.06
Mg	%	ICP	0.46	0.03
Mn	ppm	ICP	126	101
Mo	ppm	ICP	<2	<2
Mo	ppm	INAA	<1	<1
Na	%	INAA	0.04	1.95
Nd	ppm	INAA	61	10
Ni	ppm	ICP	6	2
Ni	ppm	INAA	100	<20
P	%	ICP	0.019	0.005
Pb	ppm	ICP	<5	19
Rb	ppm	INAA	96	94

Table. 8--Continued.

Map key			41	42
Sb	ppm	INAA	0.1	<0.1
Sc	ppm	INAA	2.2	1.2
Se	ppm	ICP-HY	0.5	0.5
Se	ppm	INAA	<3	<3
Sm	ppm	INAA	7.5	1.6
Sn	%	INAA	<0.01	<0.01
Sr	ppm	ICP	9	86
Sr	ppm	INAA	<500	<500
Ta	ppm	INAA	0.9	<0.5
Tb	ppm	INAA	0.6	<0.5
Te	ppm	ICP-HY	<0.2	<0.2
Th	ppm	INAA	26	5
Ti	%	ICP	0.09	0.01
U	ppm	INAA	2.2	<0.5
V	ppm	ICP	5	2
W	ppm	INAA	<1	<1
Y	ppm	ICP	8	5
Yb	ppm	INAA	1.3	0.4
Zn	ppm	ICP	3	4
Zn	ppm	INAA	<50	<50

Monida mining district (Table 9)

The Monida mining district includes a large tract of BLM land in a remote part of the Centennial Valley along Lima Reservoir. No metals have been produced from this area; the scattered historic mine workings (fig. 2) are almost all phosphate mines. Lyden (1948, p. 10) cited references to production of placer gold in 1923 from the Paul property on the shore of Lima Reservoir; the general location of the property was reported to be in sections 14, 15, 22, and 23 of T.14 S., R.6 W. (Chace and others, 1947). Lyden went on to note that if the location could be confirmed as a source of gold, testing for a large-scale dredge operation would be appropriate given the suitability of the valley for such operations. We saw no evidence for placer workings in our site visit, but we did sample a soil (fig. 3, table 9, map key 43) from the area of the reported gold production. Gold and silver are both below detection limits in the sample, and no other metals are present in any significant concentrations. The selenium content for this sample, 0.4 ppm, is within the observed range (<0.1 to 4.3 ppm) for selenium in soils in the western U.S., but above the mean western soil concentration of 0.23 ppm reported by Shacklette and Boerngen (1984).

Table 9. Analytical data for a soil sample from the Monida mining district.
[See text for explanation of methods]

Map key			43
Sample number			96JH36
Job number			AHK1787
Element	Units	Method	
Ag	ppm	ICP	<0.4
Ag	ppm	INAA	<5
Al	%	ICP	2.55
As	ppm	INAA	9.4
Au	ppb	INAA	<2
Ba	ppm	INAA	310
Be	ppm	ICP	<2
Bi	ppm	ICP-HY	<1
Bi	ppm	ICP	<5
Br	ppm	INAA	6.7
Ca	%	ICP	6.65
Ca	%	INAA	8
Cd	ppm	ICP	<0.5
Ce	ppm	INAA	44
Co	ppm	INAA	5
Cr	ppm	INAA	47
Cs	ppm	INAA	2
Cu	ppm	ICP	6
Eu	ppm	INAA	0.8
Fe	%	INAA	1.46
Ge	ppm	ICP-HY	<0.2
Hf	ppm	INAA	12
Hg	ppm	INAA	<1
Ir	ppb	INAA	<5
K	%	ICP	0.71
La	ppm	INAA	24
Lu	ppm	INAA	0.34
Mg	%	ICP	0.64
Mn	ppm	ICP	275
Mo	ppm	ICP	<2
Mo	ppm	INAA	6
Na	%	INAA	0.22
Nd	ppm	INAA	16
Ni	ppm	ICP	14
Ni	ppm	INAA	<20
P	%	ICP	0.078
Pb	ppm	ICP	9
Rb	ppm	INAA	34

Table 9.--Continued.

Map key			43
Pb	ppm	ICP	9
Rb	ppm	INAA	34
Sb	ppm	INAA	0.6
Sc	ppm	INAA	4.3
Se	ppm	ICP-HY	0.4
Se	ppm	INAA	<3
Sm	ppm	INAA	3.1
Sn	%	INAA	<0.01
Sr	ppm	ICP	132
Sr	ppm	INAA	<500
Ta	ppm	INAA	<0.5
Tb	ppm	INAA	0.6
Te	ppm	ICP-HY	0.2
Th	ppm	INAA	6.9
Ti	%	ICP	0.13
U	ppm	INAA	2.8
V	ppm	ICP	40
W	ppm	INAA	<1
Y	ppm	ICP	19
Yb	ppm	INAA	2.3
Zn	ppm	ICP	47
Zn	ppm	INAA	72

Pony mining district (Table 10)

The Pony district (includes the historic Mineral Hill district) was the largest producer of lode gold in the Tobacco Root Mountains. The numerous historic mines in the district, located in the northern part of the Tobacco Roots in Madison County, exploited structurally controlled lode veins (Woodward, 1993). Host rocks for veins include Archean gneiss and amphibolite, Proterozoic diabase dikes, and granitic rocks of the Cretaceous Tobacco Root batholith (Woodward and others, 1993). These vein systems have been interpreted as forming in Late Cretaceous time, during or shortly after emplacement of the batholith. A review of mining claim files (MCRS, 1996) shows that 516 claims are present in T.2S., R.3W.; most of these are concentrated in sections 14, 15, 16, 17, 20, 21, and 22 and many of the claims are active (last assessment date of 1996). We sampled a variety of altered rock types (fig. 3, tables 1 and 10, map key 44-52) associated with these vein deposits in sections 15 and 21 of T.2S., R.3W., in the vicinity of the historic Ben Harrison mine, Boss Tweed mine, Mountain Meadow claim, and unnamed prospects along the north side of the Cataract Creek drainage near the northern margin of the Cretaceous Tobacco Root batholith. Many of the structurally controlled, Archean gneiss-hosted, lode gold systems in the study area that are located farther south (for example, in the Virginia City and Horse Prairie district) lack any known association with Cretaceous magmatism. Therefore, a comparison of the trace element signatures of rocks associated with veins from different districts may be a useful tool in unraveling the metallogenic history of the region, classifying deposits, and evaluating the likelihood of undiscovered mineral deposits.

The Mountain Meadow claim is shown on the Vitaliano and Cordua (1979) geologic map of the Tobacco Root batholith; we have no data on production from the historic workings (caved adit on site), but a claim was staked on the property in 1994. The wallrock of the caved adit is altered (quartz-sericite-pyrite alteration) granodiorite. We observed pyrite cubes as well as chloritic and propylitic alteration, but no copper minerals, copper staining or calcite. Both samples we analyzed (table 2, table 10, map key 49 and 50) contain anomalous gold (62 and 3,270 ppb); silver is below detection limits for both samples. A number of elements that are useful pathfinders for gold, such as bismuth, antimony, and tellurium, are all present in minor concentrations in both samples. Woodward and others (1993) described the Mountain Meadow Mine as quartz veins with auriferous pyrite in a steeply dipping, northeast-striking shear zone; they reported assays for select dump samples in excess of 2 ounces of gold per ton.

The Ben Harrison Fraction mine reportedly produced $90,000 in gold and silver in the 1930's from ore in a narrow fissure vein in granite and gneiss; the vein was exploited by underground and shallow surface workings (Lorain, 1937). We focussed our sampling on the altered quartz-eye porphyry (table 1, table 10, map key 44-46) exposed in the dump and in outcrop at the partially caved adit. The samples represent three stages of alteration from relatively fresh (sample 95JH021) to moderately altered porphyry (sample 95JH022) to strongly altered (propylitic alteration) greenish porphyry (95JH023). Gold concentration increases with increasing alteration, from <2 ppb gold in the freshest samples to 70 ppb gold in the most altered sample. Silver and molybdenum are below detection limits for all three samples. Copper and lead were not analyzed; zinc is below detection limits (<50 ppm) for all three samples. Tungsten concentration increases with increasing alteration (from 89 to 210 ppm). The most altered sample contains minor amounts of arsenic, hafnium, and antimony. Tellurium is present at the 0.2 ppm concentration level in all three samples. This porphyry is quite distinct from the typical granitoid of the batholith (granodiorite to quartz monzonite) exposed at the Mountain Meadow claim. All of the rocks in this area are mapped as by Vitaliano and Cordua (1979) as silicic plutonic rocks of the composite Tobacco Root batholith. Mapping the extent of the alteration in the igneous rocks was beyond the scope of this study; the altered igneous rocks have potential for bulk minable gold deposits if sufficient grade and tonnage are present. No pervasive stockwork quartz veining or breccia zones were observed; however, previous studies have focussed on the vein systems in the district and to our knowledge, have not considered the potential of this district for porphyry-style mineral deposits.

Table 10. Analytical data for rock samples from the Pony mining district.
[See text for explanation of methods; n.d., not determined]

Map key			44	45	46	47	48	49
Sample number			95JH021	95JH022	95JH023	95JH027	95JH028	95JH019
Job number			AHK1256	AHK1256	AHK1256	AHK1256	AHK1256	AHK1256
Element	Units	Method						
Ag	ppm	INAA	<5	<5	<5	<5	<5	<5
As	ppm	INAA	<0.5	<0.5	1.4	9.9	1.3	4.1
Au	ppb	INAA	<2	9	70	322	7	62
Ba	ppm	INAA	1100	1100	720	700	1200	1600
Bi	ppm	ICP-HY	<0.2	0.2	<0.2	0.5	0.2	0.7
Br	ppm	INAA	<0.5	<0.5	<0.5	1.9	<0.5	1.6
Ca	%	INAA	<1	<1	<1	<1	<1	<1
Ce	ppm	INAA	31	35	68	120	100	44
Co	ppm	INAA	12	17	21	19	22	15
Cr	ppm	INAA	<5	<5	<5	<5	18	5
Cs	ppm	INAA	5	2	3	1	2	2
Eu	ppm	INAA	0.4	0.8	0.9	1.5	2.1	0.8
Fe	%	INAA	1.28	1.42	1.09	3.04	3.32	1.36
Ge	ppm	ICP-HY	<0.2	<0.2	<0.2	<0.2	<0.2	<0.2
Hf	ppm	INAA	<1	<1	6	11	12	4
Hg	ppm	INAA	<1	<1	<1	<1	<1	<1
Ir	ppb	INAA	<5	<5	<5	<5	<5	<5
La	ppm	INAA	28	27	55	81	72	32
Lu	ppm	INAA	0.1	0.12	0.2	0.82	0.78	0.18
Mo	ppm	INAA	<1	<1	<1	<1	<1	2
Na	%	INAA	2.34	2.59	0.09	0.86	2.32	0.1
Nd	ppm	INAA	10	11	23	43	36	14
Ni	ppm	INAA	<34	<36	<20	<27	<42	<20
Rb	ppm	INAA	110	<15	270	110	98	270
Sb	ppm	INAA	<0.1	<0.1	1.7	0.5	<0.1	0.5
Sc	ppm	INAA	2.3	3	3.5	8.6	12	2.8
Se	ppm	ICP-HY	0.2	0.2	0.2	0.2	<0.2	<0.2
Se	ppm	INAA	<3	<3	<3	<3	<3	<3
Sm	ppm	INAA	1.7	1.9	3	8.8	7.9	2.4
Sn	ppm	INAA	<100	<100	<100	<100	<100	<100
Sr	ppm	INAA	<500	<500	<500	<500	<500	<500
Ta	ppm	INAA	<0.5	<0.5	1	1.1	<0.5	1.1
Tb	ppm	INAA	<0.5	<0.5	<0.5	1.6	2.6	<0.5
Te	ppm	ICP-HY	0.2	0.2	0.2	0.2	0.2	0.2
Th	ppm	INAA	13	11	19	12	12	12
U	ppm	INAA	3	<0.5	4.8	1.9	<0.5	1.4
W	ppm	INAA	89	120	210	170	81	160
Yb	ppm	INAA	1	0.9	1.1	5.4	5.3	1.2
Zn	ppm	INAA	<50	<50	<50	<50	<50	<50

Table 10.--Continued

Map key			50	51	52
Sample number			95JH020	95JH025	95JH026A
Job number			AHK1256	AHK1256	AHK1241
Element	Units	Method			
Ag	ppm	INAA	<5	<5	<5
As	ppm	INAA	1.7	5	0.7
Au	ppb	ICP/MS	n.d.	n.d.	<1
Au	ppb	INAA	3270	7	<2
Ba	ppm	INAA	550	440	630
Bi	ppm	ICP-HY	3.3	0.6	n.d.
Br	ppm	INAA	1.1	<0.5	<0.5
Ca	%	INAA	<1	<1	4
Ce	ppm	INAA	26	47	39
Co	ppm	INAA	19	20	65
Cr	ppm	INAA	<5	280	33
Cs	ppm	INAA	1	3	1
Eu	ppm	INAA	0.4	1.2	0.9
Fe	%	INAA	4.27	4.35	15.3
Ge	ppm	ICP-HY	<0.2	<0.2	n.d.
Hf	ppm	INAA	3	5	5
Hg	ppm	INAA	<1	<1	<1
Ir	ppb	INAA	<5	<5	<5
Ir	ppb	ICP/MS	n.d.	n.d.	3.5
La	ppm	INAA	19	31	22
Lu	ppm	INAA	0.12	0.47	0.56
Mo	ppm	INAA	4	<1	<1
Na	%	INAA	0.04	0.63	0.69
Nd	ppm	INAA	7	15	10
Ni	ppm	INAA	<20	<28	180
Pd	ppb	ICP/MS	n.d.	n.d.	5.7
Pt	ppb	ICP/MS	n.d.	n.d.	7.2
Rb	ppm	INAA	170	180	62
Rh	ppb	ICP/MS	n.d.	n.d.	0.6
Sb	ppm	INAA	0.5	<0.1	0.2
Sc	ppm	INAA	1.5	29	29.0
Se	ppm	ICP-HY	<0.2	0.7	n.d.
Se	ppm	INAA	<3	<3	<3
Sm	ppm	INAA	1.2	4.6	2.8
Sn	ppm	INAA	<100	<100	<100
Sr	ppm	INAA	<500	<500	<500
Ta	ppm	INAA	0.9	<0.5	<0.5
Tb	ppm	INAA	<0.5	1	0.8
Te	ppm	ICP-HY	0.2	0.2	n.d.
Th	ppm	INAA	2.2	8.1	7.7
U	ppm	INAA	<0.5	2.4	2.1

Table 10.--Continued.

Map key			50	51	52
W	ppm	INAA	170	120	91
Yb	ppm	INAA	0.8	3.2	3.7
Zn	ppm	INAA	<50	<50	197

Red Bluff mining district (Table 11)

The Red Bluff district is situated between the Norris and Revenue districts (fig. 3). The geology and mineral deposits of the area around Red Bluff are included in older reports on the historic Norris (also known as Lower Hot Springs) mining district (Lorain, 1937). Several groups of quartz vein lode gold mines in the foothills of the Tobacco Root Mountains around Norris were developed in the early 1900's following placer gold discoveries in Norwegian Creek and Meadow Creek in 1864. From 1864 until 1930, the Norris district produced over $3 million worth of gold, silver, copper, and lead (Tansley and others, 1933). The modern Red Bluff district includes historic mines east of the town of Norris such as the Boaz mine, the Josephine mine, the Grubstake, and the Golconda. Eastern parts of sections 13 and 24 of T.3S., R.1W., and section 19 of T.3S., R.1E. are BLM lands that include, or are adjacent to, private lands holding some of these historic mine workings. More than 100 lode and placer claims were staked in section 19 between 1973 and 1995; many of these claims were last active in 1991-1993. However, nine claims were active in 1995, and 18 claims in the southern part of section 19 were active in 1996. Kellogg (1993) described the gold deposits of the Lower Hot Springs mining district and estimated total gold production from the district at about 100,000 ounces. Most of the production was pre-1900, and the Boaz mine was the most significant producer (Thurlow, 1941).

The historic workings exploit northwest-trending quartz veins in pre-Belt Supergroup gneiss and schist. This area is about 3 to 4 miles east of the exposed eastern contact of the Cretaceous Tobacco Root batholith. Lorain (1937) noted that although none of these mines were large producers, the veins in this area appeared to have higher average gold grades than most of the vein systems in the Tobacco Root region. The average grade of ore shipped from the Boaz mine, where oxidized ore was mined from an 18-inch-wide quartz fissure vein in gneiss, was reported to be 2 to 4 ounces of gold per ton. Kellogg (1994) mapped a pluton of metagranite of probable Archean age near the Grubstake mine in the Norris quadrangle; Kellogg (1993) noted that previous studies by Thurlow (1941) and Winchell (1914) described similar granite aplite "dikes" or quartz monzonite aplite intrusions in the area of the mines of the district. Kellogg (1993, 1994) suggested that an apophysis of the Tobacco Root batholith, which crops out to the west, may extend under the district. He also noted that Eocene-age igneous plugs are barren and appear to postdate the mineralization, and concluded that the Lower Hot Springs district is probably related to the Tobacco Root batholith. The descriptions of the leucogranite (aplite) are similar to the descriptions of the aplite stock associated with the Easton-Pacific mine in the Virginia City district (see below). Although the veins are all structurally controlled, we suggest that the distribution of mines and prospects, quartz veins, and mapped areas of hydrothermal alteration (Kellogg, 1994) relative to the Archean (?) leucogranite pluton presents the possibility that the gold mineralization is related to an earlier (pre-Cretaceous) magmatic event (see discussion of "Gold vein systems").

We analyzed two samples from the area between the historic Grubstake and Golconda mines. The geology of this area is shown on a recent geologic map of the Norris 7.5-minute quadrangle (Kellogg, 1994). Sample 95JH094 (map key 53 in fig. 2, tables 1 and 11) is fault gouge collected at an adit in altered gneiss. The adit appears to be aligned along a N.65W.-trending shear zone. No quartz veining or evidence of a mine dump were present on the site. Sample 95JH094 contained 18 ppb gold, but no detectable silver or zinc; copper and lead were not determined. The other sample, 95JH096 (map key 54 in fig. 2, tables 1 and 11), is an iron-stained, brecciated quartz vein from a prospect pit near the head frame of the Golconda mine site (as shown on a sketch map by Kellogg, 1993). This sample is highly anomalous in gold (50,500 ppb or 50 ppm), and also contains silver (31 ppm), arsenic (110 ppm), molybdenum (16 ppm), antimony (1.6 ppm), and tellurium (0.6 ppm). The high gold content of this randomly collected sample probably represents a nugget effect. Such gold values probably explain the continued exploration interest in area. There are probably localized pockets of high-grade gold remaining in the vein systems; the difficulty for future development likely depends on finding an economic concentration of ore of sufficient tonnage in a minable body to warrant development. Although the gold is reportedly associated with sulfide minerals, and acid-buffering carbonate rocks are absent in the area, these systems do not appear to be particularly sulfide-rich. A geoenvironmental model for low sulfide gold quartz veins (Goldfarb and others, 1995) provides a description of potential environmental considerations relevant to the types of deposits in the Red Bluff area. The potential for acid rock drainage for these types of mineral deposits is relatively low compared to massive sulfide deposits or to porphyry systems (Kwong, 1993).

Table 11. Analytical data for rock samples from the Red Bluff mining district.
[See text for explanation of methods]

Map key			53	54
Sample number			95JH094	95JH096
Job number			AHK1256	AHK1256
Element	Units	Method		
Ag	ppm	INAA	<5	31
As	ppm	INAA	2.7	110
Au	ppb	INAA	18	50,500
Ba	ppm	INAA	<50	170
Bi	ppm	ICP-HY	<0.2	0.2
Br	ppm	INAA	<0.5	2.2
Ca	%	INAA	<1	<1
Ce	ppm	INAA	6	<3
Co	ppm	INAA	43	61
Cr	ppm	INAA	<5	<5
Cs	ppm	INAA	<1	<1
Eu	ppm	INAA	<0.2	<0.2
Fe	%	INAA	0.36	9.65
Ge	ppm	ICP-HY	<0.2	<0.2
Hf	ppm	INAA	<1	<1
Hg	ppm	INAA	<1	<1
Ir	ppb	INAA	<5	<5
La	ppm	INAA	3.3	4.8
Lu	ppm	INAA	<0.05	<0.05
Mo	ppm	INAA	<1	16
Na	%	INAA	1.66	0.02
Nd	ppm	INAA	<5	<5
Ni	ppm	INAA	120	<33
Rb	ppm	INAA	52	29
Sb	ppm	INAA	<0.1	1.6
Sc	ppm	INAA	0.5	2.9
Se	ppm	ICP-HY	0.2	0.4
Se	ppm	INAA	<3	<3
Sm	ppm	INAA	0.2	0.3
Sn	ppm	INAA	<100	<100
Sr	ppm	INAA	<500	<500
Ta	ppm	INAA	<0.5	<0.5
Tb	ppm	INAA	<0.5	<0.5
Te	ppm	ICP-HY	0.2	0.6
Th	ppm	INAA	<0.5	1.6
U	ppm	INAA	<0.5	6.8
W	ppm	INAA	750	440
Yb	ppm	INAA	<0.2	<0.2
Zn	ppm	INAA	<50	260

Revenue mining district (Table 12)

The Revenue district lies immediately west of the Red Bluff district (fig.3) and includes the Revenue mine and the Galena mine, both of which were considered part of the historic Norris district (Tansley and others, 1933; Lorain, 1937). This district produced gold from vein systems. Unlike the veins of the Red Bluff district, these veins lie within the granitoid rocks of Tobacco Root batholith, near its exposed eastern margin.

The Revenue mine is in the Richmond Flat area, about 10 miles southwest of Norris. Tansley and others (1933) described the mineral deposit at the Revenue mine as a complex system of fissure veins within granite. The main Revenue vein was described as a nearly flat-lying, 2 to 3 ft wide vein that trends northeast; high-grade gold intercepts occur where this vein is cut by more steeply dipping fissure veins. Most of ore was mined as free gold from an oxidized zone composed of quartz and limonite; pyrite was reported at deeper levels (Tansley and others, 1933). The Revenue mine produced over 15,000 ounces of gold and over 16,000 ounces of silver before 1921. When we visited the area in 1995, Majesty Mining company was developing a heap leach operation, the East Revenue Mine, to recover gold from the oxidized zone exposed at the surface. We observed narrow quartz veins, open-space growth of quartz, and extensive silicification and iron-staining in fractured granodiorite (or quartz monzonite) and sampled a variety of rock types, including high-grade ore from the pit wall, quartz vein material, and altered granodiorite (map key 55-58 in fig.2, tables 1 and 12). Gold was detected in all samples (2,850 to 8,740 ppb), as was silver (13 to 15 ppm) and tellurium (1.9 to 8.3 ppm). Antimony and selenium are present at concentrations of about 1 ppm each. The relatively high tellurium values distinguish these samples from other vein systems analyzed in this study.

The Galena mine is located about two miles due north of the Revenue mine, west of the historic town of Sterling. Lorain (1937) described the deposit as a series of sheeted zones of stringers of quartz in quartz monzonite. The stringers fan out into "horsetail" veins and, although there were locally high grades, most of the stringers were difficult to mine by 1930's methods. These types of deposits might be more amenable to modern bulk mining techniques such as heap leaching. Gold was apparently produced from the oxidized zone; however, Tansley and others (1933) report galena, sphalerite, chalcocite, bornite, and pyrite on dump material from the lower mine workings. This area was explored in the early 1990's by Newmont Exploration Limited in joint venture with Westmont Gold Inc. as the Maltby's Mound project (Sagar and Childs, 1993), with plans to develop an open pit and heap leach operation to process gold from oxidized ore in a major northwest-trending shear zone of a wrench fault. Proven and probable reserves were reported as 5.7 million metric tons averaging 1.3 grams/metric ton gold as of 1992, and measured and indicated metal reserves were reported as 500,000 ounces of gold within indicated reserves of 1 million ounces (Randol, 1995). We analyzed one sample of sulfide-bearing, limonite-stained quartz vein (map key 59 on tables 1 and 12) that ran extremely high in gold (18,000 ppb) and silver (32 ppm). Copper and lead were not determined; zinc is below detection level (<50 ppm). Tellurium (1.1 ppm) and antimony (0.4 ppm) are present at lower concentrations than observed for the samples from the Revenue mine area.

Table 12. Analytical data for rock samples from the Revenue mining district.
[See text for explanation of methods; *, replicate samples]

Map key			55	56	57	58	59
Sample number			95JH083	95JH283*	95JH084	E9509	E9508
Job number			AHK1256	AHK1256	AHK1256	AHK1256	AHK1256
Element	Units	Method					
Ag	ppm	INAA	<5	13	15	14	32
As	ppm	INAA	6.3	9.7	2	9.7	4
Au	ppb	INAA	3,390	2,850	3,610	8,740	18,000
Ba	ppm	INAA	1,200	1,300	780	300	340
Bi	ppm	ICP-HY	0.2	0.6	1.3	3.9	3.9
Br	ppm	INAA	<0.5	<0.5	<0.5	1.8	1.1
Ca	%	INAA	<1	<1	<1	<1	<1
Ce	ppm	INAA	16	15	12	14	22
Co	ppm	INAA	16	27	25	29	27
Cr	ppm	INAA	5	<5	<5	<5	<5
Cs	ppm	INAA	2	<1	<1	1	<1
Eu	ppm	INAA	<0.2	<0.2	0.3	<0.2	0.4
Fe	%	INAA	1.35	1.05	0.83	1.17	3.22
Ge	ppm	ICP-HY	<0.2	<0.2	<0.2	<0.2	<0.2
Hf	ppm	INAA	<1	<1	<1	<1	3
Hg	ppm	INAA	<1	<1	<1	<1	<1
Ir	ppb	INAA	<5	<5	<5	<5	<5
La	ppm	INAA	12	12	11	11	17
Lu	ppm	INAA	<0.05	0.06	<0.05	0.06	0.1
Mo	ppm	INAA	<1	<1	3	9	7
Na	%	INAA	2.01	2.21	1.78	0.05	0.05
Nd	ppm	INAA	<5	<5	6	<5	8
Ni	ppm	INAA	<27	<27	<25	<20	<20
Rb	ppm	INAA	120	110	100	140	86
Sb	ppm	INAA	0.9	1.1	0.7	6.3	0.4
Sc	ppm	INAA	1.2	1.2	1	1.4	1.6
Se	ppm	ICP-HY	0.7	0.8	1.6	0.2	0.5
Se	ppm	INAA	<3	<3	<3	<3	<3
Sm	ppm	INAA	0.8	0.7	0.6	0.7	1.3
Sn	ppm	INAA	<100	<100	<100	<100	<100
Sr	ppm	INAA	<500	<500	<500	<500	<500
Ta	ppm	INAA	<0.5	<0.5	2.4	1.1	<0.5
Tb	ppm	INAA	<0.5	<0.5	<0.5	<0.5	<0.5
Te	ppm	ICP-HY	7.5	10	1.9	8.3	1.1
Th	ppm	INAA	3.1	3.2	2	5.2	10
U	ppm	INAA	<0.5	1	1.2	1.8	6.7
W	ppm	INAA	130	190	260	370	210
Yb	ppm	INAA	0.4	0.4	0.6	<0.2	0.8
Zn	ppm	INAA	130	120	75	150	<50

Ruby Mountains mining district (Table 13)

Archean banded iron formation of the Carter Creek iron deposit crops out along the western margin of the Ruby Mountains mining district (map key 60 and 61 on fig. 3 and tables 1 and 13). The area was mapped in detail by James and Wier (1972) and James (1990). We sampled banded iron formation and silicified dolomite near the iron formation contact. Neither sample contains gold or silver above detection limits. See the discussion of "Iron formation" for a comparison of the trace element signature of this banded iron formation with others in the study area.

Table 13. Analytical data for rock samples from the Ruby Mountains mining district.
[See text for explanation of methods]

Map key			60	61
Sample number			96JH30	96JH26
Job number			AHK1787	AHK1787
Element	Units	Method		
Ag	ppm	ICP	<0.4	<0.4
Ag	ppm	INAA	<5	<5
Al	%	ICP	0.13	0.12
As	ppm	INAA	2.5	78
Au	ppb	INAA	<2	<2
Ba	ppm	INAA	91	<50
Be	ppm	ICP	2	<2
Bi	ppm	ICP-HY	1.0	<1.0
Bi	ppm	ICP	<5	<5
Br	ppm	INAA	<0.5	<0.5
Ca	%	ICP	0.41	6.97
Ca	%	INAA	<1	7
Cd	ppm	ICP	<0.5	<0.5
Ce	ppm	INAA	14	<3
Co	ppm	INAA	1	3
Cr	ppm	INAA	13	11
Cs	ppm	INAA	<1	<1
Cu	ppm	ICP	2	2
Eu	ppm	INAA	0.3	<0.2
Fe	%	INAA	25.5	1.34
Ge	ppm	ICP-HY	0.4	<0.2
Hf	ppm	INAA	<1	<1
Hg	ppm	INAA	<1	<1
Ir	ppb	INAA	<5	<5
K	%	ICP	0.12	0.05
La	ppm	INAA	7.1	0.9
Lu	ppm	INAA	0.1	<0.05
Mg	%	ICP	0.65	3.54
Mn	ppm	ICP	217	374
Mo	ppm	ICP	<2	<2
Mo	ppm	INAA	<1	2
Na	%	INAA	0.21	0.02
Nd	ppm	INAA	6	<5
Ni	ppm	ICP	3	9
Ni	ppm	INAA	<20	<20
P	%	ICP	0.029	0.095
Pb	ppm	ICP	<5	10
Rb	ppm	INAA	<15	<15
Sb	ppm	INAA	2	2

Table 13.--Continued.

Map key			60	61
Sc	ppm	INAA	0.3	0.4
Se	ppm	ICP-HY	<0.2	<0.2
Se	ppm	INAA	<3	<3
Sm	ppm	INAA	1	0.1
Sn	%	INAA	<0.01	<0.01
Sr	ppm	ICP	13	22
Sr	ppm	INAA	<500	<500
Ta	ppm	INAA	<0.5	<0.5
Tb	ppm	INAA	<0.5	<0.5
Te	ppm	ICP-HY	<0.2	<0.2
Th	ppm	INAA	<0.2	0.2
Ti	%	ICP	0.01	0.01
U	ppm	INAA	<0.5	1
V	ppm	ICP	4	14
W	ppm	INAA	<1	7
Y	ppm	ICP	8	2
Yb	ppm	INAA	0.6	<0.2
Zn	ppm	ICP	3	4
Zn	ppm	INAA	<50	<50

Sheridan mining district (Table 14)

The Sheridan district (alternate names include Mill Creek, Ramshorn, Indian Creek, and Brandon) includes the southwestern part of the Tobacco Root Range in Madison County. The northeastern half of the district is in Beaverhead National Forest; the southwestern half of the district is a patchwork of BLM land, state lands, and private land. Between 1901 and 1935, the Sheridan district produced 29,114 ounces of gold, 185,044 ounces of silver, over 1 million pounds of lead, 151,661 pounds of copper, and 294,452 pounds of zinc (Lorain, 1937). Production came from small-scale workings along structurally controlled polymetallic veins peripheral to the Tobacco Root batholith. The mineralogy of the veins varied from pyrite-chalcopyrite to pyrite-galena-sphalerite. The veins in this district have a base-metal rich character and many of the base metal deposits in the northern part of the district are veins and replacements in carbonate rocks. We confined our sampling to an area of BLM lands around Copper Mountain (fig. 3), in section 1, T.5 S., R.4W. Copper Mountain is a small body of Archean marble in Archean hornblende gneiss and granulite interbedded with quartzite and iron formation (James and Wier, 1962; Vitaliano and Cordua, 1979). Small satellite stocks of Cretaceous intrusives of the Tobacco Root batholith crop out in the area. More than 30 lode claims were located in the Copper Mountain area between 1975 and 1991, and a few claims are actively maintained (MCRS, 1996). FMC Mineral Corporation operated a gold exploration project, the Ramshorn project, in the area and reported in their 1993 annual report that they might relinquish the property due to the small size of the geologic resource delineated in the property (Randol, 1995).

In the study of the Dillon 1° by 2° quadrangle, Loen and Pearson (1989) noted that iron, talc, chromite, thorite, and manganese are present in the Archean rocks of the Sheridan district, but none of these occurrences have been exploited. We sampled iron formation (map key 62, 64, 65 on tables 1 and 14) for gold and trace elements. The iron formation was mapped in detail by James (1981) and James and Wier (1962). All three samples are relatively iron-rich (25 to 38 weight percent iron), but gold is below or slightly above detection limits (maximum 7 ppb gold). All three samples of iron formation contained platinum (0.5 to 2.1 ppb), palladium (0.7 to 1.4 ppb), and iridium (0.9 to 1.5 ppb).

Quartzite (map key 63 on tables 1 and 14) from a pit at the Copper Mountain mine at the crest of Copper Mountain (also known as the Dictator and Belle Union prospect) is anomalous for gold (245 ppb); silver was below detection limits (<5 ppm). Copper and lead were not determined; zinc is below detection levels (<50 ppm). Most of the rock exposed in the pit is quartzite; amphibolite-rich gneiss is exposed at the north end of the pit and marble is exposed at the south end. Weathered ultramafic rocks, large blocks of white to greenish quartzite, copper-stained quartzite, and a biotite-rich reaction zone (probably developed at the ultramafic contact) are all exposed at this site. The quartzite may have potential for use as a decorative stone.

Table 14. Analytical data for rock samples from the Sheridan mining district.
[See text for explanation of methods; n.d., not determined]

Map key			62	63	64	65
Sample number			E9514	E9513	95JH110	95JH113
Job number			AHK1241	AHK1256	AHK1241	AHK1241
Element	Units	Method				
Ag	ppm	INAA	<5	<5	<5	<5
As	ppm	INAA	<0.5	3.4	1.2	<0.5
Au	ppb	ICP/MS	2	n.d.	7	<1
Au	ppb	INAA	<2	245	<2	<2
Ba	ppm	INAA	<50	310	240	210
Bi	ppm	ICP-HY	n.d.	0.4	n.d.	n.d.
Br	ppm	INAA	<0.5	2.7	<0.5	<0.5
Ca	%	INAA	<1	<1	1	<1
Ce	ppm	INAA	11	38	29	20
Co	ppm	INAA	21	62	19	14
Cr	ppm	INAA	180	210	130	120
Cs	ppm	INAA	<1	<1	<1	<1
Eu	ppm	INAA	0.3	0.3	0.5	0.3
Fe	%	INAA	37.6	0.84	25.7	31.3
Ge	ppm	ICP-HY	n.d.	<0.2	n.d.	n.d.
Hf	ppm	INAA	1	9	1	1
Hg	ppm	INAA	<1	<1	<1	<1
Ir	ppb	INAA	<5	<5	<5	<5
Ir	ppb	ICP/MS	0.9	n.d.	1.5	1
La	ppm	INAA	6.3	26	17	12
Lu	ppm	INAA	0.11	0.11	0.17	0.1
Mo	ppm	INAA	<1	<1	<1	<1
Na	%	INAA	<0.01	0.12	0.01	<0.01
Nd	ppm	INAA	<5	9	7	5
Ni	ppm	INAA	<29	270	<28	<28
Pd	ppb	ICP/MS	0.7	n.d.	1.4	0.8
Pt	ppb	ICP/MS	0.8	n.d.	2.1	0.5
Rb	ppm	INAA	<15	21	25	<15
Rh	ppb	ICP/MS	0.4	n.d.	<0.1	0.2
Sb	ppm	INAA	<0.1	1.2	0.1	<0.1
Sc	ppm	INAA	5	1.3	5.8	3.8
Se	ppm	ICP-HY	n.d.	<0.2	n.d.	n.d.
Se	ppm	INAA	<3	<3	<3	<3
Sm	ppm	INAA	0.9	1.8	2	1.3
Sn	ppm	INAA	<100	<100	<100	<100
Sr	ppm	INAA	<500	<500	<500	<500
Ta	ppm	INAA	<0.5	1.1	0.7	<0.5
Tb	ppm	INAA	<0.5	<0.5	<0.5	<0.5

Table 14.--Continued.

Map key			62	63	64	65
Te	ppm	ICP-HY	n.d.	0.5	n.d.	n.d.
Th	ppm	INAA	4.2	11	5.9	5
U	ppm	INAA	<0.5	1.3	1.6	0.9
W	ppm	INAA	110	490	55	54
Yb	ppm	INAA	0.8	0.6	1	0.7
Zn	ppm	INAA	62	<50	<50	<50

Silver Star mining district (Table 15)

The Silver Star (Iron Rod) district borders the southern margin of the Cretaceous Boulder batholith. Mineral deposits include vein and replacement base and precious metals deposits in Archean quartzofeldspathic gneiss and gold-bearing copper skarn deposits that developed in limestone along the contact of the Rader Creek pluton of the Boulder batholith (Loen and Pearson, 1989; O'Neill and others, 1996). The Archean rocks in the district also host isolated occurrences of chlorite (Golden Antler mine) and chromite (Mohawk mine, Aurora occurrence). The district produced over 10,000 ounces of gold, 18,850 ounces of silver, and 347,130 pounds of lead between 1867 and 1932 (Sahinen, 1939). Most of the historic mines are on private land, surrounded by BLM lands.

Recent exploration activity in the district has focussed on the gold-bearing oxidized skarn, which was explored most recently by BMR Gold Corporation as the Madison copper-gold project; they calculated open pit reserves of 1.3 million tons averaging 0.068 ounces of gold per ton, underground reserves of 340,000 tons averaging 0.424 ounces of gold per ton, and significant undefined copper values (Randol, 1995). The deposit is a classic zoned skarn, with well-developed zones of calc-silicate minerals. A nearly monomineralic mass of the iron-rich pyroxene mineral hedenbergite is exposed in one of the pits. Foote (1986) described the mineralogy and paragenesis of the skarn. We analyzed three varieties of skarn (garnet, epidote, and hedenbergite) from surface samples (map key 66, 67, and 68 on tables 1 and 15) to characterize the gold content and minor element signature. All three samples run in gold (13 to 5,970 ppb); silver is below detection limits (<5 ppm). Bismuth (0.7 to 211 ppm) and tellurium (0.2 to 2.3 ppm) are present in all three samples. These two elements are useful geochemical indicators for many gold-bearing skarn systems (Theodore and others, 1991). Unlike the gold skarn system at Bannack in the Dillon 1° by 2° quadrangle (Loen and Pearson, 1989), no gold placer workings are associated with the skarn at Silver Star. Although the deposit is pyrite-rich, limestone resources available on-site could be used in the design of any future mining operations to mitigate potential acid drainage.

The Mohawk mine produced a small amount of chromite during World War II (1942) from 2,000 ft of drifts, crosscuts, and raises (Trauerman and Reyner, 1950) from a block of chromite enclosed in Archean quartzofeldspathic gneiss. We observed a 50 ft wide seam of massive chromite in a pit that exposes a concordant contact between strongly foliated, possibly sheared or mylonitic, leucogneiss and a chromite-rich, cumulate ultramafic rock that grades into massive chromite. Locally, the ultramafic rock is serpentinized and coated with caliche. We analyzed one sample of fine-grained chromite (map key 69, tables 1 and 15) for gold and PGE. The sample contained 5,900 ppm chromium, negligible gold (1 ppb), and 14.1 ppb combined PGE.

Table 15. Analytical data for rock samples from the Silver Star mining district.
[See text for explanation of methods; n.d., not determined]

Map key			66	67	68	69
Sample number			E9505	E9506	E9504	E9507
Job number			AHK1256	AHK1256	AHK1256	AHK1241
Element	Units	Method				
Ag	ppm	INAA	<5	<5	<5	<5
As	ppm	INAA	13	11	4.2	1.5
Au	ppm	ICP/MS	n.d.	n.d.	n.d.	1
Au	ppb	INAA	65	13	5,970	<2
Ba	ppm	INAA	100	<50	<50	<50
Bi	ppm	ICP-HY	0.7	211	3	n.d.
Br	ppm	INAA	1.3	1.3	1	0.7
Ca	%	INAA	21	18	15	<1
Ce	ppm	INAA	<3	80	<3	3
Co	ppm	INAA	29	6	13	82
Cr	ppm	INAA	48	110	10	5,900
Cs	ppm	INAA	2	<1	<1	<1
Eu	ppm	INAA	<0.2	2.2	<0.2	<0.2
Fe	%	INAA	9.58	8.16	14.4	14.4
Ge	ppm	ICP-HY	0.5	<0.2	0.2	n.d.
Hf	ppm	INAA	2	5	<1	<1
Hg	ppm	INAA	<1	<1	<1	<1
Ir	ppb	ICP/MS	n.d.	n.d.	n.d.	5.2
Ir	ppb	INAA	<5	<5	<5	<5
La	ppm	INAA	0.7	55	<0.5	0.9
Lu	ppm	INAA	0.16	0.25	<0.05	0.05
Mo	ppm	INAA	<1	8	<1	<1
Na	%	INAA	0.08	0.02	0.44	0.02
Nd	ppm	INAA	<5	28	<5	<5
Ni	ppm	INAA	<20	<20	<20	1700
Pd	ppb	ICP/MS	n.d.	n.d.	n.d.	1.5
Pt	ppb	ICP/MS	n.d.	n.d.	n.d.	5.6
Rb	ppm	INAA	<15	<15	<15	<15
Rh	ppb	ICP/MS	n.d.	n.d.	n.d.	1.8
Sb	ppm	INAA	0.6	12	4.4	0.1
Sc	ppm	INAA	5.6	8.6	0.1	5.7
Se	ppm	ICP-HY	<0.2	1.1	0.2	n.d.
Se	ppm	INAA	<3	<3	<3	<3
Sm	ppm	INAA	0.8	5.4	<0.1	0.2
Sn	ppm	INAA	<100	<100	<100	<100
Sr	ppm	INAA	<500	<500	<500	<500
Ta	ppm	INAA	<0.5	<0.5	<0.5	<0.5
Tb	ppm	INAA	<0.5	<0.5	<0.5	<0.5

Table 15.--Continued.

Map key			66	67	68	69
Te	ppm	ICP-HY	0.2	2.3	1.8	n.d.
Th	ppm	INAA	4.2	8.2	<0.5	<0.2
U	ppm	INAA	<0.5	6.5	<0.5	<0.5
W	ppm	INAA	86	27	38	7
Yb	ppm	INAA	1.1	1.6	0.2	0.2
Zn	ppm	INAA	270	210	250	57

Virginia City mining district (Table 16)

The Virginia City mining district (also known as the Browns Gulch, Barton Gulch, Granite Creek, Williams Gulch, Fairweather, or Alder Gulch district) is one of the most significant historic placer gold districts in the United States (Lyden, 1948). More than 2.5 million ounces of gold were produced from the 1890's until the 1940's, mainly from placer workings along Alder Gulch between the towns of Nevada City and Virginia City (Yeend and Shawe, 1989). The lode source of the placer gold has been the subject of considerable scientific debate for more than 100 years (Shawe and Wier, 1989; Barnard, 1993). Recently, exploration interest in the historic lode mines along the upper reaches of the main drainage of Alder Gulch (U.S. Grant, Kearsarge, and Garrison mine areas) and the drainages to the west along Hungry Hollow Gulch and Browns Gulch (Easton-Pacific mine) has peaked, as a number of mining companies have tried to consolidate land positions and define potential mining targets in the district (Eimon, 1997). Although the lands along Alder Gulch itself and many of the historic workings are on private land, BLM lands and state lands border the private lands and some of the historic workings are on, or adjacent to, federal lands. The area of most recent exploration activity falls within the Virginia City and Cirque Lake 7.5-minute quadrangles (fig. 5). The historic lode mines of the district were developed as underground mines that followed quartz veins and lenses in highly fractured shear zones in Archean quartzofeldspathic gneiss. Although the details vary from mine to mine, most of the "veins" were a few inches to a few feet thick, or occurred as zones of closely spaced veins or lenses with pockets of high-grade ore; some ore is disseminated in wallrock adjacent to veins. The predominant vein orientations in the district are northwest and northeast. No adequate modern geologic map of the district exists. Tansley and others (1933) provided a geologic sketch map of the district. Wier (1982) prepared an outcrop map of the Virginia City 7.5-minute quadrangle and Cole (1983) included a bedrock map of the northern part of the district in his thesis, based on his own mapping and a compilation of existing maps. Hadley (1969) mapped the Varney 15-minute quadrangle, which covers the southern parts of the district in the Cirque Lake 7.5-minute quadrangle.

The key observation that must be taken into account in any exploration model for the district is the structural control of the precious metal-rich quartz veins of the district. Intersections of vein systems are likely to be the most attractive exploration targets (Eimon, 1997), and discontinuities and offsets of vein systems are likely to be the limiting factor in defining minable ore reserves. Much of the debate over the nature of the lode gold deposits revolves around the age (Archean, Proterozoic, Cretaceous, or Tertiary) and relation of the veins to one or more postulated, but unexposed, intrusive centers. The models proposed to date vary in detail, but generally espouse two different end-member mineral deposit types: (1) Archean lode gold deposits, such as those found in Archean greenstone-sedimentary belts elsewhere (Boyle, 1991); and (2) veins related to Cretaceous or younger intrusive centers. Studies in progress should clarify the age relations and genetic associations of the lode gold deposits; however, to date, the lack of a detailed geologic framework on a district-wide scale has hindered interpretation of existing data. In the following discussion, we analyze the existing published data on the district geology and age relations as a context for discussing geochemical data from samples from the central and northern parts of the district. We find none of the proposed models adequate to account for all of the existing data, and a number of different processes and events may have operated in different parts of the district over geologic time. Regardless of whether or not the lode gold deposits south of Virginia City provided all of the placer gold in Alder Gulch, there are a number of features that distinguish the area from the surrounding terrane and these features may be important in the localization of gold in the district.

Most recently, Eimon (1997) provided a comprehensive review of models proposed for the district, and defined additional exploration targets near the head of Alder Gulch in the southern part of the district, based on projected fault zone intersections. He also postulated a heat source (Garrison igneous complex) for the hydrothermal event(s). Both Barnard (1993) and Lockwood (1990) cited mineral zoning in the central part of the district and in the Easton-Pacific area as evidence for an unexposed hydrothermal source (intrusion). Barnard (1993) plotted available mineralogic data from the literature for all of the workings in the district and defined a series of mineral zones based on computed galena:pyrite ratios. He argued that these "zones" are concentric to a buried intrusion or heat source responsible for mineralization. Shawe and Wier (1989) also defined zones based on silver to gold ratios from vein production; they showed a relatively low Ag:Au zone (2:1 to 10:1) just south of Virginia City in the area of the U.S. Grant mine and also just north of Baldy Mountain near the head of Alder Gulch in the Garrison mine area. In between these two zones is a

wide area of veins characterized by silver to gold ratios ranging from 10:1 to 50:1. The silver-rich zone generally coincides with Barnard's barren zone and surrounding pyrite-galena zone, whereas the more gold-rich zone of Shawe and Wier overlaps Barnard's galena zone. Previously, Lorain (1937) suggested that the variation in the copper:silver:gold ratios of the districts in the entire region reflected zonation around the Tobacco Root batholith. Others have suggested that the lode gold deposits represent metamorphic low-sulfide gold-quartz veins that formed during the Archean or remobilized during subsequent metamorphism.

All of the lodes are hosted by Archean metamorphic rocks. To the east of Alder Gulch, the Archean rocks are covered by Tertiary volcanics. A few plugs of the volcanics are present in the area of some of the mines, and an andesite plug dated at 51.1 ±1.2 Ma (whole rock K-Ar date by Marvin and Dobson, 1979) cuts the El Fleeda vein system. This age at the El Fleeda mine—in the northern part of the district about a mile (1.5 km) south of Virginia City on the west side of Alder Gulch—suggests that at least some of the mineralization is older than Eocene (Cole, 1983). A number of workers have considered the mines of the district to be related to the Cretaceous Tobacco Root batholith, which is surrounded by lode gold vein deposits. However, the main mass of the batholith is 15 miles (24 km) north of the northern end of the district, and no satellite plutons are recognized in this district (such as those present near Copper Mountain).

On regional-scale geophysical maps, the Tobacco Root batholith is a prominent magnetic high anomaly that coincides with a gravity low anomaly; this pattern reflects the density contrast between the rocks of the batholith and the Archean metamorphic rocks they intrude (Hanna and others, 1993). No similar pattern suggestive of a large, buried intrusion is apparent in the regional-scale geophysics for the Virginia City area (Pinckney and others, 1980). Barnard (1993) noted the contrast in geophysics between the Tobacco Root and Virginia City areas and suggested that although existing geophysical data for the area is too generalized to determine a felsic intrusive in the Virginia City district, the weak magnetic and gravity lows there are permissive for a granitic intrusion of low density and low magnetic content. Tansley and others (1933) and Cole (1983) show a northwest-southeast-trending, ovoid-shaped intrusive body in the areas of the Easton and Pacific mines, west of Browns Gulch. Tansley and others (1933) called this rock a quartz monzonite aplite; Cole (1983) called it the "late Cretaceous granitic Brown's Gulch stock". The rationale for the Late Cretaceous age assigned to the stock is not apparent. Winchell (1914) described the host rock for the vein at the Easton and the Pacific mines as a feldspar-rich, lenticular mass of quartz monzonite aplite that cuts gneiss. He described the mineralogy of the aplite as quartz, microcline, orthoclase, sericitized plagioclase, and rare muscovite. Lockwood (1990) noted that the stock trends northwest, crosscuts gneissic rocks, and is hard to distinguish from luecogneisses in the area because of similar mineralogy and texture. Following the conclusions of previous wokrers, he also consdiered the stock to be of Cretaceous age. On Hadley's (1969) geologic map, the area of the "stock" near the Easton mine (northwest end) is not shown separately; it lies within an area mapped as Precambrian granite (gneiss) and migmatite. The area near the Pacific mine (southeast end) is shown to lie within biotite and hornblende gneiss of the Cherry Creek Group. The Cherry Creek Group package of rocks includes beds of dolomitic marble, schist, and quartzite of Archean age. Wier (1982) mapped at a much larger scale than Hadley (1:12,000 versus 1:62,500) and used different map units. Wier described the predominant rock type in the area as mainly non-foliated to foliated quartz-feldspar gneiss. He mapped individual outcrops of amphibolite, marble, and pegmatite separately. The maps of Wier (1982) and Hadley (1969) both show scattered, small ultramafic bodies throughout the area. Wier's map shows an unusually dense concentration of pegmatite, mainly narrow dikes of coarse quartz-feldspar pegmatite oriented in a northwesterly direction. Marginal-facies pegmatites of the Tobacco Root batholith occur within the batholith and in adjacent rocks; Cretaceous pegmatites related to the batholith contain sulfide minerals, whereas Precambrian pegmatites lack sulfides (Vitaliano and Cordua, 1979). The Tobacco Root batholith is a composite body that ranges in composition from hornblende diorite to monzonite. We consider it unlikely to have genetically-related, homogeneous aplitic plutons so far removed from the main mass of the batholith, and therefore, we suggest that the aplite "stock" of upper Browns Gulch is probably part of an older (Proterozoic?) granitic intrusion related to the pegmatites.

Wier (1982) mapped a localized swarm of northwest-trending, medium-grained granitic dikes north of Williams Creek, reported a preliminary date of 1.9 b.y. for one of these dikes, and concluded that these granitic dikes are probably genetically related to the pegmatites. We know of no reports of sulfide minerals

in pegmatites in the Virginia City district, such as are observed in Cretaceous pegmatites near the Tobacco Root batholith. The only report of a granitic intrusive rock in the northern part of the district is a description of porphyritic granite dikes and sills encountered in drill core on the third level of the U.S. Grant vein system (Sheets, 1980). Although these granites were interpreted as Cretaceous in age, the description of high concentrations of pink potassic feldspar suggests that these rocks may also represent Proterozoic(?) intrusives related to the pegmatites.

Lockwood (1990) interpreted the vein deposits at the Easton-Pacific mine as epithermal to mesothermal deposits genetically related to the Tobacco Root batholith. Although we have not mapped the area, our site visit leads us to interpret the "stock" as an aplitic facies within, or intrusive into, Precambrian granitic gneiss. Lack of a prominent metamorphic fabric (foliation) in the more granitic/aplitic bodies within the gneiss may reflect their mineralogy and grain size. For example, the rocks may have been through a metamorphism without substantial change in fabric because the dark-colored, elongate minerals that define the fabric in more mafic gneiss, such as biotite and hornblende, are absent from the mineral assemblage. The unfoliated, aplitic rocks in the Virginia City district (including the Brown's Gulch stock and Eimon's Garrison igneous complex) may be Early Proterozoic in age; O'Neill and others (1996) describe leucocratic granitic aplite and pegmatite sills of Early Proterozoic age in the southern part of the Highland Mountains. The relevance of any Proterozoic hydrothermal activity to lode gold deposition is unknown at present; however, any gold deposited at that time could have been remobilized along structures that formed, or more likely were reactivated, during the Laramide-style deformation of the Late Cretaceous.

Eimon (1997) noted that Russel J. Franklin bracketed the timing of vein formation as following the intrusion of Proterozoic pegmatite dikes and before the extrusion of Tertiary basalts, presumably on the basis of observed cross-cutting relationships. Cole (1983) reported two K-Ar mineral dates from the area of the U.S. Grant mine in the northern part of the district: (1) an age of 1572 m.y. ±51 m.y. for a biotite from a pegmatite exposed in underground workings; and (2) an age of 311 ±11 m.y. for an impure potassium feldspar sample from altered wallrock at the same mine level where the pegmatite was sampled. The biotite age is consistent with the 1.6 b.y. age of the last regional metamorphic event (Kovaric and others, 1996). The feldspar age is problematic and sheds little light on the age of mineralization in the district. Cole (1983) noted that the feldspar population of the wallrock represented a mixture of hydrothermal microcline and sericitized "Precambrian" feldspar, and interpreted the age of the sample as a composite representing a mixture of Cretaceous or Tertiary hydrothermal microcline and older feldspar. Sericite could have formed as an alteration product at any time; any sericite present in the sample will contribute to the age, and the sericite as well as the two different generations of potassium feldspar confound any interpretation of the age of this sample.

Finding suitable materials for age determinations is a problem in these rocks because there is so much intergrown potassium feldspar and sericitic alteration and because potassium is so mobile during metamorphism. Much of the potassium feldspar in the pegmatites and in the quartzofeldspathic gneiss is a distinctive salmon pink color. Masses of nearly monomineralic salmon-colored feldspar are associated with the quartz veins at the Kearsarge mine (Merlin Bingham, oral communication, 1993), and cloudy, colorless untwinned potassium feldspar (adularia) forms thin selvages or protrudes into quartz veins sampled at many of the mines in the district.

Many of the quartz veins observed on the surface and in dump materials show textures typical of epithermal to mesothermal vein systems, such as open-space growth, vugs, and doubly terminated crystals. Masses of doubly terminated quartz crystals cemented by limonite and siderite are common on the dumps at the Easton mine and at workings along Hungry Hollow Gulch. Barnard (1993) referred to this texture as "candle-quartz" and noted that it is especially common in upper Alder Gulch, associated with a distinct episode of mineralization that deposited gold, pyrite, and tellurides.

We collected 30 samples from the Virginia City district for chemical analysis (tables 1 and 16, map key 70-100). The caveats about tungsten data discussed at the beginning of this report are particularly important for data from the Virginia City district.

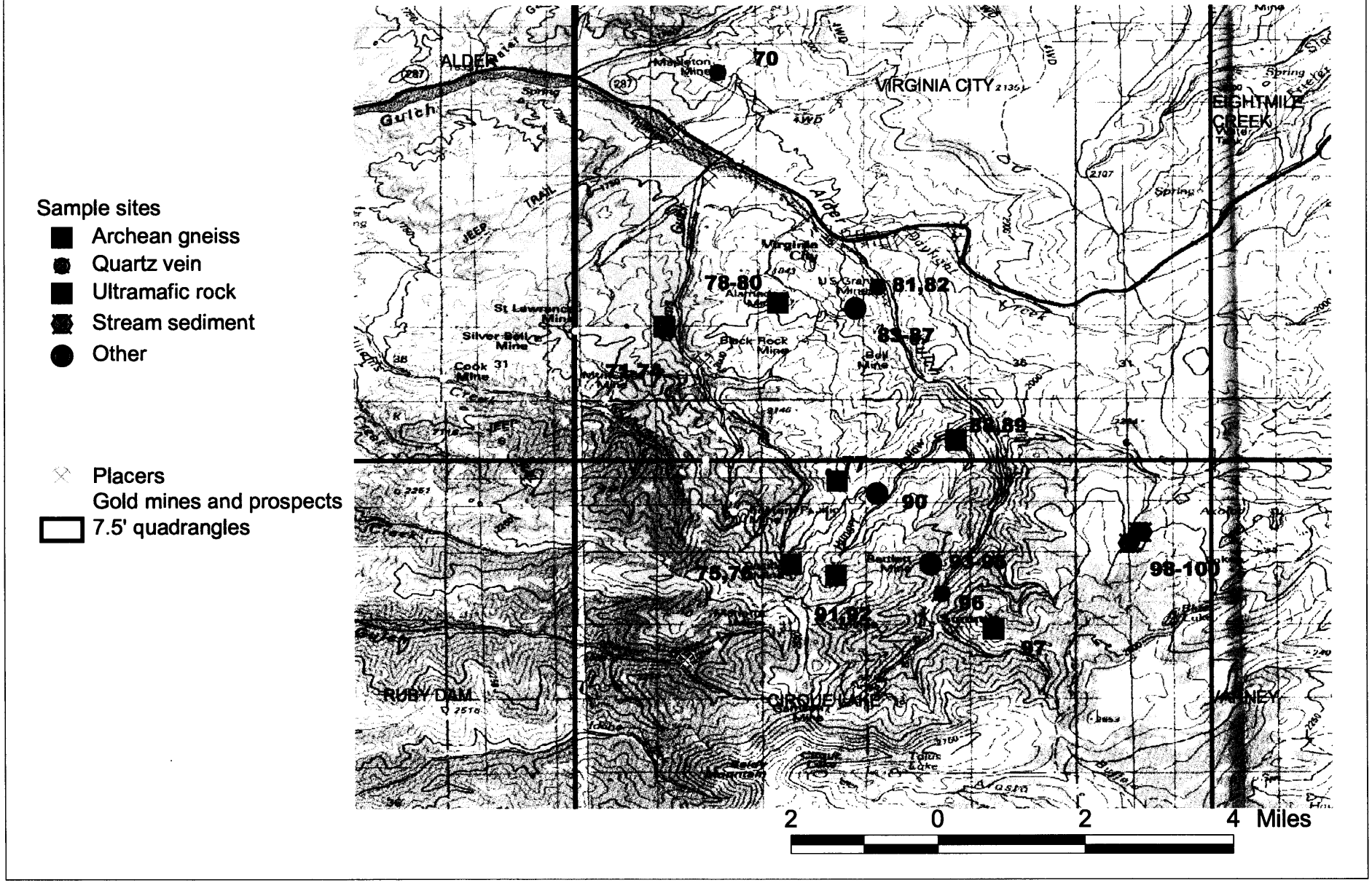

Figure 5. Sample sites in the Virginia City mining district. See tables 1 and 16 for map key. Localities for gold mines and prospects and gold placers are plotted from the MAS/MILS database (Kaas, 1996). Boundaries and names of 7.5' quadrangles are shown for reference. Base topography from parts of the Ennis and Dillon 1:100,000-scale topographic quadrangle maps.

Mapleton mine

The Mapleton mine, located north of Nevada City on the north side of Alder Gulch (fig. 5), explored a northwest-trending quartz vein for gold. Tansley and others (1933) mention the Mapleton ore body as one of many mines in the district where surficial enrichment was an important factor in producing minable metals. In other words, the oxidized zone of the orebody was exploitable whereas the sulfide-rich zone was not economic at the time. The mine was developed in 1939 on 2 patented and 6 unpatented claims as underground workings that opened 1,200 ft of drifts and 150 ft of raises and shipped about 20 tons of ore a day (Trauerman and Waldron, 1940).

We sampled a limonitic quartz vein (table 16A, map key 70, sample E9520) that ran in gold (18,000 ppb), silver (99 ppm), bismuth (1.1 ppm), antimony (17 ppm), and tellurium (1.9 ppm). Copper and lead were not determined; zinc was measured at 520 ppm. The relatively high antimony content reflects the presence of tetrahedrite in the sample. The sample also had a extremely high tungsten content (1,000 ppm). Relative to the mines south of Alder Gulch, the rocks at the Mapleton workings showed more evidence of copper staining and opaline silica.

Browns Gulch area

Three samples were collected at an unnamed adit along the west side of Brown's Gulch (table 1 and 16A, map key 71-74). The adit explored a quartz vein that appears to be about 10 ft wide and strikes approximately east-west, parallel to the foliation in the host rock gneiss at the surface. Farther into the workings, the vein appears to cross-cut the foliation. The vein carries sulfide minerals (pyrite, chalcopyrite, and tetrahedrite), and has an adularia-rich margin. Sample 007AV94 (map key 71) represents brecciated, iron-stained gneiss with quartz veins that comprises the wallrock at the adit; sample 007BV94 (map key 72) is a replicate of the gneiss. The gneiss at this locality is leucocratic and biotite appears to be the only ferromagnesian silicate mineral present. Garnet-rich amphibolite is present as float on the hill above the adit. The gneiss is locally sheared and iron-stained. Both gneiss samples contain elevated, but highly variable concentrations of gold, copper, lead, and zinc. Agreement between the two samples is excellent for some elements (9 ppm Co for both); the discrepancies in the metal analyses are probably due to a nugget effect. Samples 95JH035 and 95JH038 (map key 73 and 74) are sulfide-bearing quartz veins that run in gold (9,890 and 2,730 ppb). The gneiss samples have elevated concentrations of tellurium and antimony relative to the quartz vein samples.

The Easton and Pacific mines are located farther south, near the head of Brown's Gulch. Both mines worked splays of the same vein system within the aplitic body previously described as the Brown's Gulch stock; the vein system strikes N55° W and dips 70° NE, and the two veins reportedly merge to the southeast of the workings (Winchell, 1914; Cole, 1983). The Easton-Pacific mines produced the largest tonnage of ore in the district; from 1902 to 1935, the mines yielded more than 22,000 ounces of gold and more than 750,000 ounces of silver (Lorain, 1937). The Easton mine (about 0.5 mi northwest of the Pacific workings) was worked to a depth of about 700 ft. The underground workings are no longer accessible. According to Winchell (1914): (1) the ore minerals included argentite, auriferous pyrite, native silver, tetrahedrite, gold, sphalerite, and stibnite in a gangue of quartz, orthoclase, hematite, and limonite; (2) the ore shoot decreased in thickness with depth; (3) the vein thickness varied from 18 inches to 6 or 8 ft; and (4) a fault defined the footwall of the vein. We did not observe any rock that we would call a quartz monzonite aplite exposed at the surface or in the dump materials; we did observe a lot of pegmatite in the area. However, Lockwood (1990, fig. 23) illustrates monzonite crosscutting pegmatite dikes and quartzofeldspathic gneiss in a generalized cross-section of the geology through the Pacific Mine pit.

The vein at the Pacific mine reportedly contained antimony- and gold-bearing silver sulfide minerals in a gangue of quartz and iron oxides (Winchell, 1914). Lockwood and others (1991) noted that precious metals are generally restricted to the veins in this area, but a low-grade halo is present around some of the veins, and argillic alteration is particularly pervasive in the Pacific mine area. They also report the only published fluid inclusion data for the district. These data suggest that ore fluids in the Easton-Pacific mine area evolved from moderate-temperature, low-salinity (275 °C, 3-6 weight percent equivalent of NaCl) fluids associated with highest grade ores to more low-temperature, saline (175 °C, 10-12 weight percent

equivalent of NaCl) fluids. These data supported their conclusion that veins reflect waters from various sources that mixed. These fluid inclusion data are not typical of the porphyry copper environment, where inclusions typically record much higher temperatures (around 500° C) and salinities, and show evidence of boiling (Roedder, 1984)

We analyzed two samples of limonitic, sheared gneiss from the Pacific mine area (tables 1 and 16A, map key 75 and 76). Gold is present in both samples (31 and 56 ppb); silver is below detection limits (<0.4 ppm). Copper is variable (12 and 278 ppm), and lead and zinc values were relatively low (<30 ppm). Bismuth and selenium are below detection levels; both samples contained 0.2 ppm tellurium. Both samples are potassium-rich (>3 weight percent K).

Hadley's (1969) map of the Varney 15-minute quadrangle shows a number of small bodies of ultramafic rock. We sampled one of these bodies (tables 1 and 16B, map key 77) for PGE and metal content, and for comparison with other ultramafic rocks in the region. The small plug that crops out near the northwest corner of the Varney 15-minute quadrangle has a finer-grained margin and a coarser, pyroxene-rich core and is partly serpentinized, as reflected in the high volatile content (9.2 weight per cent for loss on ignition). This ultramafic rock is less siliceous and more magnesian than the ultramafic rocks associated with vermiculite in the Blacktail mining district (see table 4B); it also has more gold (4 ppb) and comparable PGE content (21.1 ppb), with Pt>Pd (table 17).

Alameda-Cornucopia-U.S. Grant mine area

A number of historic mines exploited a series of northeast-trending quartz veins on the west side of Alder Gulch that have been described as shallow, epithermal fissure veins containing quartz, pyrite, arsenopyrite, tetrahedrite, argentite, galena, sphalerite, chalcopyrite, and electrum (McLeod, 1986). The U.S. Grant produced about 800 ounces of gold and 46,000 ounces of silver between 1908 and 1926, and the Alameda mine produced a small amount of oxidized ore in the early 1900's (Lorain, 1937). Underground workings exploited the gold-rich, near-surface oxidized zone. Ore grades are not continuous at depth; veins are generally offset by faults. In the last 10 years, private industry has examined the possibility of reworking dumps from these mines and pursuing underground exploration, but no new mines have been developed to date.

We sampled ore from the Bamboo Chief (Alameda mine) vein system, a stockpile of ore from the lower level of the U.S. Grant workings, and a variety of rocks from the Cornucopia mine. Our three different samples from a stockpile of Bamboo Chief included iron-stained quartz veins and silicified gneiss (map key 78-80, tables 1 and 16A). All three samples ran in gold (238 to 90,400 ppb), silver (42 to 1,200 ppm), tellurium (0.7 to 5.5 ppm), and antimony (0.7 to 100 ppm). Quartz vein sample V9521B (map key 80) is also anomalous in mercury (4 ppm), molybdenum (2,000 ppm), lead (29,910 ppm), and zinc (2,000 ppm). Sample V9521A (map key 79) is also anomalous in lead and zinc, but to a lesser extent, and contains significant copper (5,650 ppm). Agreement between ICP and INAA determinations of the same element (silver and molybdenum, for example) are generally reasonable; for selenium the values reported by INAA are an order of magnitude greater than the ICP values. Nevertheless, the elevated concentrations for some of these elements indicates that they contribute to the geochemical signature of the vein deposits associated with the Bamboo Chief vein system.

Two samples of pyrite-rich quartz vein ore were collected from a stockpile of ore from the lower adit of the U.S. Grant mine (map key 81-82, tables 1 and 16A). Both samples contain anomalous gold (>2,000 ppb) and silver (>70 ppm), as well as a minor element signature that includes antimony>tellurium>selenium. Copper and lead were not determined for sample E9517; both elements are present (>100 ppm) in sample V9522, and zinc is present in both samples (>200 ppm).

Samples from the Cornucopia mine include pyrite-bearing quartz vein, red gossan, and garnetiferous amphibolite wallrock (map key 83-87, tables 1 and 16A). With the exception of the amphibolite, all samples contain gold (340 to 10,300 ppb) and silver (7 to 210 ppm). Relative to the quartz vein samples, the gossan is enriched in arsenic, molybdenum, and zinc. The gossan also contains an element suite that suggests a mafic-ultramafic rock association (chromium, nickel, PGE), although these elements are not enriched in the amphibolite.

Hungry Hollow Gulch

Hungry Hollow Gulch follows a southwest-trending creek that splits off along the west side of Alder Gulch about 2.5 miles south of Virginia City. We sampled three locations along Hungry Hollow Gulch. From north to south, these include: (1) an unnamed adit driven along a quartz vein in brecciated gneiss in a side gulch to the east of the main gulch (tables 1 and 16A, map key 88 and 89); (2) a chloritized diabase dike exposed at the Black Hawk workings on the west side of the gulch (map key 90); and (3) sulfide-bearing quartz veins in gneiss and a stream sediment from the area of the mine workings along the High Up- Irene vein system near the head of the gulch (map key 91 and 92).

The unnamed adit explores a north-trending quartz vein in gneiss interlayered with amphibolite. Some exploration drilling was conducted at this adit in the past, but the findings are unknown to us. We sampled the brecciated, iron-stained quartz vein (sample 96JH57, map key 88) and the gneiss (sample 96JH58, map key 89) adjacent to the vein. The vein is anomalous in gold (24,000 ppb), silver (>100 ppm), copper (1,111 ppm), lead (>5,000 ppm), antimony (100 ppm), tellurium (2.7 ppm), and zinc (>1,000 ppm). The gneiss contains this same element suite at concentrations well above detection limits, but below the concentrations present in the vein. For example, gold in the gneiss runs 40 ppb.

The adits and prospect pits at the Black Hawk workings appear to have been driven along the contact of a diabase dike, shown as an east-west dike within Precambrian granite (gneiss) and migmatite on Hadley's (1969) map of the Varney 15-minute quadrangle. We sampled the chloritized dike rock near the contact (sample 96JH60, map key 90). Gold content (42 ppb) is comparable to that of the country rock gneiss at the unnamed adit. The dike is anomalous in copper (>6,000 ppm), and shows somewhat elevated concentrations of chromium (230 ppm), manganese (866 ppm), and vanadium (227 ppm) relative to other samples; these concentrations are not uncommon for rocks of basaltic composition. Agreement between zinc by ICP (72 ppm) and by INAA (222 ppm) is not very good, and we have no explanation for the relatively high concentration of tellurium (1.9 ppm) in this rock. The copper staining probably attracted the attention of early prospectors.

The High Up and Irene vein systems are two parallel, northeast-trending vein systems at the head of Hungry Hollow Gulch, about one mile northeast of the Marietta Mine. Workings include several adits. Hadley (1969) showed the rock in this area as Precambrian granite (gneiss) and migmatite. We sampled quartz-veined gneiss (tables 1 and 16A, map key 91) and a stream sediment from the stream that drains the workings (map key 92). The quartz vein sample contains 1,450 ppb gold, 4.1 ppm antimony, 0.5 ppm selenium, and 2.3 ppm tellurium. Copper and zinc are present at about 100 ppm and lead concentration is low (39 ppm). The stream sediment carries a small, but measurable amount of gold (67 ppb).

Alder Gulch

A number of workings were sampled from the Alder Gulch area, north and east of the Kearsarge mine. These include the Bartlett Mine area, the Millard tunnel, and an area of historic shafts and prospects east of the old townsite of Summit and north of Bachelor Gulch (fig. 5). No data are available for the history of the Bartlett Mine; however, adits are driven along a northwest-trending quartz vein that may have followed the contact of a thick dolomite bed. The dolomite forms a prominent cliff above the workings; this particular bed of dolomite is not shown on Hadley's (1969) map. Hadley does show a northwest-trending dolomite bed within the "Cherry Creek" Group rocks that outcrop to the west in Barton Gulch, and Wier (1982) mapped numerous, mainly northeast-trending marble beds in the northern part of the district. The carbonate beds appear to be confined to the west side of Alder Gulch, but this has not been tested by mapping at appropriate scales.

The massive dolomite (table 16A, map key 93, sample 96JH21) is calcium-rich (>20 weight percent Ca), moderately magnesian (11 weight percent Mg) and, with the exception of moderate enrichment in zinc (about 130 ppm), barren of metals. Samples of magnetite-bearing quartz-carbonate rock from the caved adit area and gossan float from the mine dump (table 16A, map key 94 and 95) both ran in gold (70, 109 ppb) and other metals. These altered rocks contain about twice as much zinc as the dolomite. The zinc in the dolomite could be primary, or could be an overprint from fluid infiltration related to

mineralization.

A random sample (table 16A, map key 96) of quartz-sulfide ore from the Millard tunnel (adits on the east side of Alder Gulch about 0.8 mile north of the Kearsarge Mine) contains over 3,000 ppb gold, but no detectable silver. These workings were driven eastward from Alder Gulch, probably to intersect the Kearsarge vein system. Similarly, a dump sample (map key 97) of highly fractured, limonitic gneiss from prospects north of Bachelor Gulch contains anomalous gold (>300 ppb), but no other anomalous metal concentrations.

Butcher Gulch

Butcher Gulch drains an area of Tertiary volcanic rocks and recent gravels on BLM land east of the historic mine areas. Three sediments were sampled (tables 1 and 16A, map key 98-100) to provide background information. The area south and east of Virginia City was not covered during the NURE sampling program, probably because of the known human disturbance from historic placer mining. Two samples were collected from the active stream bed, and one sample represents sediment deposited in a terrace bank about 20 ft above the active stream channel. All three samples contain less than 10 ppb gold.

Table 16. Analytical data for rock and stream sediment samples from the Virginia City mining district.
A. Partial multielement data.
[See text for explanation of methods; n.d., not determined; *, replicate samples]

Map key			70	71	72	73	74	75
Sample number			E9520	007AV94	007BV94*	95JH035	95JH038	008AV94
Job number			AHK1256	AHK0045	AHK0045	AHK1256	AHK1256	AHK0045
Element	Units	Method	Mapleton Mine	Browns Gulch Area				
Ag	ppm	ICP	n.d.	6.9	8.5	n.d.	n.d.	<0.4
Ag	ppm	INAA	99	7	9	9	<5	<5
Al	%	ICP	n.d.	4.1	3.74	n.d.	n.d.	6.47
As	ppm	INAA	41	23	10	2.5	1.2	<0.5
Au	ppb	INAA	18,000	434	5,050	9,890	2,730	31
Ba	ppm	INAA	520	620	2,100	700	17,000	220
Be	ppm	ICP	n.d.	<2	<2	n.d.	n.d.	<2
Bi	ppm	ICP-HY	1.1	<0.2	<0.2	<0.2	<0.2	<0.2
Bi	ppm	ICP	n.d.	<5	<5	n.d.	n.d.	<5
Br	ppm	INAA	1.8	<0.5	<0.5	1.7	1.7	1.4
Ca	%	ICP	n.d.	4.71	4.83	n.d.	n.d.	1.66
Ca	%	INAA	<1	5	4	<1	<1	2
Cd	ppm	ICP	n.d.	6.2	32.9	n.d.	n.d.	<0.5
Ce	ppm	INAA	<3	38	28	<3	4	8
Co	ppm	INAA	94	9	9	81	95	1
Cr	ppm	INAA	<5	130	42	19	7	6
Cs	ppm	INAA	<1	<1	<1	<1	<1	<1
Cu	ppm	ICP	n.d.	139	403	n.d.	n.d.	12
Eu	ppm	INAA	<0.2	1.3	1.1	<0.2	<0.2	0.4
Fe	%	INAA	0.16	4.08	4.16	1.68	0.58	0.47
Ge	ppm	ICP-HY	<0.2	<0.2	<0.2	<0.2	<0.2	<0.2
Hf	ppm	INAA	<1	5	4	<1	<1	3
Hg	ppm	INAA	2	<1	<1	<1	<1	<1
Ir	ppb	INAA	<5	<5	<5	<5	<5	<5
K	%	ICP	n.d.	4.78	4.85	n.d.	n.d.	3.9
La	ppm	INAA	0.6	20	15	1.6	9	7.2
Lu	ppm	INAA	0.09	0.76	0.62	<0.05	<0.05	0.1
Mg	%	ICP	n.d.	1.69	1.96	n.d.	n.d.	0.04
Mn	ppm	ICP	n.d.	881	869	n.d.	n.d.	53
Mo	ppm	ICP	n.d.	4	7	n.d.	n.d.	<2
Mo	ppm	INAA	10	3	5	5	7	<1
Na	%	INAA	0.02	0.06	0.06	0.02	0.02	2.6
Nd	ppm	INAA	<5	16	14	<5	<5	<5
Ni	ppm	ICP	n.d.	54	42	n.d.	n.d.	2
Ni	ppm	INAA	<20	<20	67	<20	<20	<20
P	%	ICP	n.d.	0.12	0.097	n.d.	n.d.	0.002
Pb	ppm	ICP	n.d.	112	1,442	n.d.	n.d.	28

Table 16.--Continued

Map key			70	71	72	73	74	75
Rb	ppm	INAA	<15	88	59	<15	<15	160
Sb	ppm	INAA	17	15	14	1.2	1.3	0.2
Sc	ppm	INAA	0.3	13	10	2	0.2	0.8
Se	ppm	ICP-HY	0.4	<0.2	0.8	0.4	0.2	<0.2
Se	ppm	INAA	<3	<3	<3	<3	<3	<3
Sm	ppm	INAA	0.2	5.1	3.8	0.4	0.1	1.5
Sn	%	INAA	<0.01	<0.01	<0.01	<0.01	<0.01	<0.01
Sr	ppm	ICP	n.d.	207	311	n.d.	n.d.	35
Sr	ppm	INAA	<500	<500	<500	<500	<500	<500
Ta	ppm	INAA	2.2	0.7	<0.5	0.9	1.1	<0.5
Tb	ppm	INAA	<0.5	1.2	0.9	<0.5	<0.5	<0.5
Te	ppm	ICP-HY	1.9	0.6	1.4	0.2	0.2	0.2
Th	ppm	INAA	<0.5	11	7.7	1.1	<0.5	11
Ti	%	ICP	n.d.	0.11	0.07	n.d.	n.d.	0.01
U	ppm	INAA	<0.5	3.2	2.2	1.2	<0.5	<0.5
V	ppm	ICP	n.d.	183	104	n.d.	n.d.	2
W	ppm	INAA	1000	15	8	560	660	<1
Y	ppm	ICP	n.d.	26	24	n.d.	n.d.	6
Yb	ppm	INAA	0.7	4.2	3.4	0.6	0.4	0.5
Zn	ppm	ICP	n.d.	1,327	2,906	n.d.	n.d.	14
Zn	ppm	INAA	520	1,370	2,800	320	4,100	<50

Table 16.--Continued

Map key			76	78	79	80	81	82
Sample number			008BV94	E9516	V9521A	V9521B	E9517	V9522
Job number			AHK0045	AHK1256	AHK0045	AHK0045	AHK1256	AHK0045
Element	Units	Method		Alameda-Cornucopia-U.S. Grant mine area				
Ag	ppm	ICP	<0.4	n.d.	42.2	890.3	n.d.	1,040.8
Ag	ppm	INAA	<5	360	42	1,200	78	1,100
Al	%	ICP	6.66	n.d.	0.13	0.17	n.d.	0.3
As	ppm	INAA	1	1.60	210	41	4.5	27
Au	ppb	INAA	56	6,280	238	90,400	2,980	27,300
Ba	ppm	INAA	190	<50	<50	110	<50	440
Be	ppm	ICP	<2	n.d.	<2	<2	n.d.	<2
Bi	ppm	ICP-HY	<0.2	<0.2	10.2	<0.2	<0.2	<0.2
Bi	ppm	ICP	<5	n.d.	18	<5	n.d.	<5
Br	ppm	INAA	2.2	5.1	2.1	650	<0.5	5.2
Ca	%	ICP	1.77	n.d.	0.06	0.04	n.d.	<0.02
Ca	%	INAA	3	<1	<1	<1	<1	<1
Cd	ppm	ICP	<0.5	n.d.	1	1.5	n.d.	<0.5
Ce	ppm	INAA	4	<3	10	9	<3	8
Co	ppm	INAA	<1	66	<1	2	220	14
Cr	ppm	INAA	6	<5	10	17	<5	11
Cs	ppm	INAA	<1	<1	<1	<1	<1	<1
Cu	ppm	ICP	278	n.d.	5,670	158	n.d.	166
Eu	ppm	INAA	0.4	<0.2	0.5	<0.2	<0.2	<0.2
Fe	%	INAA	0.56	0.24	1.26	23.1	0.93	12
Ge	ppm	ICP-HY	<0.2	<0.2	<0.2	<0.2	<0.2	<0.2
Hf	ppm	INAA	2	<1	<1	<1	<1	1
Hg	ppm	INAA	<1	<1	<1	4	<1	<1
Ir	ppb	INAA	<5	<5	<5	<5	<5	<5
K	%	ICP	3.68	n.d.	0.06	0.01	n.d.	0.29
La	ppm	INAA	4.3	0.7	7.9	9	0.5	6.4
Lu	ppm	INAA	0.13	<0.05	0.2	0.08	<0.05	0.1
Mg	%	ICP	0.04	n.d.	0.02	0.03	n.d.	0.02
Mn	ppm	ICP	63	n.d.	116	14	n.d.	23
Mo	ppm	ICP	<2	n.d.	44	1734	n.d.	114
Mo	ppm	INAA	2	62	34	2000	30	127
Na	%	INAA	2.81	0.01	0.02	0.03	0.02	0.03
Nd	ppm	INAA	<5	<5	<5	<5	<5	<5
Ni	ppm	ICP	2	n.d.	2	7	n.d.	36
Ni	ppm	INAA	<20	<20	<20	<20	<20	<20
P	%	ICP	0.002	n.d.	0.002	0.005	n.d.	0.002
Pb	ppm	ICP	26	n.d.	17,668	29,910	n.d.	1,639

Table 16.--Continued

Map key			76	78	79	80	81	82
Rb	ppm	INAA	150	<15	<15	<15	<15	<15
Sb	ppm	INAA	<0.1	0.7	100	19	2.6	6.9
Sc	ppm	INAA	0.8	0.1	0.3	0.6	0.3	0.4
Se	ppm	ICP-HY	<0.2	0.6	0.8	8.7	0.5	0.7
Se	ppm	INAA	<3	9	<3	100	<3	5
Sm	ppm	INAA	0.9	<0.1	0.5	0.9	<0.1	0.7
Sn	%	INAA	<0.01	<0.01	<0.02	<0.02	<0.01	<0.02
Sr	ppm	ICP	38	n.d.	9	45	n.d.	16
Sr	ppm	INAA	<500	<500	<500	<500	<500	<500
Ta	ppm	INAA	<0.5	0.9	<0.5	0.6	1.7	<0.5
Tb	ppm	INAA	<0.5	<0.5	<0.5	<0.5	<0.5	<0.5
Te	ppm	ICP-HY	0.2	1.9	0.7	5.5	1.5	0.2
Th	ppm	INAA	8.5	<0.5	0.7	3.9	<0.5	1.8
Ti	%	ICP	0.01	n.d.	0.01	0.01	n.d.	0.01
U	ppm	INAA	1.7	1.5	13	<0.5	<0.5	3.2
V	ppm	ICP	2	n.d.	2	31	n.d.	25
W	ppm	INAA	<1	440	<1	<1	1,200	<1
Y	ppm	ICP	6	n.d.	4	7	n.d.	2
Yb	ppm	INAA	0.6	<0.2	1.1	0.5	<0.2	0.7
Zn	ppm	ICP	7	n.d.	672	1,900	n.d.	570
Zn	ppm	INAA	<50	95	631	2,000	290	543

Table 16.--Continued

Map key			83	84	85	86	87	88
Sample number			95JH118 A	95JH119	95JH120	E9518	009V94	96JH57
Job number			AHK1241	AHK1241	AHK1241	AHK1256	AHK0045	AHK1787
Element	Units	Method	Alameda-Cornucopia-U.S. Grant mine area					Hungry Hollow Gulch
Ag	ppm	ICP	n.d.	n.d.	n.d.	n.d.	6.9	122.6
Ag	ppm	INAA	<5	51	53	210	7	130
Al	%	ICP	n.d.	n.d.	n.d.	n.d.	0.12	0.06
As	ppm	INAA	<0.5	2.8	27.0	11	0.6	61
Au	ppb	ICP/MS	<1	3,643	511	n.d.	n.d.	n.d.
Au	ppb	INAA	<2	9,670	491	10,300	340	24,000
Ba	ppm	INAA	1,500	230	480	<50	210	5,800
Be	ppm	ICP	n.d.	n.d.	n.d.	n.d.	<2	<2
Bi	ppm	ICP-HY	n.d.	n.d.	n.d.	<0.2	<0.2	<1
Bi	ppm	ICP	n.d.	n.d.	n.d.	n.d.	<5	<5
Br	ppm	INAA	<0.5	1.0	1.1	<0.5	0.5	<0.5
Ca	%	ICP	n.d.	n.d.	n.d.	n.d.	<0.01	0.01
Ca	%	INAA	<1	<1	<1	<1	<1	<1
Cd	ppm	ICP	n.d.	n.d.	n.d.	n.d.	<0.5	1.1
Ce	ppm	INAA	120	3	150	<3	<3	<3
Co	ppm	INAA	11	65	21	98	1	5
Cr	ppm	INAA	2	<1	230	<5	8	21
Cs	ppm	INAA	<1	<1	<1	<1	<1	<1
Cu	ppm	ICP	n.d.	n.d.	n.d.	n.d.	54	1,111
Eu	ppm	INAA	2.1	<0.2	2.0	<0.2	<0.2	<0.2
Fe	%	INAA	2.8	2.7	24.0	0.69	0.96	2.9
Ge	ppm	ICP-HY	n.d.	n.d.	n.d.	<0.2	<0.2	<0.2
Hf	ppm	INAA	10	<1	<1	<1	<1	1
Hg	ppm	INAA	<1	<1	<1	<1	<1	<1
Ir	ppb	ICP/MS	0.5	0.4	0.6	n.d.	n.d.	n.d.
Ir	ppb	INAA	<5	<5	<5	<5	<5	<5
K	%	ICP	n.d.	n.d.	n.d.	n.d.	0.12	0.03
La	ppm	INAA	73.0	0.9	89.0	0.6	1.2	5.7
Lu	ppm	INAA	0.87	<0.05	0.46	<0.05	<0.05	<0.05
Mg	%	ICP	n.d.	n.d.	n.d.	n.d.	0.01	0.01
Mn	ppm	ICP	n.d.	n.d.	n.d.	n.d.	36	410
Mo	ppm	ICP	n.d.	n.d.	n.d.	n.d.	18	15
Mo	ppm	INAA	<1	28	140	27	14	30
Na	%	INAA	1.39	0.02	0.25	0.02	0.02	0.01
Nd	ppm	INAA	43	<5	43	<5	<5	<5
Ni	ppm	ICP	n.d.	n.d.	n.d.	n.d.	2	10
Ni	ppm	INAA	<31	<20	220	<20	<20	<20
P	%	ICP	n.d.	n.d.	n.d.	n.d.	0.002	0.002

Table 16.--Continued

Map key			83	84	85	86	87	88
Pb	ppm	ICP	n.d.	n.d.	n.d.	n.d.	221	5,080
Pd	ppb	ICP/MS	<0.1	0.1	0.5	n.d.	n.d.	n.d.
Pt	ppb	ICP/MS	<0.1	<0.1	0.5	n.d.	n.d.	n.d.
Rb	ppm	INAA	120	<15	120	<15	<15	<15
Rh	ppb	ICP/MS	<0.1	<0.1	<0.1	n.d.	n.d.	n.d.
Sb	ppm	INAA	<0.1	1.7	2.7	8.7	1.1	100
Sc	ppm	INAA	2.2	0.3	24.0	0.2	0.2	0.6
Se	ppm	ICP-HY	n.d.	n.d.	n.d.	0.7	0.8	0.2
Se	ppm	INAA	<3	<3	<3	<3	<3	<3
Sm	ppm	INAA	8.2	0.1	9.3	<0.1	0.1	0.5
Sn	%	INAA	<0.01	<0.01	<0.01	<0.01	<0.01	<0.01
Sr	ppm	ICP	n.d.	n.d.	n.d.	n.d.	13	83
Sr	ppm	INAA	<500	<500	<500	<500	<500	<500
Ta	ppm	INAA	<0.5	1.3	0.8	1.3	<0.5	<0.5
Tb	ppm	INAA	1.4	<0.5	1.4	<0.5	<0.5	<0.5
Te	ppm	ICP-HY	n.d.	n.d.	n.d.	1.2	0.6	2.7
Th	ppm	INAA	23.0	<0.2	9.5	<0.5	0.4	<0.2
Ti	%	ICP	n.d.	n.d.	n.d.	n.d.	0.01	0.01
U	ppm	INAA	2.5	<0.5	12.0	<0.5	<0.5	6.3
V	ppm	ICP	n.d.	n.d.	n.d.	n.d.	2	78
W	ppm	INAA	110	550	32	880	<1	<1
Y	ppm	ICP	n.d.	n.d.	n.d.	n.d.	2	4
Yb	ppm	INAA	5.5	<0.1	2.4	<0.2	<0.2	<0.2
Zn	ppm	ICP	n.d.	n.d.	n.d.	n.d.	30	1,072
Zn	ppm	INAA	152	<50	3,300	<50	<50	1,050

Table 16.--Continued

Map key			89	90	91	92	93	94
Sample number			96JH58	96JH60	96JH62	96JH63	96JH21	96JH23
Job number			AHK1787	AHK1787	AHK1787	AHK1787	AHK1787	AHK1787
Element	Units	Method	Hungry Hollow Gulch				Alder Gulch	
Ag	ppm	ICP	0.5	0.4	6.4	1	<0.4	0.6
Ag	ppm	INAA	<5	<5	10	<5	<5	<5
Al	%	ICP	7.31	6.12	5.68	6.58	0.14	7.75
As	ppm	INAA	<0.5	12	9.9	1.6	<0.5	8.4
Au	ppb	INAA	40	42	1,450	67	<2	70
Ba	ppm	INAA	920	<50	290	1,300	65	320
Be	ppm	ICP	3	<2	3	2	<2	3
Bi	ppm	ICP-HY	<1	1.0	<1	<1	<1	<1
Bi	ppm	ICP	<5	<5	<5	<5	<5	<5
Br	ppm	INAA	<0.5	2	<0.5	1.6	<0.5	<0.5
Ca	%	ICP	1.99	0.03	4.97	0.71	20.14	0.7
Ca	%	INAA	2	<1	6	<1	22	<1
Cd	ppm	ICP	<0.5	<0.5	<0.5	<0.5	<0.5	<0.5
Ce	ppm	INAA	60	48	19	64	3	79
Co	ppm	INAA	22	39	25	4	1	38
Cr	ppm	INAA	120	230	250	20	8	210
Cs	ppm	INAA	2	<1	<1	<1	<1	2
Cu	ppm	ICP	163	6,360	122	8	2	125
Eu	ppm	INAA	1.4	1.5	0.7	1.2	<0.2	1.8
Fe	%	INAA	5.05	11.7	4.94	2.13	1.04	4.03
Ge	ppm	ICP-HY	<0.2	<0.2	<0.2	<0.2	<0.2	<0.2
Hf	ppm	INAA	5	3	2	12	<1	8
Hg	ppm	INAA	<1	<1	<1	<1	<1	<1
Ir	ppb	INAA	<5	<5	<5	<5	<5	<5
K	%	ICP	2.06	0.25	3.94	3.2	0.08	3.3
La	ppm	INAA	30	23	9.2	26	1.3	37
Lu	ppm	INAA	0.49	0.35	0.25	0.52	<0.05	0.61
Mg	%	ICP	1.57	4.49	3.35	0.22	11.22	0.49
Mn	ppm	ICP	532	866	961	419	4,543	649
Mo	ppm	ICP	<2	<2	8	3	<2	3
Mo	ppm	INAA	<1	20	14	5	<1	5
Na	%	INAA	2.8	0.31	0.46	2.22	0.03	1.9
Nd	ppm	INAA	23	17	6	16	<5	27
Ni	ppm	ICP	73	74	101	7	2	109
Ni	ppm	INAA	170	<33	160	<20	<20	300
P	%	ICP	0.037	0.025	0.014	0.038	0.005	0.024
Pb	ppm	ICP	22	<5	39	44	20	19
Rb	ppm	INAA	110	<15	120	93	<15	88
Sb	ppm	INAA	0.4	0.5	4.1	0.8	0.5	2.9

Table 16.--Continued

Map key			89	90	91	92	93	94
Sc	ppm	INAA	17	32	17	4.1	0.5	22
Se	ppm	ICP-HY	<0.2	<0.2	0.5	<0.2	0.8	0.7
Se	ppm	INAA	<3	<3	<3	<3	<3	<3
Sm	ppm	INAA	5.3	4.8	1.7	3.8	0.2	5.8
Sn	%	INAA	<0.01	<0.01	<0.01	<0.01	<0.01	<0.01
Sr	ppm	ICP	182	90	248	110	63	60
Sr	ppm	INAA	<500	<500	<500	<500	<500	<500
Ta	ppm	INAA	1.1	<0.5	<0.5	<0.5	<0.5	1.8
Tb	ppm	INAA	1.1	<0.5	<0.5	<0.5	<0.5	1.2
Te	ppm	ICP-HY	1.0	1.9	2.3	0.6	0.2	<0.2
Th	ppm	INAA	11	1.3	1.3	15	0.3	13
Ti	%	ICP	0.46	0.41	0.17	0.16	0.01	0.41
U	ppm	INAA	1.8	16	8.9	3.6	<0.5	4
V	ppm	ICP	128	227	145	18	3	194
W	ppm	INAA	<1	<1	13	<1	2	6
Y	ppm	ICP	40	17	11	30	2	32
Yb	ppm	INAA	3.3	2.6	1.7	3.7	<0.2	4.5
Zn	ppm	ICP	128	72	92	84	132	219
Zn	ppm	INAA	181	222	130	88	126	279

Table 16.--Continued

Map key			95	96	97	98	99	100
Sample number			96JH24	95JH055A	012V94	96JH05	96JH03	96JH04
Job number			AHK1787	AHK1241	AHK0045	AHK1787	AHK1787	AHK1787
Element	Units	Method	Alder Gulch			Butcher Gulch		
Ag	ppm	ICP	0.8	n.d.	<0.4	<0.4	<0.4	0.4
Ag	ppm	INAA	<5	<5	<5	<5	<5	<5
Al	%	ICP	5.84	n.d.	4.99	6.65	6.97	6.66
As	ppm	INAA	45	25.0	11	6.7	2.3	3.4
Au	ppb	ICP/MS	n.d.	3,548	n.d.	n.d.	n.d.	n.d.
Au	ppb	INAA	109	3,800	398	4	2	5
Ba	ppm	INAA	220	280	2,200	1,100	1200	970
Be	ppm	ICP	2	n.d.	<2	2	2	2
Bi	ppm	ICP-HY	<1	n.d.	<0.2	<1	<1	<1
Bi	ppm	ICP	<5	n.d.	<5	<5	<5	<5
Br	ppm	INAA	<0.5	<0.5	0.7	2.6	<0.5	<0.5
Ca	%	ICP	0.04	n.d.	1.17	0.96	2.56	2.11
Ca	%	INAA	<1	10	<1	<1	2	2
Cd	ppm	ICP	<0.5	n.d.	<0.5	<0.5	<0.5	<0.5
Ce	ppm	INAA	4	25	63	58	66	53
Co	ppm	INAA	3	33	2	12	17	14
Cr	ppm	INAA	12	330	5	66	250	190
Cs	ppm	INAA	<1	<1	<1	1	1	<1
Cu	ppm	ICP	54	n.d.	69	13	22	14
Eu	ppm	INAA	0.5	1.1	1.3	1.2	1.5	1.4
Fe	%	INAA	4.15	6.4	1.11	2.7	4.39	3.89
Ge	ppm	ICP-HY	<0.2	n.d.	<0.2	<0.2	<0.2	<0.2
Hf	ppm	INAA	3	2	2	9	9	7
Hg	ppm	INAA	<1	<1	<1	<1	<1	<1
Ir	ppb	ICP/MS	n.d.	0.8	n.d.	n.d.	n.d.	n.d.
Ir	ppb	INAA	<5	<5	<5	<5	<5	<5
K	%	ICP	5.16	n.d.	5.47	2.77	2.36	2.47
La	ppm	INAA	1.8	11.0	41	27	34	28
Lu	ppm	INAA	0.15	0.38	0.5	0.42	0.46	0.5
Mg	%	ICP	0.03	n.d.	0.51	0.46	1.56	1.26
Mn	ppm	ICP	34	n.d.	154	749	1,358	1,032
Mo	ppm	ICP	26	n.d.	<2	<2	<2	<2
Mo	ppm	INAA	25	5	2	3	<1	<1
Na	%	INAA	0.94	0.22	0.65	2.01	2.02	2.02
Nd	ppm	INAA	<5	9	20	14	26	19
Ni	ppm	ICP	10	n.d.	3	22	83	59
Ni	ppm	INAA	<20	<28	<20	110	100	<20
P	%	ICP	0.005	n.d.	0.009	0.022	0.079	0.065
Pb	ppm	ICP	584	n.d.	20	18	10	17

Table 16.--Continued

Map key			95	96	97	98	99	100
Pd	ppb	ICP/MS	n.d.	3.7	n.d.	n.d.	n.d.	n.d.
Pt	ppb	ICP/MS	n.d.	5.0	n.d.	n.d.	n.d.	n.d.
Rb	ppm	INAA	110	48	120	94	64	91
Rh	ppb	ICP/MS	n.d.	<0.1	n.d.	n.d.	n.d.	n.d.
Sb	ppm	INAA	6.4	2.0	0.6	0.3	0.3	0.3
Sc	ppm	INAA	1.4	20.0	1	7.6	13	11
Se	ppm	ICP-HY	1.4	n.d.	<0.2	<0.2	0.6	0.5
Se	ppm	INAA	<3	<3	<3	<3	<3	<3
Sm	ppm	INAA	0.3	4.2	4.5	3.3	4.4	3.9
Sn	%	INAA	<0.01	<0.01	<0.01	<0.01	<0.01	<0.01
Sr	ppm	ICP	41	n.d.	86	172	329	265
Sr	ppm	INAA	<500	<500	<500	<500	<500	<500
Ta	ppm	INAA	<0.5	<0.5	<0.5	0.9	1.2	<0.5
Tb	ppm	INAA	<0.5	1.0	0.8	0.7	0.8	0.6
Te	ppm	ICP-HY	0.3	n.d.	0.2	<0.2	<0.2	<0.2
Th	ppm	INAA	23	1.6	21	8.5	8.7	7.5
Ti	%	ICP	0.01	n.d.	0.02	0.24	0.47	0.34
U	ppm	INAA	2.3	3.4	0.5	2.4	2	1.2
V	ppm	ICP	14	n.d.	59	45	91	70
W	ppm	INAA	<1	80	<1	<1	<1	<1
Y	ppm	ICP	4	n.d.	19	23	30	28
Yb	ppm	INAA	0.9	2.6	2.6	2.9	3.2	3.3
Zn	ppm	ICP	315	n.d.	19	38	47	38
Zn	ppm	INAA	274	252	<50	<50	<50	81

Table 16. Analytical data for rock samples from the Virginia City mining district.
B.Complete chemical analyses for an ultramafic rock sample.
[n.d., not determined; total iron reported as Fe_2O_3]

Major elements, in weight per cent	
Map key	77
Sample number	96JH67
Job number	AHK1787
SiO_2	40.0
Al_2O_3	2.30
Fe_2O_3	10.7
MnO	0.13
MgO	35.1
CaO	1.12
Na_2O	0.04
K_2O	<0.01
TiO_2	0.11
P_2O_5	0.02
LOI	9.2
TOTAL	98.7

Minor and trace elements			
Map key			77
Sample number			96JH67
Job number			AHK1787
Ag	ppm	ICP	<0.4
As	ppm	INAA	<1
Au	ppb	ICM/MS	4
Au	ppb	INAA	<2
Ba	ppm	ICP	10
Be	ppm	ICP	<1
Bi	ppm	ICP-HY	<1
Bi	ppm	ICP	<5
Br	ppm	INAA	2.4
Cd	ppm	ICP	<0.5
Ce	ppm	INAA	7
Co	ppm	INAA	117
Cr	ppm	INAA	4,240
Cs	ppm	INAA	<0.2

Table 16.--Continued.

Minor and trace elements			
Map key			77
Cu	ppm	ICP	7
Eu	ppm	INAA	0.08
Ge	ppm	ICP-HY	0.2
Hf	ppm	INAA	0.4
Hg	ppm	INAA	<1
Ir	ppb	ICP/MS	3.6
Ir	ppb	INAA	<1
La	ppm	INAA	1.8
Lu	ppm	INAA	0.03
Mo	ppm	INAA	<2
Nd	ppm	INAA	3
Ni	ppm	ICP	1,795
Pb	ppm	ICP	<5
Pd	ppb	ICP/MS	1.7
Pt	ppb	ICP/MS	13.4
Rb	ppm	INAA	<10
Rh	ppb	ICP/MS	2.4
Sb	ppm	INAA	<0.1
Sc	ppm	INAA	9.4
Se	ppm	ICP-HY	<0.2
Se	ppm	INAA	<0.5
Sm	ppm	INAA	0.37
Sr	ppm	ICP	6
Ta	ppm	INAA	<0.3
Tb	ppm	INAA	<0.1
Te	ppm	ICP-HY	0.3
Th	ppm	INAA	0.6
U	ppm	INAA	<0.1
V	ppm	ICP	35
W	ppm	INAA	<1
Y	ppm	ICP	3
Yb	ppm	INAA	0.3
Zn	ppm	ICP	19
Zr	ppm	ICP	16

DISCUSSION

Iron Formation

The depositional setting and age (Archean or Proterozoic) of the package of rocks that hosts banded iron formation on the east side of the Gravelly Range (Cherry Creek mining district) is a subject of some debate. The Ruby (Johnny Gulch) mine and Black Butte deposit (Granite Mountain area) rocks are of lower metamorphic grade and less deformed than other banded iron formation in Montana. In addition, their association with pillow basalts and unusual trace element signature (positive europium anomalies, low total abundance of rare earth elements) led Stanley (1988) and Bayley and James (1973) to interpret their environment of deposition as a volcanically active ocean basin. This is a depositional environment typical for Archean greenstone terranes elsewhere in the world and differs from the Proterozoic banded iron formations, which are typified by negative europium anomalies and an association with sedimentary basins and shallow water facies. While we are not suggesting that this unique chemical signature confirms an Archean age for the banded iron formation, we do suggest that contrasts in chemical signature between these occurrences of iron formation and those elsewhere in the Dillon Resource Area (Copper Mountain in the Sheridan district, Carter Creek in the Ruby Mountains district) may reflect different depositional settings that may be significant in reconstructing the Precambrian geologic history of the area. Iron concentrations of all of these occurrences of banded iron formation overlap (fig. 6). Because rare-earth elements (REE) are relatively insoluble, they can provide clues to source (Rollinson, 1994). In order to thoroughly evaluate the significance of REE patterns, more complete and better-quality data (for example, isotope dilution data) are desirable. However, these data do show significant differences in the light REE abundances for the different iron formations in the Dillon Resource Area (fig. 6A and 6B), which have all been interpretated as forming during the Archean. For chemical sediments, REE patterns are likely to reflect the composition of the seawater that precipitated the sediment. For clastic sediments, REE patterns provide clues to provenance.

Banded iron formation is a permissive, though not definitive, source of the magnetite-rich "cannonballs" associated with the Chinatown placer deposits. Iron skarn may be a more likely source rock, although no such deposits are known in the local area. Both "cannonball" samples carry trace amounts (<20 ppb) of gold (tables 1 and 6, map key 29 and 30). These "cannonballs" overlap banded iron formation (this study; also Stanley, 1988) in total iron content, tend to be enriched in scandium, cobalt, and arsenic relative to most of the banded iron formation of southwest Montana, and have distinctive chondrite-normalized rare-earth element patterns characterized by a slightly positive slope (heavy rare earth elements > light rare earth elements) and negative europium anomalies (fig. 6C).

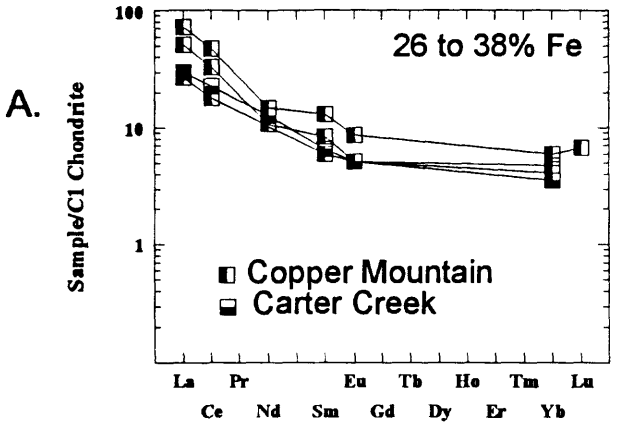

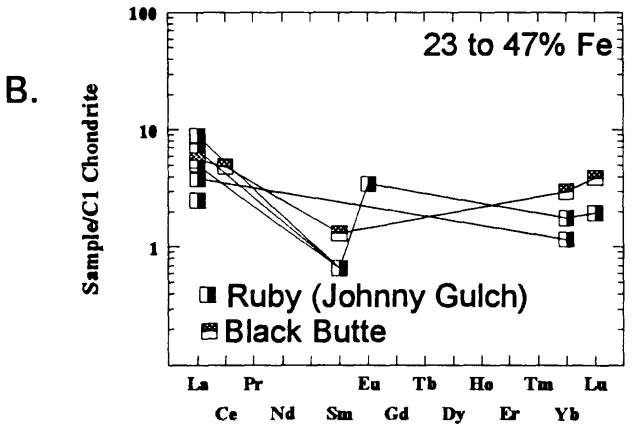

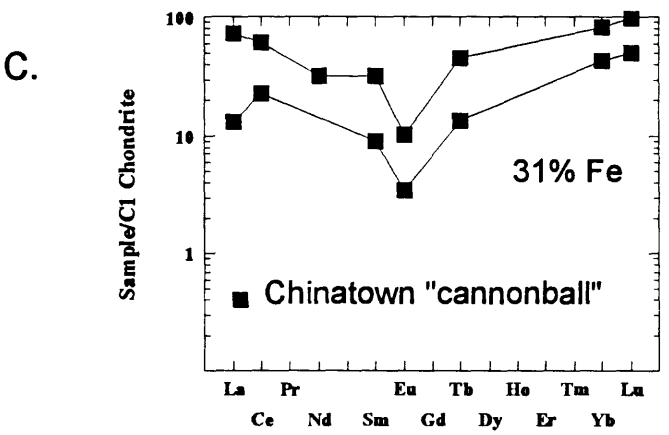

Figure 6. Chondrite-normalized rare-earth element patterns for iron formation. Element concentrations are normalized to C1 chondrite (Sun and McDonough, 1989). A. Copper Mountain and Carter Creek deposits. B. Ruby (Johnny Gulch Iron) and Black Butte deposits. C. Magnetite "cannonballs" from Chinatown placer gold tailings.

Ultramafic rocks

Ultramafic rocks occur as small plugs scattered throughout the Archean gneisses in the eastern parts of the study area. Ultramafic rocks can host significant deposits of chromium, nickel, copper, or platinum group elements (PGE) and can also be associated with vermiculite or asbestos deposits when subject to metamoprhism. On a regional scale, PGE are known to occur in a layered ultramafic complexes intrusive into Archean gneiss. Examples include: (1) the Lady of the Lake Complex in the southern part of the Tobacco Root Range, which contains up to 1,000 ppb of precious metals (gold + platinum + palladium) in sulfide-rich zones (Horn and others, 1991, 1992); and (2) the Stillwater Complex near Nye, Montana (Czamanske and Zientek, 1985; Zientek, 1993), which contains the only operating mine producing PGE in the United States. Because PGE are difficult to analyze and are not routinely sought in regional-scale stream-sediment surveys, and because the nature of the ultramafic bodies in the study area is uncertain, we focussed on acquiring new data on ultramafic rocks as part of the mineral resource assessment of the Dillon Resource Area. Anecdotal reports exist of platinum recovered from placer gold mining in the Dillon Resource Area. All of the ultramafic rocks we sampled contain measurable PGE (table 17), but none are particularly anomalous for these types of rocks or comparable to the concentrations reported for the Lady of the Lake Complex in the Tobacco Root Mountains.

Table 17. Summary of selected element concentrations in ultramafic rocks.
[n.d., not determined]

Area	Total PGE (ppb)	Gold (ppb)	Copper (ppm)	Chromium (ppm)	Nickel (ppm)
Blacktail District (Elk Creek vermiculite deposit)	13 20 27	1 1 2	11 99 n.d.	2,260 3,340 4,000	815 926 1,000
Virginia City District	21.1	4	7	4,240	1,795
Silver Star District (Mohawk Mine chromitite)	14.1	1	n.d.	5,900	1,700

Gold vein systems

One of our purposes in collecting a large number of mineralized samples of quartz veins (26 samples) from the area was to obtain minor element data to help define the geochemical signature of vein systems from different mining districts. Regional-scale stream sediment data would be useful for this purpose, but because of the extensive historic placer workings in the Virginia City district and some other districts, the stream sediments have been disturbed and may not provide useful guides to upstream sources. Some of the difficulties in classifying the vein deposits in southwest Montana are that they are hosted by Archean gneisses, lack an apparent association with volcanic rocks, and in many cases, lack an apparent association with an igneous intrusive center. Veins are typically structurally controlled and may be related to regional metamorphism and tectonics. Genetic models for low-sulfide (Motherlode type) gold quartz veins, for example, indicate that arsenic is the best pathfinder element. In these types of deposits, silver, arsenic, gold, and iron are consistently anomalous; tungsten and antimony are less consistently anomalous, and some deposits are anomalous for bismuth, copper, mercury, lead, zinc, tellurium, and (or) molybdenum (Berger, 1986; Goldfarb and others, 1995). Soils and sediments near unmined deposits may contain elevated arsenic (50 to 1,000 ppm) or antimony (>5 ppm) (Goldfarb and others, 1995). Such vein systems are zoned vertically and shallower deposits may contain anomalous mercury, whereas arsenic, tungsten, and iron are more typical of deeper, hotter parts of vein systems (greenschist to amphibolite facies conditions). Gold-rich epithermal veins are always associated with intermediate to felsic volcanic centers, and gold-silver-telluride vein deposits typically are associated with porphyritic alkaline igneous rocks. Both of these latter types of gold vein systems can also be zoned vertically, and both typically contain more sulfide minerals and a more diverse, highly variable, minor element suite; this suite can include silver, arsenic, gold, barium, bismuth, copper, fluorine, iron, mercury, molybdenum, manganese, nickel, lead, antimony, tellurium, vanadium, and zinc (Kelley and others, 1995; Plumlee and others, 1995). Selenium is more typical of the epithermal environment.

Evaluation of the quartz vein data by mining district shows that some discrete groupings exist in terms of the geochemical signatures of different vein systems (fig. 7). Quartz veins associated with iron formation in the Cherry Creek district are distinctly less gold- and zinc-rich than veins in Archean gneiss in the Virginia City and Revenue districts (fig. 7A). Ternary diagrams provide no information about variations in absolute element concentrations from district to district, but do show trends in relative concentrations of selected trace elements (figs. 7B and 7C). Relative to the Revenue and Blacktail districts, the Virginia City district veins have relatively more antimony and less tellurium (figs. 7B and 7C). All of the vein systems are enriched in arsenic relative to antimony or tellurium (fig. 7C).

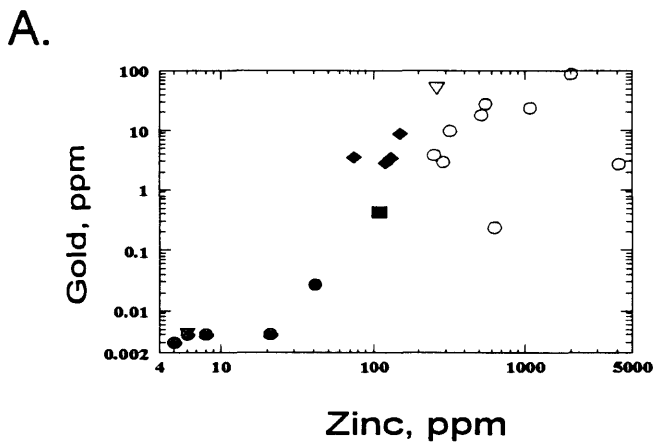

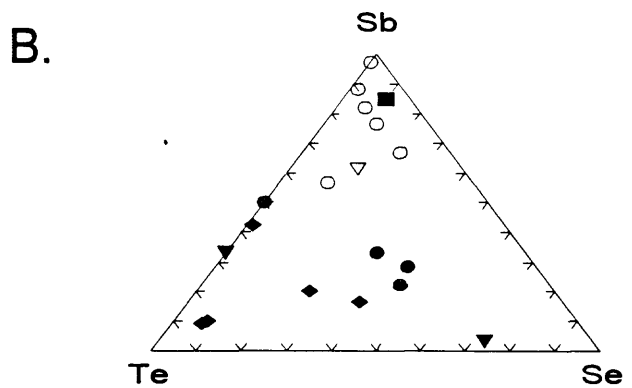

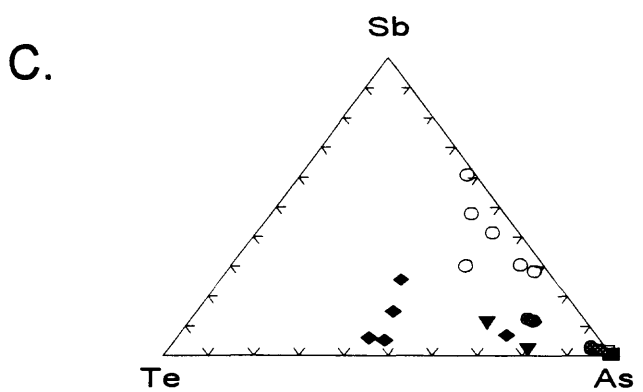

Figure 7. Minor element signature of quartz veins plotted by mining district. Open circles, Virginia City; filled circles, Cherry Creek; diamonds, Revenue; square, Horse Prairie; filled triangle, Blacktail; open triangle, Red Bluff.
A. Log plot of gold versus zinc. B. Ternary plot of antimony (Sb), tellurium (Te), and selenium (Se). C. Ternary plot of antimony (Sb), tellurium (Te), and arsenic (As).

Environmental considerations

In addition to metals that might have potential economic significance, a number of elements that were not included in previous mineral resource studies, which might be of interest for environmental studies, are covered in this report. These elements include arsenic, cadmium, chromium, mercury, selenium, and lead. Consideration of the presence or absence of such elements, along with knowledge of the mineralogy and nature of the host rock for a particular deposit, can be used to qualitatively assess the potential for negative environmental impacts on aquatic ecosystems should further development occur. The types of mineral occurrences (iron formation, low-sulfide gold quartz veins, skarn, ultramafic rocks) sampled for this study of the Dillon Resource Area do not represent types of mineral deposits likely to contribute **significant** acid drainage to aquatic ecosystems, because the near-surface deposits are typically sulfide-poor. For example, most historic lode gold workings exploited the near-surface, oxidized parts of quartz vein systems and did not develop deeper, more sulfide-rich levels because gold grades dwindled to values that were subeconomic for the technology of the time. In addition, carbonate minerals (dolomite or siderite) are present in many of the vein alteration assemblages and these minerals, though less reactive than calcite, may help neutralize any acidity generated by pyrite oxidation. This does not imply that tailings, or drainages in contact with historic tailings, are necessarily benign. Data collected for this study are intended to establish geochemical signatures of particular types of mineral occurrences, possibly indicating favorability for the occurrence of undiscovered mineral deposits or metal associations. These data coincidentally provide information about concentrations of elements in rocks and stream sediments that can help establish background and baseline conditions. However, these data are not intended for use in the evaluation of compliance with any regulatory standards.

Of the 100 samples described in this study, only 3 samples contained mercury above the detection limit of 1 ppm. One of the samples is a magnetite "cannonball" from the Chinatown placer district (tables 1 and 6, map key 29, sample E9501). This elevated mercury concentration (5 ppm) probably represents contamination of the samples from anthropogenic use of mercury because: (1) the sample is from historic placer workings where mercury was probably used in processing gold; and (2) another sample of the same type of rock, sample E9502, did not contain anomalous mercury. The other two mercury-bearing samples are from the Virginia City mining district (table 16A): (1) sample E9520 (2 ppm Hg) from the ore bin at the Mapleton Mine and sample V9521B (4 ppm Hg) from a stockpile of ore extracated from the Bamboo Chief mine. Again, these mercury values could be part of the geochemical signature of the particular orebodies, but it is suspicious that all of the other 28 samples from the Virginia City district had <1 ppm Hg and that the two anomalous samples came from concentrated ore piles. None of the four stream sediments from the district had elevated mercury. This data set is too small to evaluate mercury for the district; however, the data indicate that most random samples of ore material contain anomalous gold and lack mercury.

The data set for this report includes nine stream sediment samples representing six mining districts (see table 18). These samples were collected to augment a much larger data set collected during the NURE program. Although these data are by no means comprehensive, they can be examined in light of concentrations of elements of potential significance to benthic organisms. Measured concentrations for selected elements of environmental concern are summarized in table 18, along with limits of tolerance for sediments proscribed for most benthic species. These data indicate nothing about water quality or bioavailabilty of potentially toxic elements. Recent studies show that the total concentration of a trace metal in a sediment **cannot** be used as a measure of its toxicity and ability to bioaccumulate, because different sediments exhibit different degrees of bioavailability for the the same quantitiy of total metal (EPA, 1997). However, these data show that the total metal concentrations are well below any

values that might warrant further investigation.

A summary of abandoned hardrock mine priority sites by the Montana Department of State Lands identified a number of inactive or abandoned mine sites on both public and private lands in Beaverhead and Madison Counties which have tailings or waste rocks on-site that contain elevated metal concentrations (Pioneer Technical Services, 1995). At some sites, surface water or sediment discharges exceeded chronic aquatic life criteria for some elements. The priority sites are generally in mining districts that experienced extensive historic mining activity (Norris, Pony, Virginia City), and no seasonal monitoring of water quality over time was included in the study. The data reported for the mines in the Virginia City district indicate near-neutral pH conditions and few instances where surface water concentrations of lead or mercury exceed standards (minimum contaminant levels for drinking water or chronic aquatic life standards). Mercury probably represents an anthropogenic source because, historically, mercury was used to amalgamate gold.

Table 18. Stream sediment data for selected elements by mining district.
[Limit of tolerance is the concentration in a sediment that would be detrimental to the majority of benthic species (NYSDEC, 1991).]

Element (units)	Limit of tolerance	Big Muddy	Blacktail	Cherry Creek	Chinatown	Monida	Virginia City
Arsenic (ppm)	33	6.3	8.9	10	5.9	9.4	1.6 to 6.7
Cadmium (ppm)	10	<0.5	<0.5	0.8	<0.5	<0.5	<0.5
Copper (ppm)	114	2	15	11	11	6	8 to 22
Iron(%)	4.0	0.6	2.3	2.3	2.0	1.5	2.1 to 4.4
Mercury (ppm)	2.0	<1	<1	<1	<1	<1	<1
Nickel (ppm)	90	5	21	15	6	14	7 to 83
Lead (ppm)	250	27	17	15	27	9	10 to 44
Zinc (ppm)	800	14	59	71	71	47	38 to 84

SUMMARY AND CONCLUSIONS

A number of gold districts in the northern part of the Dillon Resource Area (Virginia City, Pony, Red Bluff, Sheridan, Revenue) have been explored more or less continuously during the past 20 years, although little development has been attempted. Should the price of gold rise in the future, many of the historic gold mining districts in the northern part of the Dillon BLM Resource Area may become more attractive to industry and present federal land managers with conflicting alternatives for future land use. Compared to the types of mineral deposits present in other parts of Montana, most of the gold deposits in the Dillon Resource Area are unlikely to pose significant threats to aquatic ecosystems from the generation of acidic waters or release of toxic metals if the near-surface, oxidized ores are processed by heap leach methods. Most of the environmental concerns associated with such operations are likely to be related to land disturbances and cyanide use. This is because these precious-metal-rich, quartz vein deposits have mainly low sulfide content. There may be significant amounts of sulfide minerals at deeper levels, and underground development could pose risks for acidic drainage to develop. However, the precious metal content of the sulfide-rich zones may be too low grade and (or) faulted, and the discontinuous nature of many of the vein systems may be not provide sufficient ore tonnage to warrant economic underground exploitation. Quartz veins associated with banded iron formation appear to be less prospective for gold than the structurally controlled vein systems. Preliminary data suggests that some of the vein systems may have distinct trace element signatures that may provide clues to their origin. The Virginia City vein systems have no apparent connection to the Tobacco Root batholith or to any dated post-Precambrain intrusive center. They may represent a hydrothermal event related to Proterozoic magmatism (represented by granitic gneiss and abundant pegmatites); gold may have been high-graded and concentrated along reactivated structures during the Laramide-style deformation of the Late Cretaceous. Structurally-controlled, gold-bearing polymetallic veins in the Horse Prairie district may represent future exploration targets in the Dillon Resource Area. Ultramafic rocks in the Resource Area contain minor concentrations of platinum-group elements, but they do not appear to have economic potential for the reasonably forseeable future because they are too small, too discontinuous, and too low in grade.

ACKNOWLEDGMENTS

Many people provided us with access to sites and background information for this study. John McKay of the Dillon BLM office and Katie Bump of the U.S. Forest Service in Dillon provided us with background information and guidance on sampling sites of particular interest to the federal land managers.

Dick Berg, Montana Bureau of Mines and Geology, showed us around in the field and graciously shared his extensive knowledge of the geology and mineral deposits of southwestern Montana. Elizabeth Brenner Younggren gave us guided tours of the Chinatown district and shared unpublished data. William Perry, USGS, Denver, led us to altered areas near Clark Canyon reservoir. Bill Jenkins, Majesty Mining Company, guided our sampling at the East Revenue mine.

We would especially like to thank the numerous geologists and the mining companies conducting exploration in the Virginia City district for providing access and discussing the local geology with us in 1995, 1996, and 1997. These include Merlin Bingham and Bill Neal of Hanover Gold Company, and Joe Bardswich of Madison Mining Corporation. Paul Eimon graciously discussed his observations of the district and provided background information. Guyan Saunders gave us access to King of Kings Mines Ltd. property in the northern part of the district and provided a forum for discussion of the district geology for all interested parties.

Our colleague, Jim Elliott, helped us sample in 1995, shared his voluminous knowledge of Montana geology and mineral deposits, and demonstrated his uncanny ability to spot the most prospective rock and interpret the field relations at any outcrop. Jeff Grossman, USGS, provided advice on geochemical data and Robert C. Carlson, USGS, reviewed the manuscript.

REFERENCES CITED

Barnard, Fred, 1993, District-scale zoning patterns, Virginia City, Montana USA: 96th National Western Mining Conference and Exhibition, Denver, Colo., March 23-26, 1993, Denver, Colorado Mining Association Reprint 93-29, 18 p.

Bayley, R.W., and James, H.L., 1973, Precambrian iron formations of the United States: Economic Geology, v. 68, p. 934-959.

Berg, R.B., 1988, Barite in Montana: Montana Bureau of Mines and Geology Memoir 61, 100 p.

_____1995, Geology of the Elk Creek vermiculite deposit, Madison and Beaverhead Counties, Montana: Montana Bureau of Mines and Geology Open-File Report 335, pamphlet, 9 p., 2 plates.

Berger, B.R., 1986, Descriptive model of low-sulfide Au-quartz veins, *in* Cox, D.P. and Singer, D.A., eds. Mineral deposit models: U.S. Geological Survey Bulletin 1693, p. 239-243.

Berger, B.R., Snee, L.W., Hanna, W.F., and Benham, J.R., 1983, Mineral resource potential of the West Pioneer Wilderness Study Area, Beaverhead County, Montana: U.S. Geological Survey Miscellaneous Field Studies Map MF-1565-A, scale 1:50,000, includes pamphlet, 21 p.

Bolivar, S.L., 1980, Uranium hydrogeochemical and stream sediment reconnaissance of the Bozeman NTMS Quadrangle, Montana, including concentrations of forty-two elements: U.S. Department of Energy Open-File Report GJBX-235(80), 169 p., available from USGS Open-File Services.

Boyle, R.W., 1991, Auriferous Archean greenstone-sedimentary belts: Economic Geology, Monograph 8, p. 164-191.

Brenner Younggren, Elizabeth, 1995, Chinatown Prospect, Beaverhead County, Montana: Unpublished report, 6 p.

Carlson, R.R. and Lee, G.K., in prep., Geochemistry—Stream sediments, *in* Hammarstrom, J.M., Wilson, A.B., and Van Gosen. B.S., eds., Mineral and energy resource assessment of the Gallatin National Forest (exclusive of the Absaroka-Beartooth study area), in Gallatin, Madison, Meagher, Park, and Sweet Grass Counties, south-central Montana: U.S. Geological Survey Professional Paper, Chapter D.

Chace, F.M., Carter, Fred, and Byers, Virginia, 1947, Map showing metallic mineral deposits of Montana: U.S. Geological Survey Missouri Basin Studies no. 16, scale 1:1,000,000.

Chavez, Joel, 1994, Mining districts of Montana: Helena, Montana State Library, National Resource Information System Map #94-NRIS-230, scale 1:1,000,000.

Cole, M.M., 1983, Nature, age, and genesis of quartz-sulfide-precious-metal vein systems in the Virgina City mining district, Madison County, Montana: Bozeman, Montana State University, M.S. thesis, 76 p.

Czamanske, G.K., and Zientek, M.L., eds., 1985, The Stillwater Complex, Montana—Geology and guide: Montana Bureau of Mines and Geology Special Publication 92, 396 p., 4 plates.

Desmarais, N.R., 1978, Structural and petrologic study of Precambrian ultramafic rocks, Ruby Range, southwestern Montana: Missoula, University of Montana, M.S. thesis, 88 p.

_____1981, Metamorphosed Precambrian ultramafic rocks in the Ruby Range, Montana: Precambrian Research, v. 16, p. 67-101.

Eimon, P.I., 1997, The economic geology of Montana's Virginia City mining district: Society of Economic Geologists Newsletter, no. 28, January, 1997, 6 p.

EPA (Environmental Protection Agency), 1997, The incidence and severity of sediment contamination in surface waters of the United States, Volume 1, National sediment quality survey: U.S. Environmental Protection Agency, Report to Congress, Document EPA 823-R-97-006, variously paginated.

Foote, M.W., 1986, Contact metamorphism and skarn development of the precious and base metal deposits at Silver Star, Madison County, Montana: Laramie, University of Wyoming, Ph.D. Dissertation, 233 p.

Garihan, J.M., 1979, Geology and structure of the central Ruby Range, Madison County, Montana—Summary: Geological Society of America Bulletin, Part I, v. 90, p. 323-326.

Geach, R.D., 1972, Mines and mineral deposits (except fuels), Beaverhead County, Montana: Montana Bureau of Mines and Geology Bulletin 85, 194 p.

Goldfarb, R.J., Berger, B.R., Klein, T.L., Pickthorn, W.J., and Klein, D.P., 1995, Low-sulfide Au quartz vein deposits, *in* du Bray, E.A., ed., Preliminary compilation of descriptive geoenvironmental mineral deposit models: U.S. Geological Survey Open-File Report 95-831, p. 261-267.

Hadley, J.B., 1969, Geologic map of the Varney quadrangle, Madison County, Montana: U.S. Geological Survey Geologic Quadrangle Map GQ-814, scale 1:62,500.

Haley, J.C., and Perry, W.J., Jr., 1991, The Red Butte conglomerate—A thrust-derived conglomerate of the Beaverhead Group, southwestern Montana: U.S. Geological Survey Bulletin 1945, 19 p.

Hanna, W.F., Kaufmann, H.E., Hassemer, J.H., Ruppel, B.D., Pearson, R.C., and Ruppel, E.T., 1993, Maps showing gravity and aeromagnetic anomalies in the Dillon 1° x 2° quadrangle, Idaho and Montana: U.S. Geological Survey Miscellaneous Investigations Series Map I-1803-I, scale 1:250,000, includes pamphlet, 27 p.

Hawkes, H.E., and Webb, J.S., 1962, Geochemistry in mineral exploration: New York, Harper & Row, 415 p.

Heinrich, E.W., 1949, Sillimanite deposits of the Dillon, region Montana: Montana Bureau of Mines and Geology Memoir 30, 43 p.

_____1960, Geology of the Ruby Mountains, *in* Pre-Beltian geology of the Cherry Creek and Ruby Mountains areas, southwestern Montana: Montana Bureau of Mines and Geology Memoir 38, p. 15-40.

Hogberg, R.K., 1960, Geology of the Ruby Creek iron deposit, Madison County, Montana, *in* Campau, D.E., Anisgard, H.W., and Egbert, R.L., eds., West Yellowstone-earthquake area, Billings Geological Society, annual field conference, 11th, September 7-10, 1960, Guidebook: Billings Geological Society, p. 268-272.

Horn, L., Coyner, S., Mueller, P., Heatherington, A., and Mogk, D., 1991, The Lady of the Lake Complex—A newly discovered, layered, mafic intrusion, Tobacco Root Mountains, SW Montana: Geological Society of America Abstracts with Programs, v. 23, no. 5, p. A329.

Horn, L., Mueller, P. Heatherington, A., and Mogk, D., 1992, Geochemistry of a layered mafic intrusion—The Lady of the Lake Complex, Tobacco Root Mountains, southwestern Montana: Geological Society of America Abstracts with Programs, v. 24, no. 7, p. A262.

James, H.L., 1981, Bedded Precambrian iron deposits of the Tobacco Root Mountains: U.S. Geological Survey Professional Paper 1187, 16 p.

_____1990, Precambrian geology and bedded iron deposits of the southwestern Ruby Range, Montana, *with a section on* The Kelly iron deposit of the northeastern Ruby Range: U.S. Geological Survey Professional Paper 1495, 39 p., 2 plates.

James, H.L., and Wier, K.L., 1962, Magnetic and geologic map of iron deposits near Copper Mountain, Madison County, Montana: U.S. Geological Survey Open-File Report [unnumbered], scale 1:2,400, 2 sheets.

_____1972, Geologic map of the Carter Creek iron deposit, secs. 3, 9, and 10, T. 8 S., R. 7 W., Madison and Beaverhead Counties, Montana: U.S. Geological Survey Miscellaneous Field Studies Map MF-359, scale 1:3,600.

Kaas, L.M., ed., 1996, Indices to U.S. Bureau of Mines Mineral Resources Records: U.S. Bureau of Mines Special Publication 96-2 (CD-ROM).

Kelley, K.D., Armbrustmacher, T.J., and Klein, D.P., 1995, Au-Ag-Te vein deposits, *in* du Bray, E.A., ed., Preliminary compilation of descriptive geoenvironmental mineral deposit models: U.S. Geological Survey Open-File Report 95-831, p. 130-136.

Kellogg, K.S., 1993, Gold deposits of the Lower Hot Springs mining district near Norris, Montana, *in* Childs, J.F., and Lageson, D.R., eds., Economic and regional geology of the Tobacco Root-Boulder Batholith region, Montana, Tobacco Root Geological Society, annual field conference, 18th, Bozeman, Mont., July 16-18, 1993: Northwest Geology, v. 22, p. 19-23.

_____1994, Geologic map of the Norris quadrangle, Madison County, Montana: U.S. Geological Survey Geologic Quadrangle Map GQ-1738, scale 1:24,000.

Kovaric, D.N., Brady, J.B., Cheney, J.T., Grove, Marty, Jacob, L.J., and King, J.T., 1996, $^{40}Ar/^{39}Ar$ evidence for reheating events affecting basement rocks in the Tobacco Root, Ruby, and Highland Mountains, SW Montana: Geological Society of America Abstracts with Programs, v. 28, no. 7, p. A-493.

Kwong, Y.T. John, 1993, Prediction and prevention of acid rock drainage from a geological and mineralogical perspective: National Hydrology Research Institute (NHRI) Contribution CS-92054, Environment Canada, MEND project 1.32.1, Saskatoon, Saskatchewan, Canada, 47 p.

Lockwood, M.S., 1990, Controls on precious-metal mineralization, Easton-Pacific Vein, Virginia City mining district, Madison County, Montana: Socorro, New Mexico Institute of Mining and Technology, M.S. thesis, 136 p.

Lockwood, M.S., Campbell, A.R., and Chavez, W.X., Jr., 1991, Evolution of mineralizing fluids, Virginia City mining district, Montana: Geological Society of America Abstracts with Programs, v. 23, no. 4, p. 43.

Loen, J.S., 1995, Geological curiosities of southwestern Montana, *in* Thomas, R.C., ed., Geologic history of the Dillon area, southwestern Montana, Proceedings volume from the 20th annual field conference of the Tobacco Root Geological Society, Western Montana College, Dillon, Mont., Aug. 11-13, 1995: Northwest Geology, v. 25, p. 79-90.

Loen, J.S., and Pearson, R.C., 1989, Map showing locations of mines and prospects in the Dillon 1° x 2° quadrangle, Idaho and Montana: U.S. Geological Survey Miscellaneous Investigations Series Map I-1803-C, scale 1:250,000, accompanying pamphlet, 85 p.

Lorain, S.H., 1937, Gold lode mining in the Tobacco Root Mountains, Madison County, Montana: U.S. Bureau of Mines Information Circular 6972, 74 p.

Lowell, W.R., 1965, Geologic map of the Bannack-Grayling area, Beaverhead County, Montana: U.S. Geological Survey Miscellaneous Geologic Investigations Map I-433, scale 1:31,680.

Lyden, C.J., 1948, Gold placers of Montana: Montana Bureau of Mines and Geology Memoir 26, 151 p. [**Note** that this memoir was reprinted in 1987 as Montana Bureau of Mines and Geology Reprint 6.]

Marvin, R.F., and Dobson, S.W., 1979, Radiometric ages—Compilation B, U.S. Geological Survey: Isochron /West, no. 26, p. 3-32.

McCulloch, Robin, 1994, Montana mining directory—1993: Montana Bureau of Mines and Geology Open-File Report 329, 84 p.

McLeod, J.W., 1986, Report on the U.S. Grant gold mine, Virginia City area, Madison County, Montana: Unpublished report prepared in behalf of the U.S. Grant Gold Mining Company Ltd. of Vancouver, British Columbia, 19 p.

MCRS (Mining Claim Recordation System), 1996, Data base maintained by the Bureau of Land Management, Denver Service Center, Denver, CO.

M'Gonigle, J.W., and Dalrymple, G.B., 1996, $^{40}Ar/^{39}Ar$ ages of some Challis Volcanic Group rocks and the initiation of Tertiary sedimentary basins in southwestern Montana: U.S. Geological Survey Bulletin 2132, 17 p., 1 plate.

M'Gonigle, J.W. and Hait, M.H., Jr., 1997, Geologic map of the Jeff Davis Peak quadrangle and the eastern part of the Everson Creek quadrangle, Beaverhead County, southwest Montana: U.S. Geological Survey Geologic Investigations Map I-2604, scale 1:24,000.

Nockolds, S.R., 1954, Average chemical compositions of some igneous rocks: Bulletin of the Geological Society of America, v. 65, p. 1007-1032.

NYSDEC, 1991, New York State Department of Environmental Conservation (NYSDEC), Sediment Criteria: Report of the Sediment Medium Committee.

O'Neill, J.M., Klepper, M.R., Smedes, H.W., Hanneman, D.L., Frazer, G.D., and Mehnert, H.H., 1996, Geologic map and cross sections of the central and southern Highland Mountains, southwestern Montana: U.S. Geological Survey Miscellaneous Investigations Series Map I-2525, scale 1:50,000.

Page, N. J, 1986, Deposit model of synorogenic-synvolcanic Ni-Cu, *in* Cox, D.P. and Singer, D.A., eds., Mineral deposit models: U.S. Geological Survey Bulletin 1693, p. 28.

Pearson, R.C., Trautwein, C.M., Ruppel, E.T., Hanna, E.F., Rowan, L.C., Loen, J.S., and Berger, B.R., 1992, Mineral resource assessment of the Dillon 1° x 2° quadrangle, Idaho and Montana: U.S. Geological Survey Circular 1077, 15 p.

Perry, W.J., Jr., Haley, J.C., Nichols, D.J., Hammons, P.M., and Ponton, J.D., 1988, Interactions of Rocky Mountain foreland and Cordilleran thrust belt in Lima region, southwest Montana, *in* Schmidt, C.J., and Perry, W.J., Jr., eds., Interaction of the Rocky Mountain foreland and Cordilleran thrust belt: Geological Society of America Memoir 171, p. 267-290.

Pinckney, D.M., Hanna, W.F., Kaufman, H.A., and Larsen, C.E., 1980, Resource potential of the Bear Trap Canyon Instant Study Area, Madison County, Montana: U.S. Geological Survey Open-File Report 80-835, 32 p.

Pioneer Technical Services, Inc. 1995, Abandoned hardrock mine priority sites, 1995, Summary Report, Prepared for Montana Department of State Lands, Abandoned Mine Reclamation Bureau, Helena, MT, variously paginated.

Plumlee, G.S., Smith, K.S., Berger, B.R., Foley-Ayuso, N., and Klein, D.P., 1995, Creede, Comstock, and Sado epithermal vein deposits, *in* du Bray, E.A., ed., Preliminary compilation of descriptive geoenvironmental mineral deposit models: U.S. Geological Survey Open-File Report 95-831, p. 152-161.

Randol 1994/1995, 1995, Mining directory 1994/95, U.S. mines and mining companies: Golden, Colo., Randol International Ltd., Randol Mining Directory, p. 287-301.

Roedder, Edwin, 1984, Fluid inclusions: Chelsea, MI, Bookcrafters, Inc., Mineralogical Society of America, Reviews in Mineralogy, v. 12, 644 p.

Rollinson, Hugh, 1994, Using geochemical data—Evaluation, presentation, interpretation: Singapore, Longman Scientific and Technical, 352 p.

Ruppel, E.T., O'Neill, J.M., and Lopez, D.A., 1993, Geologic map of the Dillon 1° x 2° quadrangle, Idaho and Montana: U.S. Geological Survey Miscellaneous Investigations Series Map I-1803-H, scale 1:250,000.

Sagar, Joe, and Childs, John, 1993, Field trip #2, Maltby's Mound: Northwest Geology, v. 22, p. 103-116.

Sahinen, U.M., 1939, Geology and ore deposits of the Rochester and adjacent mining districts, Madison County, Montana: Montana Bureau of Mines and Geology Memoir 19, 53 p.

Shacklette, H.T., and Boerngen, J.G., 1984, Element concentrations in soils and other surface materials of the conterminous United States: U.S. Geological Survey Professional Paper 1270, 105 p.

Shannon, S.S., Jr., 1980, Uranium hydrogeochemical and stream sediment reconnaissance data release for the Ashton NTMS Quadrangle, Idaho/Montana/Wyoming, including concentrations of forty-two elements: U.S. Department of Energy Open-File Report GJBX-189(80), 168 p. [Available from USGS Open-File Services.]

Shawe, D.R., and Wier, K.L., 1989, Gold deposits in the Virginia City-Alder Gulch District, Montana, *in* Gold in placer deposits: U.S. Geological Survey Bulletin 1857-G, p. G14-G19.

Sheets, M.R., 1980, A geological investigation and evaluation of R and D Minerals, Inc., Virginia City, Madison County, Montana: Unpublished report prepared for the Kemmerer Corporation, 83 p.

Sinkler, Helen, 1942, Geology and ore deposits of the Dillon nickel prospect, southwestern Montana: Economic Geology, v. 37, no. 2, p. 136-152.

Sonderegger, J.L., Schofield, J.D., Berg, R.B., and Mannick, M.L., 1982, The upper Centennial Valley, Beaverhead and Madison Counties, Montana, *with a section on* The Madison Valley thermal springs by G.J. Weinheimer: Montana Bureau of Mines and Geology Memoir 50, 53 p., 4 plates.

Stanley, D.R., 1988, Geochemical investigation of some Archean banded iron formations from southwest Montana: Gainesville, University of Florida, M.S. thesis, 129 p.

Sun, S.S., and McDonough, W.F., 1989, Chemical and isotopic systematics of oceanic basalts—Implication for mantle composition and processes, *in* Magmatism in the ocean basins: Geological Society of America Special Publication 42, p. 313-345.

Tansley, Wilfred, Schafer, P.A., and Hart, L.H., 1933, A geological reconnaissance of the Tobacco Root Mountains, Madison County, Montana: Montana Bureau of Mines and Geology Memoir 9, 57 p.

Theodore, T.G., Orris, G.J., Hammarstrom, J.M., and Bliss, J.D., 1991, Gold-bearing skarns: U.S. Geologcal Survey Bulletin 1930, 61 p.

Thurlow, E.E., 1941, Geology and ore deposits of the lower Hot Springs mining district, Madison County, Montana: Butte, Montana School of Mines and Geology, M.S. thesis, 85 p.

Trauerman, C.J., and Reyner, M.L., 1950, Directory of Montana mining properties, 1949: Montana Bureau of Mines and Geology Memoir 31, 125 p.

Trauerman, C.J., and Waldron, C.R., Supervisors, 1940, Directory of Montana mining properties, 1949: Montana Bureau of Mines and Geology Memoir 20, 135 p.

Vitaliano, C.J., and Cordua, W.S., 1979, Geologic map of southern Tobacco Root Mountains, Madison County, Montana: Geological Society of America Map and Chart Series MC-31, scale 1:62,500.

Wier, K.L., 1965, Preliminary geologic map of the Black Butte iron deposit, Madison County, Montana: U.S. Geological Survey Open-File Report [unnumbered, dated June 4, 1965], scale 1:9,600.

_____1982, Maps showing geology and outcrops of part of the Virginia City and Alder quadrangles, Madison County, Montana: U.S. Geological Survey Miscellaneous Field Studies Map MF-1490, 2 sheets, scales 1:12,000 and 1:4,750.

Winchell, A.N., 1914, Mining districts of the Dillon quadrangle, Montana, and adjacent areas: U.S. Geological Survey Bulletin 574, 191 p.

Winters, Richard, Graham, Don, Hillman, Tom, Hughes, Curt, and Johnson, Rick, 1994, Mineral resource appraisal of the Beaverhead National Forest, Montana: U.S. Bureau of Mines Mineral Land Assessment Open-File Report MLA 18-94, 84 p., plus appendixes A-I.

Woodward, L.A., 1993, Structural control of lode gold deposits in the Pony mining district, Tobacco Root Mountains, Montana: Economic Geology, v. 88, no. 7, p. 1,850-1,861.

Woodward, L.A., Miller, D.R., and Kendall, T.K., 1993, Geology and ore deposits of the Mineral Hill mining district, Madison County, Montana, *in* Childs, J.F., and Lageson, D.R., eds., Economic and regional geology of the Tobacco Root-Boulder Batholith region, Montana, Tobacco Root Geological Society, annual field conference, 18th, Bozeman, Mont., July 16-18, 1993: Northwest Geology, v. 22, p. 9-17.

Yeend, Warren, and Shawe, D.R., 1989, Gold placers, *in* Gold in placer deposits: U.S. Geological Survey Bulletin 1857-G, p. G1-G13.

Zientek, M.L., 1993, Mineral resource appraisal for locatable minerals—The Stillwater Complex [chapter F], *in* Hammarstrom, J.M., Zientek, M.L., and Elliott, J.E., eds., Mineral resource assessment of the Absaroka-Beartooth study area, Custer and Gallatin National Forests, Montana: U.S. Geological Survey Open-File Report 93-207, p. F1-F83.